Energy, Mines and Resources Canada
Énergie, Mines et Ressources Canada

CANMET

Canada Centre for Mineral and Energy Technology
Centre canadien de la technologie des minéraux et de l'énergie

Mining Research Laboratories
Laboratoires de recherche minière

Canada

Canada/NB MDA project on mine-shaft rope testing; testing of 1 1/2 in., 6×30, H.R. (our rope #7)

L.B. Geller, D. Poffenroth, J.E. Udd, and D. Hutchinson

MRL report #90-071 (TR) August, 1990

This document is an internal
report which was prepared primarily
for use [illegible] and internal
[illegible] purposes. It does not
necessarily a final expression of
the opinion of the Canada Centre
for Mineral and Energy Technology
(CANMET)

Ce document est un rapport
[illegible] interne et rédigé
[illegible] pour fin de
discussion et de documentation
[illegible] nécessaire-
ment [illegible] définitive de
l'opinion du Centre canadien de
la technologie des minéraux et de
l'énergie (CANMET)

132 pp

91-01595/

CANADA/NB MDA PROJECT ON MINE-SHAFT ROPE TESTING; TESTING OF $1\frac{1}{2}$ IN., 6 × 30, H.R. (OUR ROPE #7)

by

L.B. Geller*, D. Poffenroth†, J.E. Udd**, and D. Hutchinson††

ABSTRACT

In this report the authors analyse the test-results obtained both non-destructively, and destructively, on a $1\frac{1}{2}$ in., 6×30, stranded hoist-rope (H.R.). The rope was examined both in situ and on the shop-floor as part of CANMET's project to comparatively evaluate the performance of a range of EM wire-rope testers. This is the first time a project of this magnitude and diversity has been undertaken.

The rope in question was reported to contain localised strength losses (LBS) of up to 21.0%, with slight to moderate corrosion, and some interstrand wear. Its size and construction is very representative of the hoist-ropes currently being used in Canadian mine shafts. Moreover, this test-series is of great interest because it entails the widest range of EM instruments that were used on a single rope during the current CANMET project.

In the field, EM testing was performed with one American (the LMA-250) and three Canadian (the Rotesco AC, Rotescograph, and Magnograph) instruments. The same instruments, as well as a prototype version of a West German tester, designed by WBK's rope testing laboratory, were used on the shop-floor.

The large number of results obtained are analysed with special reference to such important parameters as their repeatability, comparability, and levels of accuracy. Moreover, calculations are presented to document the legitimacy of comparing in situ EM test results with reel-to-reel results.

---

* Research Scientist, and ** Director, Mining Research Laboratories, CANMET, Energy Mines and Resources Canada, Ottawa; and † Electronics Engineer, and ††Chief, Industrial and Electrical Safety Division, MSHA, United States Dept. of Labor, Denver.

Keywords: New Brunswick; Mineral Development Agreement; wire-ropes; Non-destructive-testing; Electro-magnetic instruments; stranded ropes

ENTENTE CANADA/NOUVEAU-BRUNSWICK SUR L'EXPLOITATION MINÉRALE
PROJET D'ESSAIS DE CÂBLES POUR LES PUITS DE MINE
ESSAI D'UN CÂBLE DE LEVAGE DE 1½ po, 6 X 30 (NOTRE CÂBLE #7)

par

L.B. Geller*, D. Poffenroth+, J.E. Udd** et D. Hutchison++

RÉSUMÉ

Dans le présent rapport, les auteurs analysent les résultats d'essais, à la fois non destructifs et destructifs, réalisés sur un câble de levage toronné de 1½ po, 6 x 30. Le câble a été examiné dans le puits de mine et en atelier dans le cadre d'un projet de CANMET visant à comparer les performances de plusieurs instruments d'essai EM des câbles métalliques. C'est la première fois qu'un projet d'une telle ampleur et d'une telle diversité a été entrepris.

Les essais ont montré que le câble en question présentait des pertes de résistance localisées atteignant 21,0 %, avec une corrosion légère à moyenne et une certaine usure entre les torons. Par sa taille et sa construction, ce câble est très représentatif des câbles de levage actuellement utilisés dans les puits de mine canadiens. En outre, cette série d'essais présente un grand intérêt car elle fait intervenir la plus grande gamme d'instruments EM jamais utilisés avec un seul câble dans le cadre de ce projet de CANMET.

Sur le terrain, les essais EM ont été réalisés à l'aide d'un instrument américain (le LMA-250) et de trois instruments canadiens (le Rotesco AC, le Rotescograph et le Magnograph). En atelier, on a utilisé les mêmes instruments ainsi qu'un prototype d'un instrument ouest-allemand, conçu par le laboratoire d'essais de câbles de la WBK.

Le grand nombre de résultats obtenus sont analysés en fonction, plus particulièrement, de paramètres importants tels que leur répétabilité, leur comparabilité et leurs niveaux de précision. Sont également présentés des calculs montrant qu'il est justifié de comparer les résultats d'essais EM in situ et les résultats d'essais entre tourets.

---

*Chercheur et **directeur, Laboratoires de recherche minière, CANMET, Énergie, Mines et Ressources, Canada, Ottawa; + ingénieur électronicien et ++ chef, Industrial and Electrical Safety Division, MSHA, United States Dept. of Labor, Denver.

Mots clés : Nouveau-Brunswick ; entente sur l'exploitation minérale ; câbles métalliques ; essais non destructifs ; instruments électromagnétiques ; câbles toronnés.

CONTENTS

page No.

ABSTRACT i

RÉSUMÉ ii

BACKGROUND 1

ROPE DETAILS 1

IN SITU TEST RESULTS — AS REPORTED AND REVIEWED 2

SHOP FLOOR TEST RESULTS — AS REPORTED AND REVIEWED . 4

DESTRUCTIVE TESTING 8

ANALYSIS OF TEST RESULTS 10

REFERENCES 14

APPENDIX 1: Calculation of difference in LMA chart readings 16

APPENDIX 2: Tables 1 to 5, as well as Figures 1 to 14 21

BACKGROUND

The results described in this report constitute an integral part of the contracted phase of CANMET's project, undertaken in 1986 in response to requests by both the mining industry and the mine regulatory authorities. The basic project objectives specified that the continuing rope failures, or near failures — occurring despite mandatory wire-rope examinations with electro-magnetic (EM) instruments at regular intervals — be examined, documented, analysed, and the reasons for these occurrences clarified. This is the first time a project of this scope and depth has been undertaken, anywhere.

CANMET's work included both in-house and contracted work phases. The in-house phase resulted in a range of conclusions and recommendations, reported elsewhere (1, 2, 3, 4). We are now in the process of reporting the results obtained during the contracted project-phase, which included an extensive series of both in situ and shop-floor tests. The first six reports of this series were published in February, May, June, and July, 1990 (5, 6, 7, 8, 9, 10). This is the seventh such report. More are to follow.

ROPE DETAILS

The rope which is the subject of this report (referred to as "our rope #7") was designated #909989-01-1 Head Rope in Shaft #1 of Lac Minerais Ltée's Doyon mine at Cadillac, Quebec. Its reel number was 641700-1.

It was of a $1\frac{1}{2}$ in. diameter, 6 × 30 stranded (FS) construction (12 × .105-.106; 12 × .065-.066; 3 × .033-.034; and 3 × .103-.104 in. wires). Its breaking strength was 261,500 lb, as per Ontario MOL test certificate #66583, dated 4.11.86*. It was installed on 7.2.87, and removed on 27.8.88 (i.e., it was in use for $19\frac{1}{2}$ months). As is well known, and has been pointed out in our previous reports (3, 6, 8), non-destructive testing (NDT) with EM instruments must not be done in isolation. Instead, one must be aware of the previous NDT test-results that have been obtained on the rope tested, and if possible, also on its companion-ropes and predecessors. In the present case we obtained copies of three previous Magnograph test-reports.

---

* for consistency with all previous reports in this series (reference numbers 1–10) dates are given in this order: day; month; year.

IN SITU TEST RESULTS — AS REPORTED AND REVIEWED

General procedure

The in situ tests were undertaken, under standard operating conditions, with three Canadian (the Magnograph, Rotesco AC, and Rotescograph) and one American (the LMA-250) instruments. All of the tests were performed completely independently of each other by operators known to, and approved by, the instrument makers/designers. None of the operators knew about each other's results before these were submitted to us.

The Magnograph data

Previous in situ test results were obtained with a Magnograph instrument at regular intervals along a rope length of some 628-630 yards (1,884-1,890 ft). These tests were undertaken on 15.6.87 (report #87-033A); on 16.9.87 (report #87-146B); and on 13.4.88 (report #88-163B). The maximum reported LMA values were 1.5% (Fig. 1a); 1.5% (Fig. 1b); and 4.0% (Fig. 1c), respectively. The maximum losses were reported some 101-104 yards from test-start.

Our own Magnograph test was performed on 23.8.88. The operator submitted the strip-charts reproduced in Figures 1d$_1$ and 1d$_2$. The rope length tested was 630 yards (1,890 ft). The maximum reported LMA (LMA_{max}) was 11.5% (report #88-383B) at 67 yards from the start of the test. Five LBS estimates were also submitted by the instrument operator (report #88-495) for the 67, 90, 264, 430, and 477 yard rope segments. These segments contained, or were near to, the characteristic rope-flaws #1b; #3; #4; #5; and #6 (Fig. 1d$_1$). The respective LBS estimates — with the coresponding reported LMA values in brackets — were: 17.4% (11.5%); 17.6% (11.0%); 17.1% (9.0%); 19.2% (10.0%); and 17.7% (9.0%).

On reviewing the operator's charts, we noted the following:

Fig. 1a: the LMA_{max} is in the order of 0.5%, rather than the reported 1.5%;
Fig. 1b: we agree with the reported $1\frac{1}{2}$% LMA_{max} value;
Fig. 1c: we agree with the reported 4.0% LMA_{max}. It is interesting to note the initial development of some of the characteristic rope-defects (identified as points #2, #5, #7, and #8 in Fig. 1c) at this test-stage already;
Fig. 1d$_1$: report #88-383B refers to an LMA_{max} of 11.5% at 67 yards from test start. At this location the operator wrote 9.0% LMA on his chart. We agree with the latter marking, but note the unexplained discrepancy of some 28.0% between the two foregoing

LMA values. We added our own markings to Fig. $1d_1$: (a) of the 0%LMA level, and (b) of the characteristic rope defect locations #1 to #8.

Fig. $1d_2$: the operator only marked the location of one broken wire on this chart, but no LMA data. Our own LMA_{max} reading is 8.5%. We added our own markings to Fig. $1d_2$: (a) of the 0%LMA level, and (b) of the characteristic rope defect locations #1 to #8.

The Rotesco AC data

Our in situ test was performed on 9.9.88. A copy of the instrument chart is reproduced in Fig. 2a. The rope length tested was some 1,810 ft. The operator reported (test #DPQ-1) a general strength reduction of some 18.0% between 150 ft and 240 ft from test start above the conveyance, with localised losses in the order of 19.0% at 150-160 ft; 170-175 ft; 200-205 ft; and 230-240 ft from the test start. Between 250-755 ft additional localised strength losses of some 11.5%-16.0% were also reported. In addition, some 16.0%-17.0% LBS was reported at 1,230-1,235 ft from the start of the test. Elsewhere, a 16.0% LBS was noted.

We added our own markings to Fig. 2a, notably: (a) the 0%LMA level and (b) the characteristic flaw-locations #1 to #8, inclusive.

The Rotescograph data

Our in situ Rotescograph test was also performed on 9.9.88. A copy of the instrument chart is reproduced in Fig. 3a. The rope length tested was some 1,831 ft. The operator reported (tests #DPQR-1A and -1B) an LBS of some 18.0%-20.0% at 172-227 ft, and at 250-266 ft from the start of the test. Estimated LBS_{max} was 21.0% at 193-195 ft, and at 262-264 ft from the test start. At 1,283-1,285 ft the reported LBS estimate was 18.0%. Elsewhere, the estimated LBS was of the order of 17.0-18.0%. Slight to moderate corrosion, as well as interstrand wear, was reported over the first 1,790 ft, and at 1,807-1,821 ft above the conveyance.

Broken wires were reported at 519 ft, 1,428 ft, and at 1,550 ft from the start of the test. The operator did not mark the test-chart. We added our own markings to Fig. 3a, notably: (a) the 0%LMA reference level, and (b) the characteristic flaw locations #1 to #8, inclusive.

The LMA-250 data

Our in situ LMA-250 test was performed on 9.9.88. A copy of the instrument chart, as submitted to us by the operator, is reproduced in Fig. $4a_1$. The rope length tested was 1,882 ft. The operator reported an LMA_{max} of 12.0% at 1,620 ft from the test-start (i.e., at characteristic rope-flaw #3), and 11.0% LMA at 605 ft from the test-start (i.e., at rope flaw #5). We agree with these chart readings.

Another copy of the original instrument chart, marked by ourselves, is reproduced in Fig. $4a_2$. We added: (a) the 0% LMA reference level, (b) the characteristic flaw locations #1 to #8 inclusive, and (c) the %LMA chart-readings at rope-flaws #3 and #5. We also reproduced a copy of a second original instrument chart (Fig. 4b), adding the following: (a) the 0% LMA reference level, and (b) the characteristic flaw locations #1 to #8, inclusive. While the conveyance was "rising" in case of Fig. 4a, it was "descending" in Fig. 4b. A comparison of the latter two figures, therefore, provides a good opportunity for establishing the LMA-250 tester's ability to accurately repeat measurements.

We noted that the "descending" chart-trace provided to us by the operator (Fig. 4b) went off-scale at the 1,795 ft chart-location, and remained off-scale (except for the #8 flaw location) until the end of the test. Consequently, we are unable to accurately determine the location of the 0% LMA level for this chart. It is unfortunate that this should be so, because, as shown in Figures 6–9, otherwise the repeatability of the EM chart traces is quite remarkable. Also, we think that the complete "descending" trace was probably recorded on the magnetic test-tape, and could, therefore, have been printed out in its entirety. Under the given circumstances, though, we could merely make the "acceptable" assumption that the 0% LMA reference levels in both Figures 4a and 4b are at the same level relative to flaw #8, i.e., that in both cases there is a 3.0% LMA chart-reading at flaw #8. We drew the "true" 100% reference level in Fig. 4b accordingly.

SHOP FLOOR TEST RESULTS — AS REPORTED AND REVIEWED

General procedure

The shop-floor tests were undertaken with three Canadian, one American, and a West German tester, namely with the Rotesco AC, Rotescograph, Magnograph, and the LMA-250 instruments, as well as with the prototype version of the latest German WBK instrument. None of the operators knew about each other's results before these were submitted to us. All of the details of the testing process have been described, and illustrated, elsewhere (5).

The Magnograph data

Shop-floor testing with the Magnograph was undertaken on 18.1.89 and on 4.4.89. The operator reported an LMA_{max} of 11.5% on 18.1.89 (report #89-045) at 830-860 yards from test-start, and 13.5% at 60-90 yards from test-start on 4.4.89 (report #89-286D). The rope moved through the sensor-head in opposite directions on these two occasions. The test-chart from the first date is reproduced in Fig. 1e, and from the second in Fig. 1f. The rope lengths tested were reported to be 908 yards and 944 yards, respectively. The latter length seems excessive, presumably due to the uncertainty introduced by a change of the magnetic tape during testing. The operator marked the 11.5% LMA_{max} reading on the 18.1.89 chart. None of the other LMA readings were marked. We added our own marking of: (a) the 0% LMA reference level, and (b) the characteristic flaw locations #1 to #11, inclusive, to both charts (Figures 1e and 1f). In both figures the three broken wires (flaws #9 to #11) are conspicuous at the drum-end of the rope. These locations could not be EM tested in the field. It will be noted that only some 630 yards were EM tested in the field (Fig. $1d_1$) vs some 908 yards on the shop-floor (Fig. 1e). Comparing the in situ and the shop-floor results further, we also noted that the %LMA difference between the conveyance- and drum-rope-ends was about 4.0% in the field (Fig. $1d_1$) vs 5.0% (Fig. 1e) and even 7.0% (Fig. 1f) on the shop-floor. In other words, the %LMA data recorded in situ should, in fact, be increased by, at least, another 1.0% (or possibly even 3.0%), due to the fact that the "best" rope section itself had a 1.0% (or even worse) loss-of-metallic-area relative to an inaccessible rope segment. It is unclear to us why there should have been a 2.0% LMA difference between the chart-readings at the conveyance-rope-ends in Figures 1e and 1f. We assume that a human error of improper instrument calibration, in one case or the other, was the cause.

The question often arises as to how useful, and instructive, the LBS test results are from those tests that are routinely obtained — on a mandatory basis — with rope samples cut from the conveyance-end of an operational hoist-rope. In the present case the difference between the %LMA chart-readings at the conveyance-rope-end and at the "worst" rope segment (i.e., at rope-flaws #1b and #2a) is: (a) 5.0% for the in situ situation (Fig. $1d_1$), and (b) 5.5% (Fig. 1e) or 7.5% (Fig. 1f) for the shop-floor situation. Assuming that the %LMA chart-readings are directly proportional to the corresponding "true" LBS data, we conclude that, in the present case, a destructive test at the conveyance-rope-end would suggest that the rope is some 5.0% to 7.5% stronger than it actually is.

Except for the drum-rope-end noted in Fig. 1f, the operator omitted to indicate the location of the seizing-wire rope-markers on his shop-floor charts. LBS estimates for both the 18.1.89 and 4.4.89 test runs were submitted, however. We shall discuss the operator's algorithm for obtaining the LBS estimates in a future report. At this time we only wish to mention that the calculations were based on a consideration of both the LMA and the LF chart-traces, including the instrument's sensitivity setting. This is indicated in the relevant chart-segments (Figures $1e_1$ to $1e_5$, inclusive) for the 18.1.89 test run. As marked in these figures, the %LBS estimates at chart-locations 455 yard (flaw #6); 521 yard; 609 yard (close to flaw #4); 722 yard; and 844 yard (flaw #2a), are as follows (together with the corresponding %LMA chart-readings in brackets): 16.2% (8.5%); 10.7% (7.5%); 8.3% (6.0%); 12.9% (7.5%); and 18.5% (11.0%), respectively.

The operator also submitted LBS estimates for the 4.4.89 test-run (report #89-286D). In this case, for the 52.5, 58.0, 62.5, 68.5, and 81.0 yard chart-locations (Fig. 1f). These rope-segments contained the following flaws: #1a; #1b; #2; #2a; and #3. The LBS estimates were: 20.7%; 24.2%; 25.5%; 23.0%; and 22.2%, respectively.

The Rotesco AC data

Shop-floor testing with the Rotesco AC was performed on 3.4.89. The rope length tested was 2,730 ft. The operator reported an LMA_{max} of 13.0% some 225 ft from the test-start (Fig. 2b). Applying a conversion factor of 1.53, a corresponding 19.9% LBS was estimated. The 0% LMA reference level was placed at the 2,730 ft tested rope-end.

We cut, realigned, and marked the operator's test-chart (Fig. 2c) — notably with the 0.0% LMA reference level and the characteristic flaw locations #1 to #8 — for a clearer overview of rope-conditions. It was not possible to locate the position of rope-flaws #9 to #11, since the Rotesco AC instrument only records the %LMA trace, and also because of the relatively slow strip-chart advance, which results in a crowded sequence of events.

Apart from reading an LMA_{max} of 14.0% at 225 ft from the start of the test (vs the operator's 13.0%) we agreed with the report submitted.

The Rotescograph data

Shop-floor testing with the Rotescograph was performed on 5.4.89 (actually, this date was wrongly noted on the test-chart. It should have been 4.4.89), and on 10.4.89. The respective instrument charts are reproduced in Figures 3b and 3c. The rope lengths tested were 2,880 ft and 2,668 ft. The rope moved in opposite directions on these two occasions. The operator marked the seizing-wire rope-locations and the footages on both charts. However, LMA chart-readings were added only to the 10.4.89 chart. In addition a report was submitted only for the latter test-run. In this the LMA_{max} was quoted at 7.6% at 2,465 ft from test start. Other LMA readings were reported as follows: 0.0% (at 30 ft); 0.4% (at 55 ft); 0.8% (at 185 ft); 2.6% (at 960 ft); 4.8% (at 1,160 ft); 5.8% (at 1,200 ft); 6.4% (at 1,260 ft); 6.2% (at 1,305 ft); and 6.6% (at 1,380 ft). We agree with these chart readings.

We added our own markings to Figures 3b and 3c, notably the 0% LMA level, and the flaw-locations #1 to #11, inclusive. It may be noted that flaws #8, #7, #6, #5, and #1b−#2 coincided with the 960 ft, 1,260 ft, 1,305 ft, 1,380 ft, and 2,465 ft rope-locations, respectively, chosen by the operator for the abovenoted LMA chart readings.

The operator also submitted LBS estimates. These were calculated by doubling the respective LMA chart readings at the corresponding rope-locations.

The three broken wires at the drum-rope-end (flaws #9 to #11) are much in evidence on both the LMA and the LF traces, in both Figures 3b and 3c.

The LMA-250 data

Shop-floor testing with the LMA-250 instrument was performed on 18.1.89 (Fig. 4c) and on 4.4.89 (Fig. 4d). The rope lengths tested were 2,700 ft and 2,790 ft, respectively. The operator did not mark the chart, or submit a report, for the 18.1.89 test run. We marked Fig. 4c with: (a) the 0% LMA level, (b) the footages tested, (c) the LMA_{max}, and (d) with the location of rope-flaws #1 to #11, inclusive. It is unclear why the 100% reference level in Fig. 4c was not at the drum-rope-end, as it was on all the other charts (except for Fig. 1c).

With the 4.4.89 chart (Fig. 4d) the operator did submit a report, besides marking on the chart: (a) the 0% LMA level, (b) the location of the seizing-wire rope-markers, (c) the footages tested, and (d) the respective (as per the report) LMA chart readings. We have added the location of rope flaws #1 to #11, inclusive. We agree with the operator's chart readings.

The operator's report referred to broken wire indications in the corroded rope section between markers M1 to M8. The three broken wires at the drum-rope-end (flaws #9 to #11) are much in evidence.

The WBK data

Shop-floor testing with the German WBK instrument was undertaken on 10.4.89 — side-by-side with the second Rotescograph test-run. The rope length tested was 2,867 ft (874 m). The strip-chart contains, reading from top-to-bottom: five LF traces, a %LMA trace, and a length indication scale (in meters). There is also space for a second %LMA trace (e.g., note 'Fig. 7.27' of our Fig. 5), and for a rope-diameter indication-trace (not used in the current test-series). With the sensor-head closed, the individual measuring coils LF #1 and LF#2 are joined together, and so are #3 and #4. The fifth LF chart-trace summarizes the output of these two individual traces.

The operators carefully annotated their charts, including the seizing-wire markers (M1 to M12), besides submitting written reports. Where feasible, we added the location of the characterisitic rope defects #1 to #11.

We did not receive a copy of the complete strip-chart. Instead copies of the important chart sections were submitted, numbered Figures 7.1 to 7.32, inclusive. We reproduce these as our Fig. 5. As may be seen, the 0.0% LMA reference level was set along the 2m–5m rope section, and the %LMA scale was 0.353% per mm of diagram ('Fig. 7.1' of our Fig. 5).

We include the %LMA chart-readings in Table 1b, and the defect distances in Table 3b. The German report also included a tabulation of the M1 to M12 marker locations. It is interesting to note that the tabulated distances between these markers was almost consistently 76 m (249.3 ft). The corresponding 'true' distance was 250 ft.

DESTRUCTIVE TESTING

Three 16-ft samples were cut from our rope #7 for destructive testing. From these, contiguous samples, each 8-ft long, were used for destructive testing, and for external and internal visual inspection. Results of the latter work are not yet available.

The general test procedure has been described and illustrated elsewhere (6).

The samples were designated as sample #7a, #7b, and #7c. With reference to Fig. 1f:

Sample #7a: cut from defect #2a rope-segment (at 78 yard chart marking in Fig. 1f), i.e., from rope section containing an LMA chart-reading of 14.5% per Fig. 1f (or 11.5% per Fig. 1e);

Sample #7b: cut from 769–785 ft rope segment (at 256–262 yard chart marking), i.e., from rope section containing an LMA chart-reading of 11.0% per Fig. 1f (or 8.5% per Fig. 1e);

Sample #7c: cut from drum-end of rope, i.e., from rope section containing the 0%LMA reference level. In the field this rope section was always on the drum. Its EM chart trace shows no evidence of broken wires or of corrosion.

Destructive testing was performed in the laboratories of Wire Rope Industries (WRI) Ltd., at Pointe Claire, Quebec. Standard procedures were followed, as monitored by Messrs. G. Rousseau (of CANMET) and R. Boles (of WRI).

As mentioned before, the original breaking strength of our rope #7 was determined by the Rope Testing Laboratory of the Ontario Ministry of Labour, in Toronto. According to their test certificate #66583 of 4.11.86 it was found to be 261,500 lb.

The test results were as follows:

Sample #7a: 218,500 lb, i.e., a loss of 16.0% of the original 261,500 lb strength, at a point where the maximum LMA chart reading is 14.5% (Fig. 1f). The sample diameter was 1.520 in.;

Sample #7b: 250,000 lb, i.e., a loss of 4.0% of the original 261,500 lb strength, at a point where the maximum LMA chart reading is 11.0% (Fig. 1f). The sample diameter was 1.525 in.;

Sample #7c: 240,000 lb, i.e., a loss of 8.0% of the original 261,500 lb strength, at a point where the maximum LMA chart reading is 0.0% (Fig. 1f). The sample diameter was 1.560–1.610 in.

The conditions of the broken samples are illustrated in Figures 11–13. These were as follows:

Sample #7a: complete break at cone. Heavy wear and heavy rust. Breaks were partly tensile- and partly shear-failures. The recoil at rope-failure exposed completely, or nearly completely, rusted fillers and inners;

Sample #7b: three strands broke at sample-centre. The general appearance of this sample was the same as that of sample #7a. Breaks were mostly tensile-failures, with some shear-failures at the notches;

Sample #7c: several strands broke at cone. The sample showed minimum wear and good lubrication. The appearance was somewhat oval, with some crushing.

The results of sample #7c seem to be misleading, presumably due to sample-failure at the cone. Otherwise it is hard to understand why this sample should show a greater LBS than does sample #7b — unless there might, perhaps, have been a mix-up in reporting the test-results for samples 7b and 7c.

ANALYSIS OF TEST RESULTS

(1) Repeatability and general comments

We tabulated the in situ chart-readings in Table 1a, and the shop-floor ones in Table 1b. The details of all relevant test set-ups are listed in Table 2.

Our comparisons are based on a number of characteristic rope-defects — identified as #1 to #11 flaws. It is easy to locate them, mostly by their characteristic LMA traces, i.e., "fingerprints" (Figures 1–8), and by the consistency of their location on the distance counter along the chart-edge (Tables 3a and 3b). In case of flaws #9 to #11 the conspicuous perturbation of the LF traces should also be noted.

As mentioned in previous reports (5, 6, 8, 9) the repeatability of the EM test-charts, *per se*, is quite remarkable. This is documented in Figures 6 to 9 — in which we compared the characteristic rope flaw-sections of Figures 1 to 4 — and in the juxtaposition of Fig. 10. Unfortunately, the corresponding %LMA chart-readings are not equally consistent (Table 1b). We believe that this is due, primarily, to human, rather than to instrument related, causes.

(2) LMA chart readings

On reviewing the LMA chart-readings, we noted the following:

Table 1a (in situ tests): it is interesting to note that several of the characteristic rope flaws are already clearly present in the Magnograph test-chart trace (Fig. 1c) obtained on 13.4.88, less than a year after the initial EM testing of this rope.

Unfortunately, the Rotescograph and Rotesco AC field operators only reported to us their LBS estimates. The listed LMA data are, therefore, our own chart-readings. We have noted in earlier reports (6, 8) that the Rotesco AC's LMA chart-readings are below the ones obtained with the other EM instruments. On this occasion the Magnograph's LMA chart-readings are also well below those of the Rotescograph and of the LMA-250. The difference between these various LMA chart-readings is unacceptably large, insofar as it exceeds, in many cases, the ±2.0% range that we set as a benchmark level in an earlier report (5). Moreover, in Fig. 4b it was noted that the "true" 100% reference level was not even available on the instrument chart submitted to us.

Apart from the %LMA readings at the eight characteristic rope defect locations, we also noted the %LMA difference between the two rope ends. Here again the data-range is unacceptably large. It is uncertain whether this is due: (a) to improper instrument calibration, (b) to difficulties with properly setting the 100% reference level, and/or (c) to zero drift along the LMA trace.

Table 1b (shop-floor tests): in this case the difference between the %LMA chart-readings of the various instruments is again unacceptably large.

It may be noted that the German operators were the only ones to record the use of calibration rods during these test-runs ('Fig. 7.1' of our Fig. 5). With their special LF channel arrangement the location of the seizing-wire markers M1–M12 (note that these are surface flaws) is very noticeable, even in badly corroded rope sections (e.g., M11 in 'Fig. 7.28' of our Fig. 5). As a result it is also easy to pick out at these locations the corresponding LMA peaks. Interestingly, the +1.34% LMA chart-reading at the 103–105 m location ('Fig. 7.8' of our Fig. 5), conspicuous on both the LF and LMA traces of the WBK strip-chart, is noticeable only on the LF trace of the corresponding Rotescograph chart (Fig. 3c).

In addition, one may note: (a) the low LMA readings on the Rotescograph chart, and (b) the excessive differences in the Magnograph and the LMA-250 chart-readings that were obtained by the same operators on two separate occasions under identical circumstances, with identical instruments, and on the same rope. In case of the LMA-250 the location of the 100% reference level in Fig. 4c seems questionable.

Since the 'best' rope section is at the drum-end, we again, as in Table 1a, added readings of the %LMA differences at the two rope-ends. The range is unacceptably large.

In view of the unacceptably wide %LMA range in both Tables 1a and 1b, it is uncertain how well the "true" in situ and shop-floor %LMA chart-readings, *per se*, compare. We suggest, though, that the present results confirm our previous statement (6, 7, 8) to the effect that the two readings can be legitimately compared. This is borne out by our theoretical examination of the situation, as discussed later in this report.

Table 2 (details of testing): it is interesting to note details of the very wide-ranging series of test-runs we were able to perform on our rope #7.

(3) Accuracy of tested rope-length indications

In Tables 3a and 3b we tabulated the footage readings on the instrument-charts at the various characteristic defect locations along the rope. As stated elsewhere (9), it is remarkable how well these length-readings match each other. Since the rope passed through the sensor-heads in different directions on different occasions, and since the overall tested rope lengths differ on the various charts, the accuracy of the footage readings is easier to observe by comparing the distances between the various flaws, rather than their distances from the test-starts.

(4) LBS estimates

We tabulated the operators' LBS estimates, the "true" LBS data, as well as related data, in Tables 4a and 4b.

The Rotesco AC, Rotescograph, and Magnograph operators submitted estimates, while none were received from the LMA-250 operators. As mentioned earlier in this report: (a) the Magnograph operator's estimates were based on a consideration of both the LMA and LF chart-traces, in conjunction with the sensitivity settings used, (b) the operator of the shop-floor Rotescograph doubled the respective LMA chart-readings to obtain the corresponding LBS estimates, (c) the shop-floor Rotesco AC operator used an LMA to LBS conversion factor of 1.53, and (d) the operators of the Rotescograph and Rotesco AC instruments in the field did not explain to us their method for obtaining LBS estimates. We assume, though, that they too used conversion factors. An examination of their %LBS to %LMA ratios in Table 4a indicates that, on the whole, the factor in case of the Rotesco AC field data is in the order of 2.3–2.5, and in case of the Rotescograph field data the factor, in general, is 1.7–1.9.

On comparing the estimated and "true" LBS data in Table 4b we note that the 16.0% LBS of sample #7a is the only one that supports the corresponding estimates. The sample #7b and #7c test results — i.e., the 4.0% and 8.0% values — are unacceptable unless, perhaps, the destructive test-results themselves are questionable.

(5) Comparability: in situ vs shop-floor test results

The question of how comparable in situ and reel-to-reel EM results are is of considerable interest. In case of the LF chart-trace one can say that: (a) the broken wire-ends are further apart when the rope is heavily loaded, as compared to when it is under no load; consequently some breaks might be overlooked in the no-load case. However, the true number, and locations, of the local faults is the same in each case.

The situation with the%LMA chart-readings is less straightforward. Currently, the LMA readings are always relative ones, i.e., any "local" chart-reading is a value relative to the situation at the "best" rope segment, at the time of investigation. But how is this metallic-area ratio of the "best" to "local" rope-segments affected, as the loading on the rope changes? Our answer is that within the accuracy limitation of current EM testing-techniques, and within the range of rope sizes and rope loadings that are of practical interest, this ratio is unaffected. This is illustrated in Tables 5a to 5f. Here we list the %Error that arises when measuring %LMA, at the same location, once at no-load and once at full-load conditions — or vice versa. In other words, if the tabulated error is, say, 0.15%, then a 9.0% LMA reading in one case will be a 9.0% ±0.15% LMA reading in the other case. In Tables 5a to 5f we used metallic-cross-sectional areas that — according to manufacturers' catalogues — apply, approximately, to various rope sizes and constructions of practical interest. The top loads (P) and metallic-area-ratios (α) are in excess of any practical situations. However, we included them in order to make the trend clearer; namely that the error increases as the rope-loading increases, and as the rope-size decreases. This trend is also illustrated in graphical representations (Figures 14a to 14c).

The values in Tables 5a to 5f were calculated from the following equation:

$$\text{Error } (\%) = \alpha \times \left[1 - \frac{1 - \frac{2X}{\alpha} + \left(\frac{X}{\alpha}\right)^2}{(1-X)^2} \right] \times 100$$

Where:

Error = difference between %LMA readings obtained at the same "local" rope segment (a) in situ, and (b) reel-to-reel;

α = the metallic cross-sectional-area ratio (a_1/A_1) of the "local" rope segment (a_1) to that of the "best" segment (A_1), under the "original" test circumstances ("original" being whatever was measured first, be it the fully-loaded, or the un-loaded, condition); and

$X = \frac{\mu \times P}{E \times A_1}$ with:

μ = Poisson's ratio;
P = loading;
A_1 = metallic cross-sectional-area of wire-rope;
E = Young's modulus.

It follows from this equation: (a) that the Error = 0 if X = 0 (no loading), or if $\alpha = 1$ (no rope defect); (b) that the Error is a maximum, with $\text{Error}_{max} = \alpha$, if $\frac{X}{\alpha} = 1$; and (c) that the Error increases with decreasing A; with incrasing P; and with decreasing α.

A step-by-step derivation of foregoing %Error equation is given in Appendix 2.

REFERENCES

1. Geller, L.B.; Udd, J.E.; and Mitchell, E.W. "Comparative evaluation of mine-shaft wire-rope NDT instruments: a search for, and analysis of, background information — contribution to the Canada/USBM/Ontario MOL joint R&D program"; CANMET Division Report MRL 88-78, 139 pp; July, 1988.

2. Geller, L.B.; Anderson, G.L.; Miscoe, A.J.; and Mitchell, E.W. "The safety of mine-shaft wire-ropes — cooperative work by Canada and the U.S.A."; CANMET Division Report MRL 89-14, 28 pp; February, 1989.

3. Geller, L.B.; Udd, J.E.; Blanchard, R.; and Daniel, K.E. "About electro-magnetic wire-rope testing in New Brunswick mines, and related data"; CANMET Division Report MRL 89-40, 51 pp; October, 1989.

4. Geller, L.B.; and Rousseau, G. "Effect of trapped wire-rope debris upon an EM instrument's LMA chart-trace"; CANMET Division Report MRL 90-08, 29 pp; February, 1990.

5. Geller, L.B.; Rousseau, G.; and Poffenroth, D. "Canada/NB MDA project on mine-shaft rope testing; stranded ropes with artificial defects"; CANMET Division Report MRL 90-015, 117 pp; February, 1990.

6. Geller, L.B.; Poffenroth, D.; Udd, J.E.; and Hutchinson, D. "Canada/NB MDA project on mine-shaft rope testing; testing of 1 1/4 in., FLC, H.R. (our rope #4)"; CANMET Division Report MRL 90-044, 76 pp; May, 1990.

7. Geller, L.B.; Poffenroth, D.; Udd, J.E.; and Hutchinson, D. "Evaluation of EM rope testers: Canada/US joint work"; CANMET Division Report MRL 90-052, 24 pp; June, 1990.

8. Geller, L.B.; Poffenroth, D.; Udd, J.E.; and Hutchinson, D. "Canada/NB MDA project on mine-shaft rope testing; testing of 1 7/16 in., FLC, H.R. (our rope #5)"; CANMET Division Report MRL 90-053, 46 pp; June, 1990.

9. Geller, L.B.; Poffenroth, D.; Udd, J.E.; and Hutchinson, D. "Canada/NB MDA project on mine-shaft rope testing; testing of 1 7/8 in., 34×7, NR, T R., (our rope #9)"; CANMET Division Report MRL 90-060, 48 pp; July, 1990.

10. Geller, L.B.; Poffenroth, D.; Udd, J.E.; and Hutchinson, D. "Canada/NB MDA project on mine-shaft rope testing; testing of 1 7/8 in., 34×7, NR, T.R., (our rope #12)"; CANMET Division Report MRL 90-069, 30 pp; July, 1990.

APPENDIX 1

Calculation of difference in LMA chart-readings when EM testing wire-ropes in situ and reel-to-reel

To obtain the equation:

$$\text{Error } (\%) = \alpha \times \left[1 - \frac{1 - \frac{2X}{\alpha} + \left(\frac{X}{\alpha}\right)^2}{(1-X)^2} \right] \times 100$$

Where:

Error = difference between %LMA readings obtained at the same "local" rope segment (a) in situ, and (b) reel-to-reel;

α = the metallic cross-sectional-area ratio (a_1/A_1) of the "local" rope segment (a_1) to that of the "best" segment (A_1), under the "original" test circumstances ("original" being whatever was measured first, be it the fully-loaded, or the un-loaded, condition); and

X = $\frac{\mu \times P}{E \times A}$ with:

μ = Poisson's ratio;
P = loading;
A = metallic cross-sectional-area of wire-rope;
E = Young's modulus;

we made the assumption that, for purposes of our calculations, the wire-rope can be replaced by a solid cylindrical steel bar. With this simplifying assumption, the derivation of the equation is as follows:

Let the rope be initially unloaded, i.e., let $P=P_1=0$

With $P=P_1$, let:

A_1 = metallic cross-sectional-area of 'best' rope section, with diam (R_1) and length (L_1);

a_1 = metallic cross-sectional-area of 'worst' rope section, with diam (r_1) and length (l_1);

With rope loaded, let $P=P_2$

With $P=P_2$, let:

A_2 = metallic cross-sectional-area of 'best' rope section, with diam (R_2) and length (L_2);

a_1 = metallic cross-sectional-area of 'worst' rope section, with diam (r_2) and length (l_2);

It follows that:

$A_1 > A_2$; $R_1 > R_2$; $L_2 > L_1$; $a_1 > a_2$; $r_1 > r_2$; and $l_2 > l_1$. Also, that: $R_2 = R_1 - \delta R_1$; $r_2 = r_1 - \delta r_1$; and $r_1 = r_2 + \delta r_2$. Moreover, that: $\delta A_1 = A_1 - A_2$; $\delta A_2 = A_1 - A_2$; $\delta a_1 = a_1 - a_2$; and $\delta a_2 = a_1 - a_2$.

Consequently:

$$\frac{\delta A_1}{A_1} = \frac{\pi\left[2R_1\delta R_1 - (\delta R_1)^2\right]}{\pi R_1^2} = \frac{2\delta R_1}{R_1} - \left(\frac{\delta R_1}{R_1}\right)^2$$

But, by definition:

$$\alpha = \frac{a_1}{A_1}, \text{ and Poisson's ratio} = \mu = \frac{\delta R_1/R_1}{\delta L_1/L_1}$$

$$\text{i.e., } \frac{\delta R_1}{R_1} = \mu\frac{\delta L_1}{L_1}$$

On substitution, therefore:

$$\frac{\delta A_1}{A_1} = 2\mu\frac{\delta L_1}{L_1} - \left(\mu\frac{\delta l_1}{L_1}\right)^2 \qquad Eq\ (1)$$

where, by definition:

$$\epsilon = \frac{\delta L_1}{L_1} = \text{ strain} = \frac{stress}{Young's\ modulus} = \frac{\sigma}{E}$$

In our case: $\mu_{steel} = 0.3; E_{steel} = 215.3$ GPa, and $\sigma = \frac{P}{A_1}$. It should be noted that 1 GPa = 10^9 Pa = 10^9 N/m^2, and that 9.81 N = 1 kg$_{force}$.

Similarly, it can be shown that:

$$\frac{\delta A_2}{A_2} = 2\mu\frac{\delta L_2}{L_2} + \left(\mu\frac{\delta L_2}{L_2}\right)^2 \qquad Eq\ (2)$$

$$\frac{\delta a_1}{a_1} = 2\mu\frac{\delta l_1}{l_1} - \left(\mu\frac{\delta l_1}{l_1}\right)^2 \qquad Eq\ (3)$$

and,

$$\frac{\delta a_2}{a_2} = 2\mu\frac{\delta l_2}{l_2} + \left(\mu\frac{\delta l_2}{l_2}\right)^2 \qquad Eq\ (4)$$

If instead of initial no-load and subsequent full-load conditions, as is the case above, we reverse the process, only the signs in front of the quadratic terms need to be changed in the foregoing equations (1) to (4).

Now, by definition:

$$\text{Error} = \frac{a_1}{A_1} - \frac{a_2}{A_2} = \alpha - \frac{a_2}{A_2} = \alpha - \frac{(a_1 - \delta a_1)}{(A_1 - \delta A_1)}$$

However, remembering that:

$$\delta a_1 = a_1\left[2\mu\frac{\delta l_1}{l_1} - \left(\mu\frac{\delta l_1}{l_1}\right)^2\right] \text{ and that, } \delta A_1 = A_1\left[2\mu\frac{\delta L_1}{L_1} - \left(\mu\frac{\delta L_1}{L_1}\right)^2\right]$$

and also that,

$$\frac{\delta l_1}{l_1} = \frac{P/a_1}{E} = \frac{P/(\alpha A_1)}{E} = \frac{1}{\alpha}\frac{\delta L_1}{L_1}, \quad \text{we see that:}$$

$$\text{Error} = \alpha - \frac{a_1 - a_1\left[2\mu\frac{\delta l_1}{l_1} - \left(\mu\frac{\delta l_1}{l_1}\right)^2\right]}{A_1 - A_1\left[2\mu\frac{\delta L_1}{L_1} - \left(\mu\frac{\delta L_1}{L_1}\right)^2\right]} = \alpha - \frac{a_1}{A_1} \times \frac{\left[1 - 2\mu\frac{\delta l_1}{l_1} + \left(\mu\frac{\delta l_1}{l_1}\right)^2\right]}{\left[1 - 2\mu\frac{\delta L_1}{L_1} + \left(\mu\frac{\delta L_1}{L_1}\right)^2\right]}$$

Consequently, since

$$\alpha = \frac{a_1}{A_1}, \quad \text{and} \quad \frac{\delta L_1}{L_1} = \epsilon_1 = \frac{stress}{Young's\ modulus} = \frac{P/A_1}{E} = \alpha\frac{\delta l_1}{l_1}$$

we have:

$$\text{Error} = \alpha - \alpha \times \frac{\left[1 - 2\frac{\mu}{\alpha}\frac{\delta L_1}{L_1} + \left(\frac{\mu}{\alpha}\frac{\delta L_1}{L_1}\right)^2\right]}{\left[1 - 2\mu\frac{\delta L_1}{L_1} + \left(\mu\frac{\delta L_1}{L_1}\right)^2\right]} = \alpha\left\{1 - \frac{\left[1 - 2\frac{\mu}{\alpha}\frac{P}{A_1 E} + \left(\frac{\mu}{\alpha}\frac{P}{A_1 E}\right)^2\right]}{\left[1 - 2\mu\frac{P}{A_1 E} + \left(\mu\frac{P}{A_1 E}\right)^2\right]}\right\}$$

Finally, on substituting:

$$X = \frac{\mu \times P}{E \times A}$$

we obtain:

$$\text{Error (\%)} = \alpha \left\{ 1 - \frac{\left[1 - \frac{2X}{\alpha} + \left(\frac{X}{\alpha}\right)^2\right]}{\left[1 - 2X + X^2\right]} \right\} \text{ ....q.e.d.}$$

As an example, let: $\mu = 0.3$; $E = 215.3$ GPa; $\alpha = 0.9$; $P = 500$ metric tonnes $= 500 \times 1{,}000 \times 9.81\ \mathrm{kg}_{force}$; $A = 1.0344\ \mathrm{in}^2 = 1.0344 \times 6.452 \times 10^{-4}\ \mathrm{m}^2$.

Then:

$$X = \frac{0.3}{215.3} \times \frac{500 \times 1{,}000 \times 9.81 \times 10^{-9}}{1.0344 \times 6.452 \times 10^{-4}} = 0.01024$$

and,

$$\text{Error} = 0.9\,[1 - 0.9977] = 0.0021.$$

In this example, therefore, the Error that is committed when one measures under full-load rather than reel-to-reel conditions, is 0.21% LMA chart reading. This is well within the error limitations of current EM instruments.

APPENDIX 2

Tables 1 to 5,

as well as Figures 1 to 14, inclusive

Table 1a

LMA chart-readings — in situ tests

Rope defect	Magnograph		Rotesco AC	Rotescograph	LMA-250	
	Fig. 1c	Fig. $1d_1$	Fig. 2a	Fig. 3a	Fig. $4a_2$	Fig. 4b*
#1	—	7.6%	6.8%	10.4%	9.5%	10.7%
#1a	—	8.7%	—	10.2%	9.0%	10.7%
#1b	—	9.1%	—	11.0%	11.0%	12.4%
#2	1.7%	8.2%	8.4%	11.2%	11.5%	13.5%
#2a	—	8.7%	—	10.8%	11.0%	12.7%
#3	—	8.7%	8.0%	11.0%	12.0%	13.0%
#4	—	1.9%	2.2%	2.2%	1.5%	2.7%
#5	0.8%	7.7%	6.8%	9.4%	11.0%	11.2%
#6	—	6.9%	5.2%	8.0%	9.0%	9.2%
#7	1.0%	7.6%	5.6%	8.4%	9.4%	9.8%
#8	1.4%	2.9%	1.6%	2.8%	3.0%	3.0%
**	nil	4.0%	4.0%	5.7%	2.5%	2.5%
Rope, total chart footage	1,869	1,890	1,810	1,831	1,882	1,885

*: with "true" 100% reference level

**: difference between %LMA chart-readings at the two rope-ends

Table 1b

LMA chart-readings — shop-floor tests

Rope defect	Magnograph		Rotesco AC	Rotescograph		LMA-250		WBK
	Fig. 1e	Fig. 1f	Fig. 2c	Fig. 3b	Fig. 3c	Fig. 4c	Fig. 4d	Fig. 5
Marker*	—	0.4%	—	0.4%	0.8%	—	1.8%	4.9%
#1	9.0%	12.5%	12.0%	5.6%	6.6%	8.0%	14.0%	—
#1a	10.2%	13.5%	13.0%	6.0%	7.2%	—	16.0%	13.7%
#1b	10.5%	14.0%	14.0%	7.0%	7.6%	—	17.0%	14.8%
#2	10.6%	14.0%	14.0%	7.0%	7.6%	10.5%	17.0%	14.4%
#2a	10.7%	14.5%	12.7%	7.1%	7.7%	10.0%	17.0%	14.8%
#3	10.0%	13.7%	13.1%	6.2%	7.4%	11.5%	16.0%	14.3%
#4	2.5%	3.6%	3.8%	1.2%	1.3%	1.1%	2.0%	—
#5	9.0%	11.0%	10.2%	5.6%	6.6%	8.0%	14.8%	12.7%
#6	8.0%	10.5%	9.3%	5.2%	6.2%	6.5%	13.3%	12.3%
#7	8.5%	11.0%	10.0%	5.6%	6.4%	7.0%	14.0%	12.7%
#8	2.8%	3.8%	2.7%	2.0%	2.6%	2.5%	4.0%	4.2%
#9	—	0.5%	—	0.6%	0.9%	0.5%	1.5%	2.5%
#10	—	—	—	0.2%	—	0.2%	—	0.8%
#11	—	—	—	0.3%	0.3%	0.2%	1.0%	1.4%
**	5.0%	7.0%	4.8%	2.8%	2.4%	1.5%	6.0%	6.0%
Rope, total chart footage	2,724	2,832	2,730	2,880	2,668	2,700	2,790	2,867

*: closest to drum-end of rope

**: difference between %LMA chart-readings at the two rope-ends

Table 2

Details of EM testing of the 1 1/2 in., stranded, H.R.

Item No.	Test Instr.	Test No.	Test date	Test location	Instr. operator*	Test chart: Fig. #
1	Magnograph	#87-033A	15.6.87	in situ	(2)	1a
2	Magnograph	#87-146B	16.9.87	in situ	(2)	1b
3	Magnograph	#88-163B	13.4.88	in situ	(2)	1c
4	Magnograph	#88-383B	23.8.88	in situ	(2)	$1d_1$, & $1d_2$
5	Rotesco AC	DPQ-1	9.9.88	in situ	(1)	2a
6	Rotescograph	DPQR-1	9.9.88	in situ	(1)	3a
7	LMA-250	—	9.9.88	in situ	(3)	$4a_1$, $4a_2$, & 4b
8	Magnograph	#89-045	18.1.89	shop-floor	(2)	1e
9	Magnograph	#89-286D	4.4.89	shop-floor	(2)	1f
10	Rotesco AC	—	3.4.89	shop-floor	(4)	2b & 2c
11	Rotescograph	—	5.4.89	shop-floor	(6)	3b
12	Rotescograph	—	10.4.89	shop-floor	(6)	3c
13	LMA-250	—	18.1.89	shop-floor	(5)	4c
14	LMA-250	—	4.4.89	shop-floor	(5)	4d
15	WBK	—	10.4.89	shop-floor	(7)	5

*: (1), (3), and (7): instr. designer/maker and service company

(2) service company

(4) and (6): mining company

(5) government organization

Table 3a

In situ tests — accuracy of chart length-indications

	Distance from test-start – ft, and, in brackets, — (distance between defects – ft)				
	Magnograph	Rotesco AC	Rotescograph	LMA-250	
Rope defect	23.8.88 Fig. $1d_1$	9.9.88 Fig. 2a	9.9.88 Fig. 3a	9.9.88 Fig. $4a_2$	9.9.88 Fig. 4b
	— (87)	— (65)	— (89)	— (84)	— (90)
#1	87	65	89	1,798	90
	— (96)		— (69)	— (75)	— (75)
#1a	183		158	1,723	165
	— (16)	— (105)	— (14)	- (21)	— (19)
#1b	199		172	1,702	184
	— (14)		— (16)	— (15)	— (17)
#2	213	170	188	1,687	201
	— (18)		— (32)	— (33)	— (31)
#2a	231	— (60)	220	1,655	232
	— (39)		— (37)	— (37)	— (36)
#3	270	230	257	1,618	268
	— (633)	— (650)	— (648)	— (658)	— (662)
#4	903	880	905	960	930
	— (390)	— (352)	— (346)	— (354)	— (360)
#5	1,293	1,232	1,251	606	1,290
	— (138)	— (138)	— (135)	— (137)	— (137)
#6	1,431	1,370	1,386	469	1,427
	— (63)	— (65)	— (62)	— (63)	— (64)
#7	1,494	1,435	1,448	406	1,491
	— (327)	— (315)	— (375)	— (327)	— (329)
#8	1,821	1,750	1,761	79	1,820
	— (69)	— (60)	— (70)	— (79)	— (65)
Rope length*	1,890 ft	1,810 ft	1,831 ft	1,882 ft	1,885 ft

*: total rope length, as recorded on instrument chart

Table 3b

Shop-floor tests — accuracy of chart length-indications

	Distance from test-start – ft, and, in brackets, — (distance between defects – ft)							
	Magnograph		Rotesco AC	Rotescograph		LMA-250		WBK
Rope defect	18.1.89 Fig. 1e	4.4.89 Fig. 1f	3.4.89 Fig. 2c	5.4.89 Fig. 3b	10.4.89 Fig. 3c	18.1.89 Fig. 4c	4.4.89 Fig. 4d	10.4.89 Fig. 5
	— (48)	— (78)	— (100)	— (85)	— (91)	— (45)	— (80)	
#1	2,676	78	100	85	2,577	2,685	80	— (181)
	— (97)	— (95)	— (80)	— (100)	— (97)		— (98)	
#1a	2,579	173	180	185	2,480		178	2,686
	— (17)	— (18)		— (15)	- (16)	— (100)	— (14)	— (14)
#1b	2,562	191	— (45)	200	2,464		192	2,672
	— (12)	— (13)		— (18)	— (14)		— (14)	— (16)
#2	2,550	204	225	218	2,450	2,585	206	2,656
	— (21)	— (15)		— (17)	— (18)		— (18)	— (18)
#2a	2,529	219	— (35)	235	2,432	— (45)	224	2,638
	— (33)	— (39)		— (43)	— (37)		— (36)	— (38)
#3	2,496	258	260	278	2,395	2,540	260	2,600
	— (648)	— (663)	— (720)	— (662)	— (640)	— (645)	— (650)	
#4	1,848	921	980	940	1,755	1,895	910	— (1,020)
	— (354)	— (360)	— (290)	— (360)	— (365)	— (390)	— (355)	
#5	1,494	1,281	1,270	1,300	1,390	1,505	1,265	1,580
	— (129)	— (138)	— (130)	— (145)	— (88)**	— (130)	— (143)	— (140)
#6	1,365	1,419	1,400	1,445	1,302	1,375	1,408	1,440
	— (60)	— (62)	— (60)	— (60)	— (44)**	— (70)	— (62)	— (65)
#7	1,305	1,481	1,460	1,505	1,258	1,305	1,470	1,375
	— (312)	— (325)	— (290)	— (330)	— (298)	— (223)	— (317)	— (326)
#8	993	1,806	1,750	1,835	960	1,082	1,787	1,049
	— (838)	— (837)	— (980)	— (845)	— (774)	— (892)	— (817)	— (850)
#9	155	2,643	—	2,680	186	190	2,604	199
	— (60)	— (63)		— (63)	(60)	— (52)	— (58)	— (63)
#10	95	2,706	—	2,743	126	138	2,662	136
	— (72)	— (72)		— (75)	— (73)	— (73)	— (65)	— (74)
#11	23	2,778	—	2,818	53	65	2,727	62
	— (23)	— (64)		— (62)	— (53)	— (65)	— (63)	— (62)
Rope length*	2,724 ft	2,832 ft	2,730 ft	2,880 ft	2,668 ft	2,730 ft	2,790 ft	2,867 ft

*: total rope length, as recorded on instrument chart

**: these chart-footages are in error

Table 4a

In situ tests — LBS estimates and related data

LBS	LMA*	LMA**	chart	associated defect	
(%)	(%)	(%)	location	#	location
Magnograph; Fig. $1d_1$					
17.4	11.5	9.1	201 ft	1b	199 ft
17.6	11.0	8.7	270 ft	3	270 ft
17.1	9.0	7.0	792 ft	4	903 ft
19.2	10.0	7.7	1,290 ft	5	1,293 ft
17.7	9.0	6.9	1,431 ft	6	1,431 ft
Rotesco AC; Fig. 2a					
18.0	chart not marked	8.4 & 8.0	150−240 ft	2 & 3	170 & 230 ft
19.0		8.4	150−160 ft	2	170 ft
19.0		8.4	170−175 ft	2	170 ft
19.0		8.0	230−240 ft	3	230 ft
11.5−16.0		4.8−3.6	250−755 ft	4	880 ft
16.0−17.0		6.8	1,230−1,235 ft	5	1,232 ft
Rotescograph; Fig. 3a					
	chart not marked	11.0		1b	172 ft
18.0−20.0		11.2 & 10.8	172−227 ftt	2 & 2a	188 & 220 ft
18.0−20.0		11.0	250−266 ft	3	257 ft
21.0		11.2	193−195 ft	2	188 ft
21.0		11.0	262−264	3	257 ft
18.0		9.4	1,283−1,285 ft	5	1,251 ft
17.0−18.0		8.0	elsewhere	6	1,386 ft

*: per operator report #88-495

**: per our own chart-readings

Table 4b

Shop-floor tests — LBS estimates and related data

LBS (%)		LMA (%)		chart	associated defect	
†	††	*	**	location	#	location
Magnograph; 18.1.89; Figures 1e; and 1e$_1$ to 1e$_8$						
8.0			0.0	drum end		
	16.2	8.5	8.0	1,365 ft	6	1,365 ft
	10.7	7.5	7.5	1,563 ft	—	—
	8.3	6.0	6.0	1,827 ft	4	1,848 ft
4.0			8.5	1,989 ft		
	12.9	7.5	7.0	2,166 ft	—	—
16.0			10.7	2,553 ft		
	18.5	11.0	10.7	2,682 ft	2a	2,529 ft
Magnograph; 4.4.89 ; Fig. 1f						
	20.7		12.0	157.5 ft	—	—
	24.2	chart	13.5	174.0 ft	1a	173 ft
	25.5	not	14.0	187.5 ft	1b	191 ft
	23.0	marked	14.0−14.5	205.5 ft	2 & 2a	204 & 219 ft
16.0			14.5	234.0 ft		
	22.2		13.7	243.0 ft	3	258 ft
4.0			11.0	777.0 ft		
8.0			0.0	drum end		
Rotesco AC; Figures 2b and 2c						
	19.9	13.0	14.0	225 ft	2	225 ft
16.0			14.0	234 ft		
Rotescograph; Fig. 3c						
8.0			0.0	drum end		
	0.0		0.0	30 ft		
	0.8		0.4	55 ft		
	1.6		0.8	185 ft		
	5.2	2.6	2.6	960 ft	8	960 ft
	9.6		4.8	1,160 ft		
	11.6	5.8	5.8	1,200 ft		
	12.8	6.4	6.4	1,260 ft	7	1,258 ft
	12.4	6.2	6.2	1,305 ft	6	1,302 ft
	13.2	6.6	6.6	1,380 ft	5	1,390 ft
4.0			6.2	1,875 ft		
	15.2	7.6	7.6	2,465 ft	1b−2	2,450−2,464 ft
16.0			7.6	2,465 ft		

†: "true" LBS (destructive testing results)

††: estimates by instrument operators

*: per operator reports (#89-286D for Magnograph) and charts

**: per our own chart-readings

Table 5a

%Error, on comparing reel-to-reel with in situ %LMA chart readings: $\underline{\alpha = 0.95}$

A = 0.0540 sq. in.

P METRIC TONNES	ERROR (%)
50.	0.200
100.	0.408
150.	0.624
200.	0.850
250.	1.084
300.	1.329
350.	1.586
400.	1.852
450.	2.132
500.	2.425

A = 0.2480 sq. in.

P METRIC TONNES	ERROR (%)
50.	0.043
100.	0.086
150.	0.130
200.	0.174
250.	0.218
300.	0.263
350.	0.308
400.	0.353
450.	0.399
500.	0.446

A = 0.8380 sq. in.

P METRIC TONNES	ERROR (%)
50.	0.013
100.	0.025
150.	0.038
200.	0.051
250.	0.064
300.	0.077
350.	0.089
400.	0.102
450.	0.115
500.	0.128

A = 1.4800 sq. in.

P METRIC TONNES	ERROR (%)
50.	0.007
100.	0.014
150.	0.021
200.	0.029
250.	0.036
300.	0.043
350.	0.050
400.	0.057
450.	0.064
500.	0.072

A = 3.4020 sq. in.

P METRIC TONNES	ERROR (%)
50.	0.003
100.	0.006
150.	0.009
200.	0.012
250.	0.016
300.	0.019
350.	0.022
400.	0.025
450.	0.028
500.	0.031

A = 0.0620 sq. in.

P METRIC TONNES	ERROR (%)
50.	0.174
100.	0.353
150.	0.539
200.	0.732
250.	0.932
300.	1.139
350.	1.354
400.	1.577
450.	1.808
500.	2.049

A = 0.3380 sq. in.

P METRIC TONNES	ERROR (%)
50.	0.031
100.	0.063
150.	0.095
200.	0.127
250.	0.159
300.	0.192
350.	0.224
400.	0.257
450.	0.290
500.	0.323

A = 0.9920 sq. in.

P METRIC TONNES	ERROR (%)
50.	0.011
100.	0.021
150.	0.032
200.	0.043
250.	0.054
300.	0.064
350.	0.075
400.	0.086
450.	0.097
500.	0.108

A = 1.6100 sq. in.

P METRIC TONNES	ERROR (%)
50.	0.007
100.	0.013
150.	0.020
200.	0.026
250.	0.033
300.	0.039
350.	0.046
400.	0.053
450.	0.059
500.	0.066

A = 0.1010 sq. in.

P METRIC TONNES	ERROR (%)
50.	0.106
100.	0.214
150.	0.325
200.	0.437
250.	0.553
300.	0.670
350.	0.791
400.	0.914
450.	1.039
500.	1.166

A = 0.4400 sq. in.

P METRIC TONNES	ERROR (%)
50.	0.024
100.	0.048
150.	0.073
200.	0.097
250.	0.122
300.	0.147
350.	0.171
400.	0.196
450.	0.221
500.	0.247

A = 1.1600 sq. in.

P METRIC TONNES	ERROR (%)
50.	0.009
100.	0.018
150.	0.027
200.	0.036
250.	0.046
300.	0.055
350.	0.064
400.	0.073
450.	0.082
500.	0.092

A = 2.0400 sq. in.

P METRIC TONNES	ERROR (%)
50.	0.005
100.	0.010
150.	0.016
200.	0.021
250.	0.026
300.	0.031
350.	0.036
400.	0.042
450.	0.047
500.	0.052

$\alpha = 0.95$

A = 0.1720 sq. in.

P METRIC TONNES	ERROR (%)
50.	0.062
100.	0.125
150.	0.188
200.	0.252
250.	0.317
300.	0.383
350.	0.450
400.	0.518
450.	0.586
500.	0.655

A = 0.6880 sq. in.

P METRIC TONNES	ERROR (%)
50.	0.016
100.	0.031
150.	0.046
200.	0.062
250.	0.078
300.	0.093
350.	0.109
400.	0.125
450.	0.140
500.	0.156

A = 1.3530 sq. in.

P METRIC TONNES	ERROR (%)
50.	0.008
100.	0.016
150.	0.024
200.	0.031
250.	0.039
300.	0.047
350.	0.055
400.	0.063
450.	0.071
500.	0.079

A = 2.5530 sq. in.

P METRIC TONNES	ERROR (%)
50.	0.004
100.	0.008
150.	0.013
200.	0.017
250.	0.021
300.	0.025
350.	0.029
400.	0.034
450.	0.038
500.	0.042

Table 5b

%Error, on comparing reel-to-reel with in situ %LMA chart readings: $\underline{\alpha = 0.92}$

A = 0.0640 sq. in.

P METRIC TONNES	ERROR (%)
50.	0.329
100.	0.662
150.	0.999
200.	1.357
250.	1.732
300.	2.122
350.	2.529
400.	2.954
450.	3.396
500.	3.863

A = 0.2400 sq. in.

P METRIC TONNES	ERROR (%)
50.	0.068
100.	0.138
150.	0.208
200.	0.279
250.	0.349
300.	0.420
350.	0.492
400.	0.566
450.	0.639
500.	0.713

A = 0.5360 sq. in.

P METRIC TONNES	ERROR (%)
50.	0.020
100.	0.041
150.	0.061
200.	0.081
250.	0.102
300.	0.123
350.	0.143
400.	0.164
450.	0.184
500.	0.205

A = 1.4000 sq. in.

P METRIC TONNES	ERROR (%)
50.	0.011
100.	0.023
150.	0.034
200.	0.046
250.	0.057
300.	0.069
350.	0.080
400.	0.092
450.	0.103
500.	0.115

A = 3.4220 sq. in.

P METRIC TONNES	ERROR (%)
50.	0.005
100.	0.010
150.	0.015
200.	0.020
250.	0.025
300.	0.030
350.	0.035
400.	0.040
450.	0.045
500.	0.050

A = 0.0820 sq. in.

P METRIC TONNES	ERROR (%)
50.	0.278
100.	0.565
150.	0.862
200.	1.170
250.	1.488
300.	1.818
350.	2.161
400.	2.516
450.	2.884
500.	3.267

A = 0.3380 sq. in.

P METRIC TONNES	ERROR (%)
50.	0.050
100.	0.101
150.	0.152
200.	0.203
250.	0.255
300.	0.306
350.	0.358
400.	0.411
450.	0.464
500.	0.517

A = 0.6820 sq. in.

P METRIC TONNES	ERROR (%)
50.	0.017
100.	0.034
150.	0.051
200.	0.069
250.	0.086
300.	0.103
350.	0.120
400.	0.138
450.	0.155
500.	0.173

A = 1.5100 sq. in.

P METRIC TONNES	ERROR (%)
50.	0.010
100.	0.021
150.	0.032
200.	0.042
250.	0.053
300.	0.063
350.	0.074
400.	0.084
450.	0.095
500.	0.106

A = 0.1010 sq. in.

P METRIC TONNES	ERROR (%)
50.	0.170
100.	0.342
150.	0.518
200.	0.699
250.	0.883
300.	1.071
350.	1.263
400.	1.460
450.	1.660
500.	1.866

A = 0.4480 sq. in.

P METRIC TONNES	ERROR (%)
50.	0.038
100.	0.077
150.	0.116
200.	0.156
250.	0.195
300.	0.234
350.	0.274
400.	0.314
450.	0.354
500.	0.394

A = 1.1680 sq. in.

P METRIC TONNES	ERROR (%)
50.	0.015
100.	0.029
150.	0.044
200.	0.058
250.	0.073
300.	0.088
350.	0.102
400.	0.117
450.	0.132
500.	0.147

A = 2.0480 sq. in.

P METRIC TONNES	ERROR (%)
50.	0.008
100.	0.017
150.	0.025
200.	0.033
250.	0.041
300.	0.050
350.	0.058
400.	0.066
450.	0.075
500.	0.083

$\alpha = 0.92$

A = 0.1720 sq. in.

P METRIC TONNES	ERROR (%)
50.	0.099
100.	0.199
150.	0.301
200.	0.404
250.	0.508
300.	0.613
350.	0.719
400.	0.827
450.	0.937
500.	1.047

A = 0.5880 sq. in.

P METRIC TONNES	ERROR (%)
50.	0.025
100.	0.049
150.	0.074
200.	0.099
250.	0.124
300.	0.149
350.	0.174
400.	0.199
450.	0.225
500.	0.250

A = 1.3520 sq. in.

P METRIC TONNES	ERROR (%)
50.	0.013
100.	0.025
150.	0.038
200.	0.050
250.	0.063
300.	0.076
350.	0.088
400.	0.101
450.	0.114
500.	0.126

A = 2.5280 sq. in.

P METRIC TONNES	ERROR (%)
50.	0.007
100.	0.013
150.	0.020
200.	0.027
250.	0.034
300.	0.040
350.	0.047
400.	0.054
450.	0.061
500.	0.067

Table 5c

%Error, on comparing reel-to-reel with in situ %LMA chart readings: $\underline{\alpha = 0.90}$

A = 0.0540 sq. in.

P METRIC TONNES	ERROR (%)
50.	0.400
100.	0.815
150.	1.246
200.	1.685
250.	2.162
300.	2.648
350.	3.155
400.	3.684
450.	4.237
500.	4.815

A = 0.2480 sq. in.

P METRIC TONNES	ERROR (%)
50.	0.086
100.	0.172
150.	0.259
200.	0.347
250.	0.436
300.	0.525
350.	0.615
400.	0.706
450.	0.798
500.	0.890

A = 0.8380 sq. in.

P METRIC TONNES	ERROR (%)
50.	0.025
100.	0.051
150.	0.076
200.	0.102
250.	0.127
300.	0.153
350.	0.179
400.	0.205
450.	0.231
500.	0.256

A = 1.4960 sq. in.

P METRIC TONNES	ERROR (%)
50.	0.014
100.	0.028
150.	0.043
200.	0.057
250.	0.071
300.	0.086
350.	0.100
400.	0.114
450.	0.129
500.	0.143

A = 3.4320 sq. in.

P METRIC TONNES	ERROR (%)
50.	0.006
100.	0.012
150.	0.019
200.	0.025
250.	0.031
300.	0.037
350.	0.043
400.	0.050
450.	0.056
500.	0.062

A = 0.0820 sq. in.

P METRIC TONNES	ERROR (%)
50.	0.347
100.	0.708
150.	1.077
200.	1.461
250.	1.858
300.	2.270
350.	2.698
400.	3.139
450.	3.598
500.	4.074

A = 0.3300 sq. in.

P METRIC TONNES	ERROR (%)
50.	0.063
100.	0.126
150.	0.190
200.	0.254
250.	0.318
300.	0.383
350.	0.448
400.	0.514
450.	0.580
500.	0.648

A = 0.9920 sq. in.

P METRIC TONNES	ERROR (%)
50.	0.021
100.	0.043
150.	0.064
200.	0.086
250.	0.107
300.	0.129
350.	0.151
400.	0.172
450.	0.194
500.	0.216

A = 1.6100 sq. in.

P METRIC TONNES	ERROR (%)
50.	0.013
100.	0.026
150.	0.039
200.	0.053
250.	0.066
300.	0.079
350.	0.092
400.	0.105
450.	0.119
500.	0.132

A = 0.1010 sq. in.

P METRIC TONNES	ERROR (%)
50.	0.212
100.	0.428
150.	0.649
200.	0.874
250.	1.103
300.	1.338
350.	1.578
400.	1.822
450.	2.073
500.	2.328

A = 0.4400 sq. in.

P METRIC TONNES	ERROR (%)
50.	0.048
100.	0.097
150.	0.145
200.	0.194
250.	0.244
300.	0.293
350.	0.343
400.	0.392
450.	0.442
500.	0.493

A = 1.1690 sq. in.

P METRIC TONNES	ERROR (%)
50.	0.018
100.	0.036
150.	0.055
200.	0.073
250.	0.091
300.	0.110
350.	0.128
400.	0.146
450.	0.165
500.	0.183

A = 2.0480 sq. in.

P METRIC TONNES	ERROR (%)
50.	0.010
100.	0.021
150.	0.031
200.	0.041
250.	0.052
300.	0.062
350.	0.073
400.	0.083
450.	0.094
500.	0.104

$\alpha = 0.90$

A = 0.1720 sq. in.

P METRIC TONNES	ERROR (%)
50.	0.124
100.	0.249
150.	0.376
200.	0.504
250.	0.634
300.	0.766
350.	0.899
400.	1.033
450.	1.170
500.	1.308

A = 0.6880 sq. in.

P METRIC TONNES	ERROR (%)
50.	0.031
100.	0.062
150.	0.093
200.	0.124
250.	0.155
300.	0.186
350.	0.218
400.	0.249
450.	0.281
500.	0.312

A = 1.3620 sq. in.

P METRIC TONNES	ERROR (%)
50.	0.016
100.	0.031
150.	0.047
200.	0.063
250.	0.079
300.	0.094
350.	0.110
400.	0.126
450.	0.142
500.	0.158

A = 2.5280 sq. in.

P METRIC TONNES	ERROR (%)
50.	0.008
100.	0.017
150.	0.025
200.	0.034
250.	0.042
300.	0.050
350.	0.059
400.	0.067
450.	0.075
500.	0.084

Table 5d

%Error, on comparing reel-to-reel with in situ %LMA chart readings: $\underline{\alpha = 0.85}$

A = 0.0540 sq. in.

P METRIC TONNES	ERROR (%)
50.	0.609
100.	1.221
150.	1.866
200.	2.535
250.	3.231
300.	3.955
350.	4.709
400.	5.498
450.	6.310
500.	7.164

A = 0.2480 sq. in.

P METRIC TONNES	ERROR (%)
50.	0.129
100.	0.258
150.	0.389
200.	0.521
250.	0.653
300.	0.787
350.	0.922
400.	1.058
450.	1.196
500.	1.333

A = 0.8380 sq. in.

P METRIC TONNES	ERROR (%)
50.	0.038
100.	0.076
150.	0.114
200.	0.153
250.	0.191
300.	0.229
350.	0.2[illegible]
400.	0.307
450.	0.346
500.	0.386

A = 1.4880 sq. in.

P METRIC TONNES	ERROR (%)
50.	0.021
100.	0.043
150.	0.064
200.	0.086
250.	0.107
300.	0.129
350.	0.150
400.	0.172
450.	0.193
500.	0.215

A = 3.4320 sq. in.

P METRIC TONNES	ERROR (%)
50.	0.009
100.	0.019
150.	0.028
200.	0.037
250.	0.046
300.	0.056
350.	0.065
400.	0.074
450.	0.084
500.	0.093

A = 0.0620 sq. in.

P METRIC TONNES	ERROR (%)
50.	0.521
100.	1.058
150.	1.613
200.	2.186
250.	2.779
300.	3.392
350.	4.027
400.	4.683
450.	5.364
500.	6.069

A = 0.3380 sq. in.

P METRIC TONNES	ERROR (%)
50.	0.094
100.	0.189
150.	0.284
200.	0.380
250.	0.477
300.	0.574
350.	0.672
400.	0.770
450.	0.869
500.	0.968

A = 0.9820 sq. in.

P METRIC TONNES	ERROR (%)
50.	0.032
100.	0.064
150.	0.096
200.	0.129
250.	0.161
300.	0.193
350.	0.226
400.	0.258
450.	0.291
500.	0.324

A = 1.6100 sq. in.

P METRIC TONNES	ERROR (%)
50.	0.020
100.	0.039
150.	0.059
200.	0.079
250.	0.099
300.	0.118
350.	0.138
400.	0.158
450.	0.178
500.	0.198

A = 0.1010 sq. in.

P METRIC TONNES	ERROR (%)
50.	0.318
100.	0.642
150.	0.972
200.	1.308
250.	1.652
300.	2.003
350.	2.360
400.	2.726
450.	3.099
500.	3.479

A = 0.4400 sq. in.

P METRIC TONNES	ERROR (%)
50.	0.072
100.	0.145
150.	0.218
200.	0.291
250.	0.365
300.	0.439
350.	0.513
400.	0.588
450.	0.663
500.	0.738

A = 1.1060 sq. in.

P METRIC TONNES	ERROR (%)
50.	0.027
100.	0.055
150.	0.082
200.	0.109
250.	0.137
300.	0.164
350.	0.192
400.	0.220
450.	0.247
500.	0.275

A = 2.0490 sq. in.

P METRIC TONNES	ERROR (%)
50.	0.016
100.	0.031
150.	0.047
200.	0.062
250.	0.078
300.	0.093
350.	0.109
400.	0.125
450.	0.140
500.	0.156

$\alpha = 0.85$

A = 0.1720 sq. in.

P METRIC TONNES	ERROR (%)
50.	0.186
100.	0.374
150.	0.564
200.	0.756
250.	0.950
300.	1.147
350.	1.346
400.	1.548
450.	1.751
500.	1.957

A = 0.6880 sq. in.

P METRIC TONNES	ERROR (%)
50.	0.046
100.	0.093
150.	0.139
200.	0.186
250.	0.233
300.	0.280
350.	0.327
400.	0.374
450.	0.421
500.	0.468

A = 1.3520 sq. in.

P METRIC TONNES	ERROR (%)
50.	0.024
100.	0.047
150.	0.071
200.	0.094
250.	0.118
300.	0.142
350.	0.165
400.	0.189
450.	0.213
500.	0.237

A = 2.5280 sq. in.

P METRIC TONNES	ERROR (%)
50.	0.013
100.	0.025
150.	0.038
200.	0.050
250.	0.063
300.	0.076
350.	0.088
400.	0.101
450.	0.114
500.	0.126

Table 5e

%Error, on comparing reel-to-reel with in situ %LMA chart readings: $\underline{\alpha = 0.80}$

A = 0.0640 sq. in.

P METRIC TONNES	ERROR (%)
50.	0.798
100.	1.625
150.	2.482
200.	3.370
250.	4.281
300.	5.247
350.	6.240
400.	7.273
450.	8.348
500.	9.464

A = 0.2480 sq. in.

P METRIC TONNES	ERROR (%)
50.	0.171
100.	0.344
150.	0.518
200.	0.694
250.	0.871
300.	1.049
350.	1.228
400.	1.409
450.	1.591
500.	1.776

A = 0.6360 sq. in.

P METRIC TONNES	ERROR (%)
50.	0.051
100.	0.102
150.	0.153
200.	0.204
250.	0.255
300.	0.306
350.	0.358
400.	0.409
450.	0.461
500.	0.513

A = 1.4000 sq. in.

P METRIC TONNES	ERROR (%)
50.	0.028
100.	0.057
150.	0.085
200.	0.114
250.	0.143
300.	0.171
350.	0.200
400.	0.228
450.	0.257
500.	0.286

A = 3.4220 sq. in.

P METRIC TONNES	ERROR (%)
50.	0.012
100.	0.025
150.	0.037
200.	0.049
250.	0.062
300.	0.074
350.	0.087
400.	0.099
450.	0.111
500.	0.124

A = 0.0820 sq. in.

P METRIC TONNES	ERROR (%)
50.	0.694
100.	1.409
150.	2.146
200.	2.907
250.	3.693
300.	4.504
350.	5.342
400.	6.208
450.	7.103
500.	8.030

A = 0.3380 sq. in.

P METRIC TONNES	ERROR (%)
50.	0.126
100.	0.252
150.	0.379
200.	0.507
250.	0.636
300.	0.765
350.	0.896
400.	1.028
450.	1.157
500.	1.289

A = 0.8620 sq. in.

P METRIC TONNES	ERROR (%)
50.	0.043
100.	0.086
150.	0.129
200.	0.171
250.	0.215
300.	0.258
350.	0.301
400.	0.344
450.	0.388
500.	0.431

A = 1.6180 sq. in.

P METRIC TONNES	ERROR (%)
50.	0.026
100.	0.053
150.	0.079
200.	0.105
250.	0.131
300.	0.158
350.	0.184
400.	0.211
450.	0.237
500.	0.264

A = 0.1010 sq. in.

P METRIC TONNES	ERROR (%)
50.	0.423
100.	0.855
150.	1.294
200.	1.742
250.	2.199
300.	2.664
350.	3.139
400.	3.622
450.	4.115
500.	4.618

A = 0.4400 sq. in.

P METRIC TONNES	ERROR (%)
50.	0.097
100.	0.193
150.	0.291
200.	0.389
250.	0.487
300.	0.586
350.	0.684
400.	0.784
450.	0.883
500.	0.984

A = 1.1660 sq. in.

P METRIC TONNES	ERROR (%)
50.	0.036
100.	0.073
150.	0.109
200.	0.146
250.	0.183
300.	0.219
350.	0.256
400.	0.293
450.	0.330
500.	0.367

A = 2.0480 sq. in.

P METRIC TONNES	ERROR (%)
50.	0.021
100.	0.041
150.	0.062
200.	0.083
250.	0.104
300.	0.124
350.	0.145
400.	0.166
450.	0.187
500.	0.208

A = 0.1720 sq. in.

P METRIC TONNES	ERROR (%)
50.	0.248
100.	0.498
150.	0.751
200.	1.007
250.	1.266
300.	1.527
350.	1.792
400.	2.060
450.	2.330
500.	2.604

A = 0.5600 sq. in.

P METRIC TONNES	ERROR (%)
50.	0.062
100.	0.124
150.	0.186
200.	0.248
250.	0.310
300.	0.373
350.	0.436
400.	0.499
450.	0.561
500.	0.624

A = 1.2820 sq. in.

P METRIC TONNES	ERROR (%)
50.	0.031
100.	0.063
150.	0.094
200.	0.126
250.	0.157
300.	0.189
350.	0.220
400.	0.252
450.	0.284
500.	0.316

A = 2.5300 sq. in.

P METRIC TONNES	ERROR (%)
50.	0.017
100.	0.034
150.	0.050
200.	0.067
250.	0.084
300.	0.101
350.	0.118
400.	0.134
450.	0.151
500.	0.168

$\alpha = 0.80$

Table 5f

%Error, on comparing reel-to-reel with in situ %LMA chart readings: $\underline{\alpha = 0.75}$

A = 0.0840 sq. in.

P METRIC TONNES	ERROR (%)
50.	0.997
100.	2.028
150.	3.084
200.	4.187
250.	5.339
300.	6.522
350.	7.748
400.	9.019
450.	10.337
500.	11.706

A = 0.2480 sq. in.

P METRIC TONNES	ERROR (%)
50.	0.214
100.	0.430
150.	0.648
200.	0.867
250.	1.087
300.	1.309
350.	1.533
400.	1.759
450.	1.986
500.	2.214

A = 0.8360 sq. in.

P METRIC TONNES	ERROR (%)
50.	0.063
100.	0.127
150.	0.191
200.	0.254
250.	0.318
300.	0.383
350.	0.447
400.	0.511
450.	0.576
500.	0.640

A = 1.4800 sq. in.

P METRIC TONNES	ERROR (%)
50.	0.036
100.	0.071
150.	0.107
200.	0.143
250.	0.179
300.	0.214
350.	0.250
400.	0.286
450.	0.322
500.	0.358

A = 3.4320 sq. in.

P METRIC TONNES	ERROR (%)
50.	0.015
100.	0.031
150.	0.046
200.	0.062
250.	0.077
300.	0.093
350.	0.108
400.	0.124
450.	0.139
500.	0.155

A = 0.0920 sq. in.

P METRIC TONNES	ERROR (%)
50.	0.867
100.	1.759
150.	2.677
200.	3.623
250.	4.596
300.	5.602
350.	6.639
400.	7.707
450.	8.810
500.	9.940

A = 0.3380 sq. in.

P METRIC TONNES	ERROR (%)
50.	0.157
100.	0.315
150.	0.474
200.	0.633
250.	0.794
300.	0.956
350.	1.117
400.	1.280
450.	1.444
500.	1.609

A = 0.9920 sq. in.

P METRIC TONNES	ERROR (%)
50.	0.053
100.	0.107
150.	0.161
200.	0.214
250.	0.268
300.	0.322
350.	0.377
400.	0.430
450.	0.484
500.	0.539

A = 1.6160 sq. in.

P METRIC TONNES	ERROR (%)
50.	0.033
100.	0.066
150.	0.098
200.	0.131
250.	0.164
300.	0.197
350.	0.230
400.	0.263
450.	0.296
500.	0.330

$\alpha = 0.75$

A = 0.1010 sq. in.

P METRIC TONNES	ERROR (%)
50.	0.529
100.	1.067
150.	1.616
200.	2.174
250.	2.742
300.	3.320
350.	3.909
400.	4.510
450.	5.121
500.	5.744

A = 0.4400 sq. in.

P METRIC TONNES	ERROR (%)
50.	0.121
100.	0.242
150.	0.363
200.	0.485
250.	0.608
300.	0.731
350.	0.854
400.	0.979
450.	1.103
500.	1.228

A = 1.1600 sq. in.

P METRIC TONNES	ERROR (%)
50.	0.045
100.	0.091
150.	0.137
200.	0.182
250.	0.228
300.	0.274
350.	0.320
400.	0.365
450.	0.412
500.	0.458

A = 2.0400 sq. in.

P METRIC TONNES	ERROR (%)
50.	0.026
100.	0.052
150.	0.078
200.	0.104
250.	0.130
300.	0.156
350.	0.182
400.	0.208
450.	0.234
500.	0.260

A = 0.1720 sq. in.

P METRIC TONNES	ERROR (%)
50.	0.310
100.	0.622
150.	0.936
200.	1.258
250.	1.580
300.	1.906
350.	2.236
400.	2.568
450.	2.906
500.	3.246

A = 0.6960 sq. in.

P METRIC TONNES	ERROR (%)
50.	0.077
100.	0.154
150.	0.232
200.	0.310
250.	0.387
300.	0.465
350.	0.544
400.	0.622
450.	0.701
500.	0.780

A = 1.3620 sq. in.

P METRIC TONNES	ERROR (%)
50.	0.039
100.	0.078
150.	0.118
200.	0.157
250.	0.197
300.	0.236
350.	0.276
400.	0.315
450.	0.355
500.	0.394

A = 2.5200 sq. in.

P METRIC TONNES	ERROR (%)
50.	0.021
100.	0.042
150.	0.063
200.	0.084
250.	0.105
300.	0.126
350.	0.147
400.	0.168
450.	0.189
500.	0.210

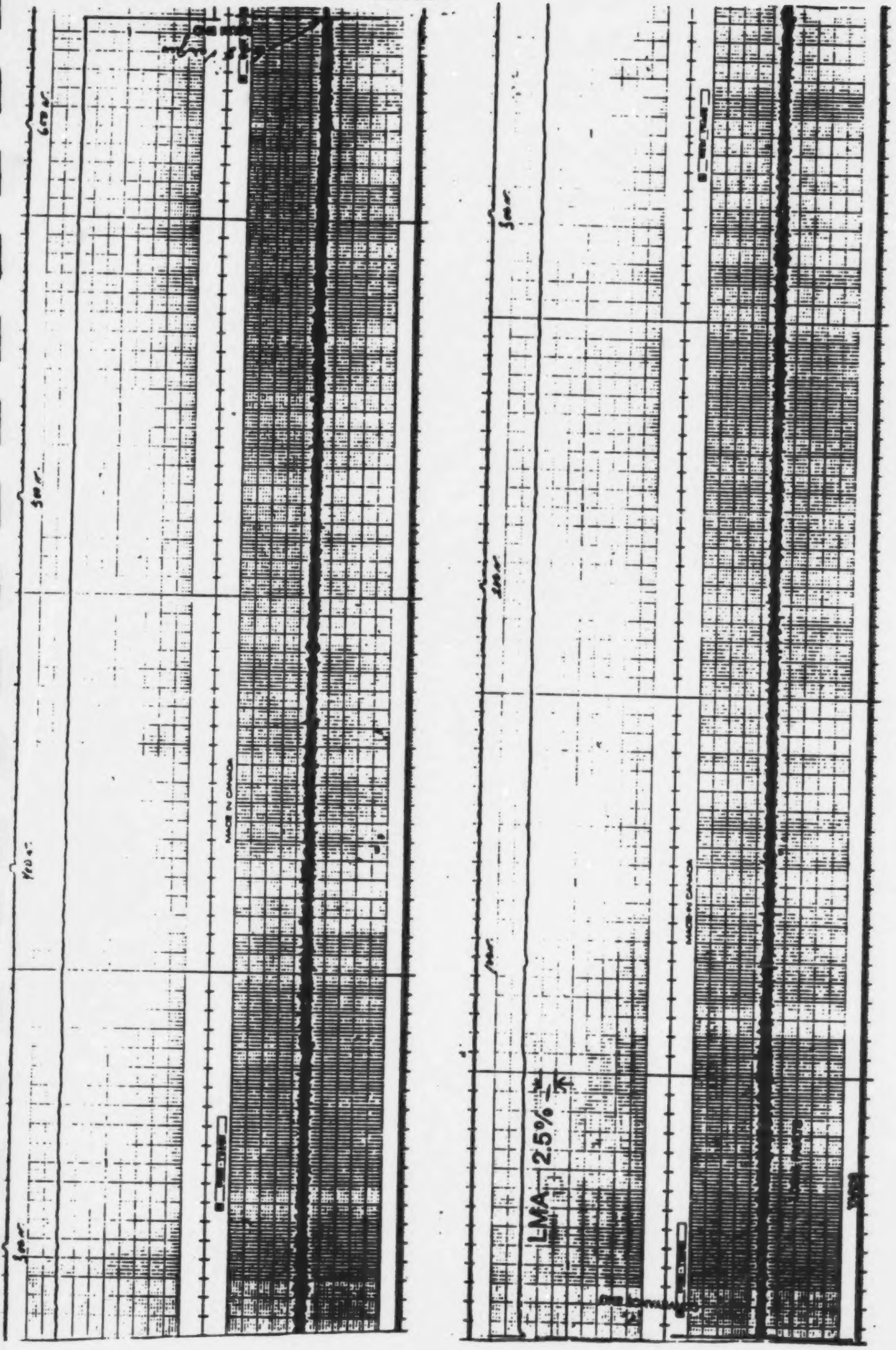

Fig. 1a — 15.6.87 in situ Magnograph test

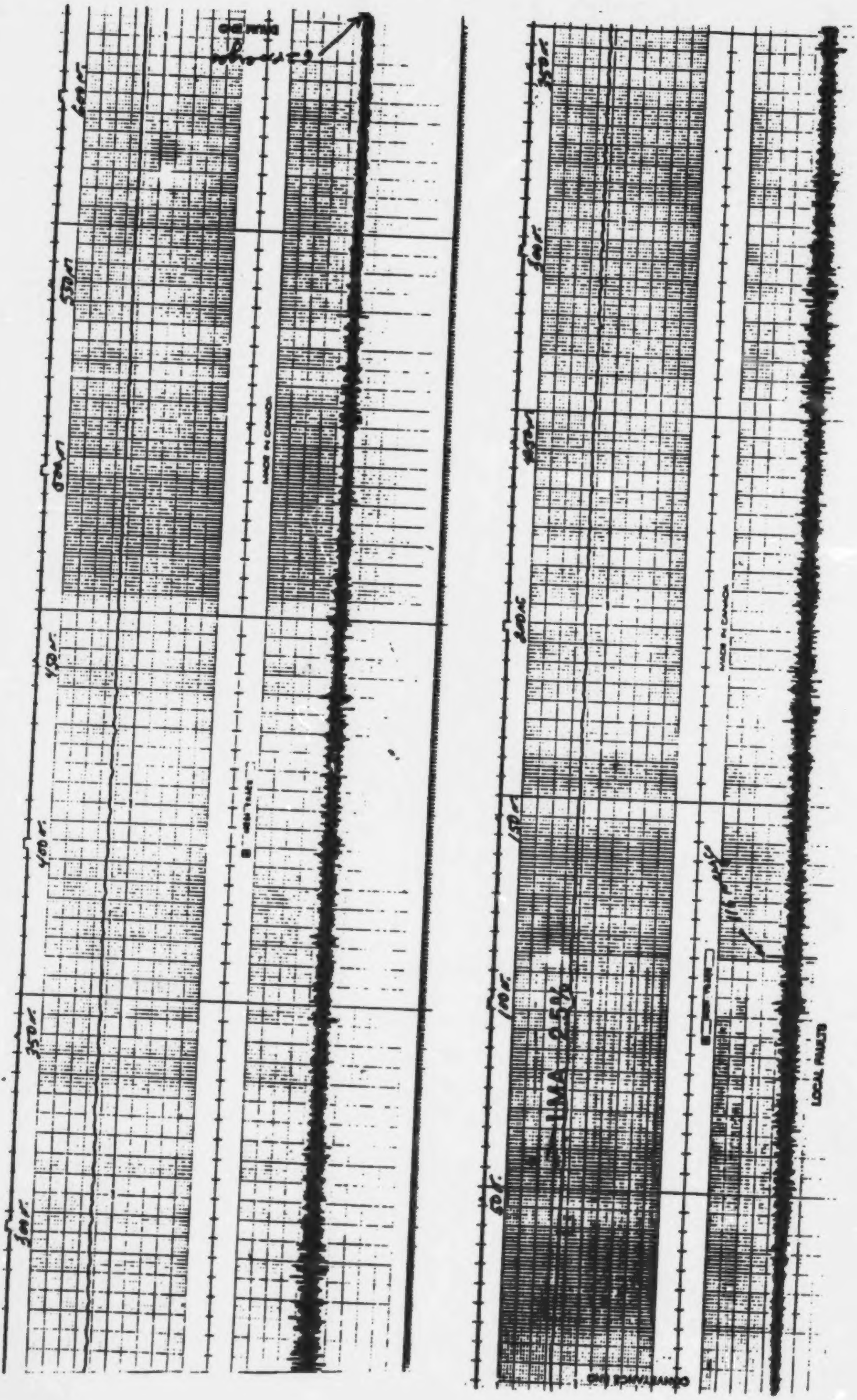

Fig. 1b — 16.9.87 in situ Magnograph test

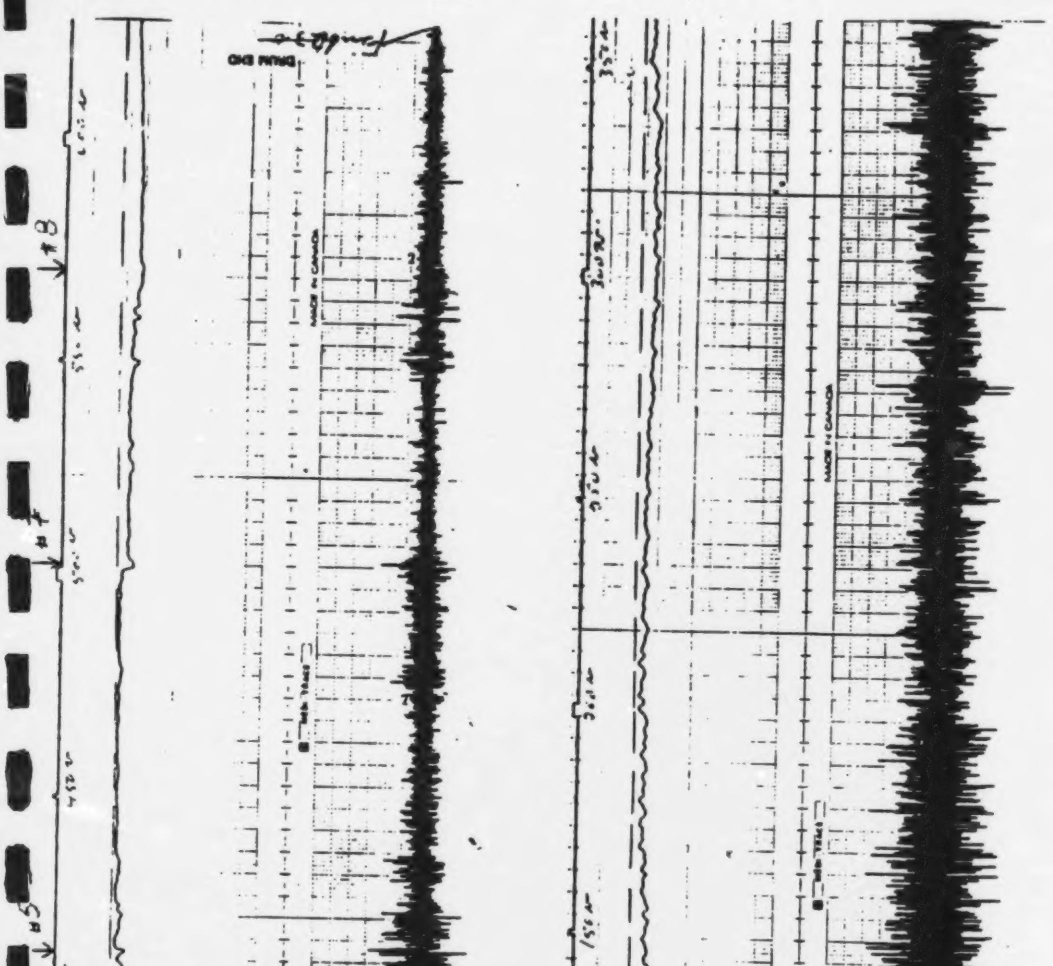

Fig. 1c — 13.4.88 in situ Magnograph test

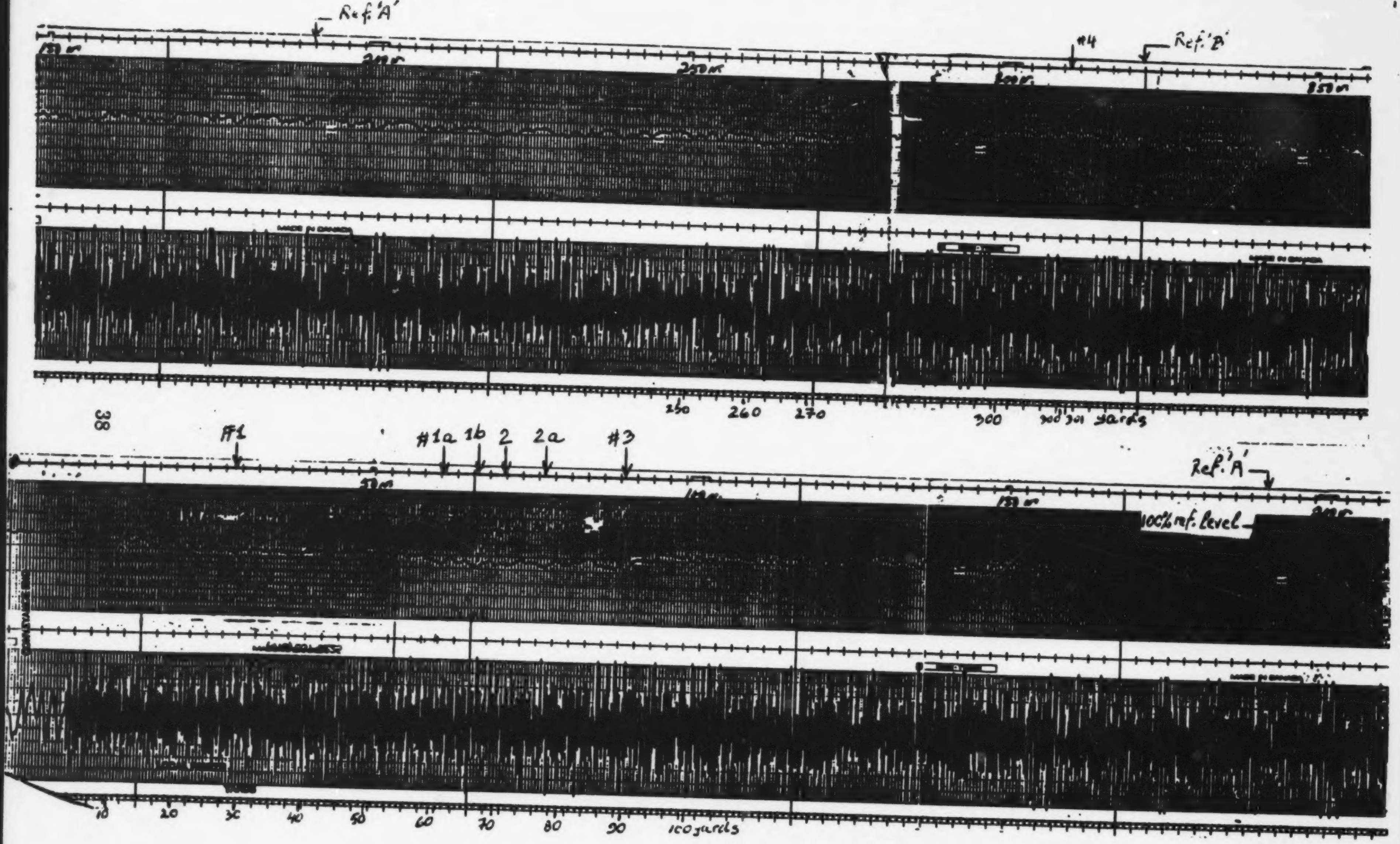

Fig. 1d$_1$ — 23.8.88 in situ Magnograph test — regular chart speed (100 yards/125 chart mm)

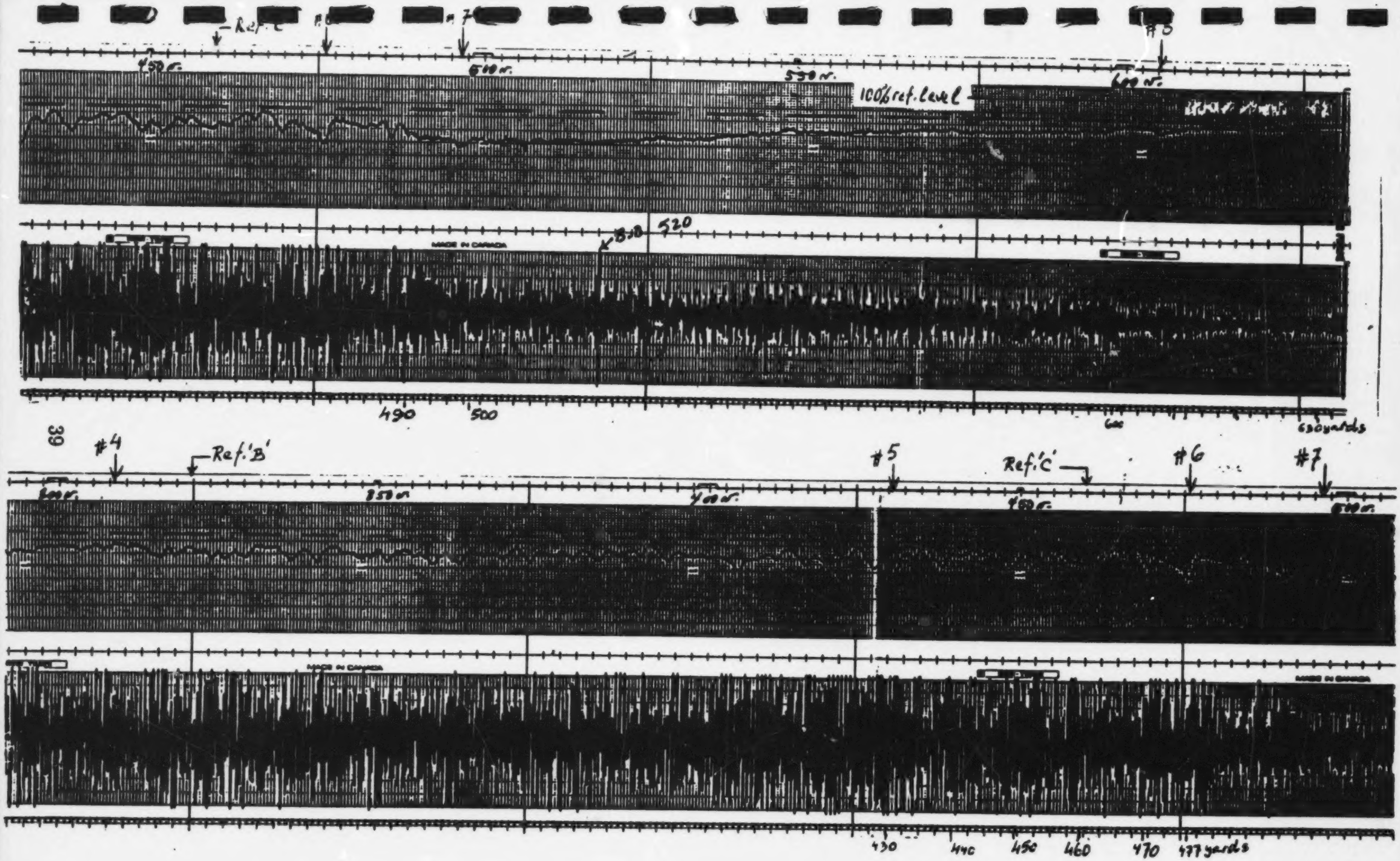

Fig. 1d₁ (continued) — 23.8.88 in situ Magnograph test — regular chart speed (100 yards/125 chart mm)

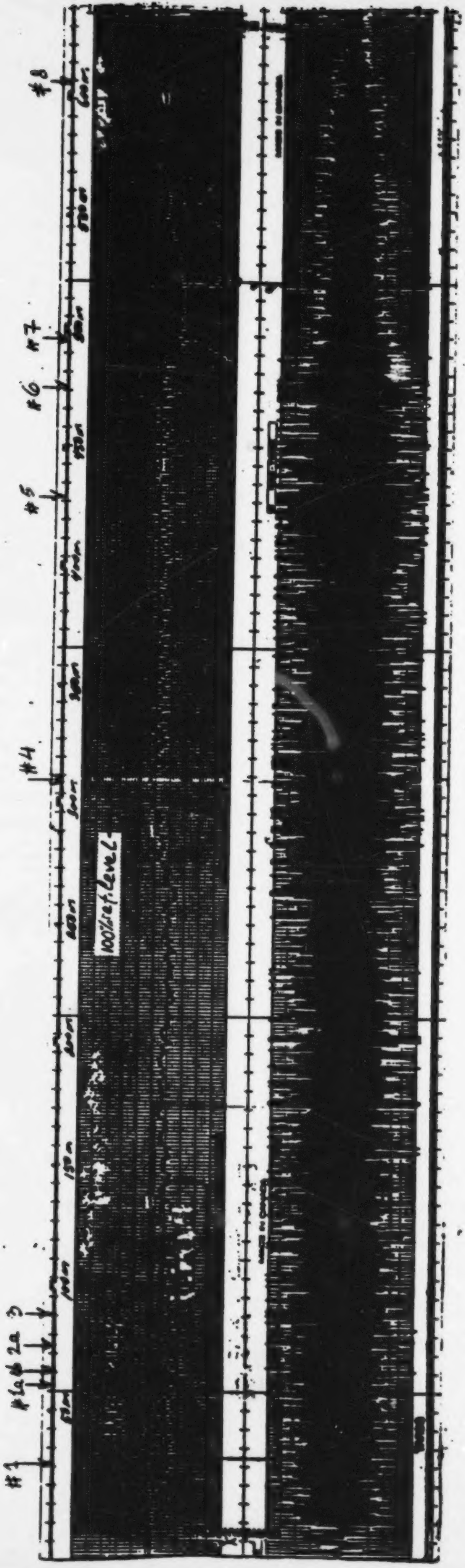

Fig. $1d_2$ — 23.8.88 in situ Magnograph test — fast chart speed (100 yards/42 chart mm)

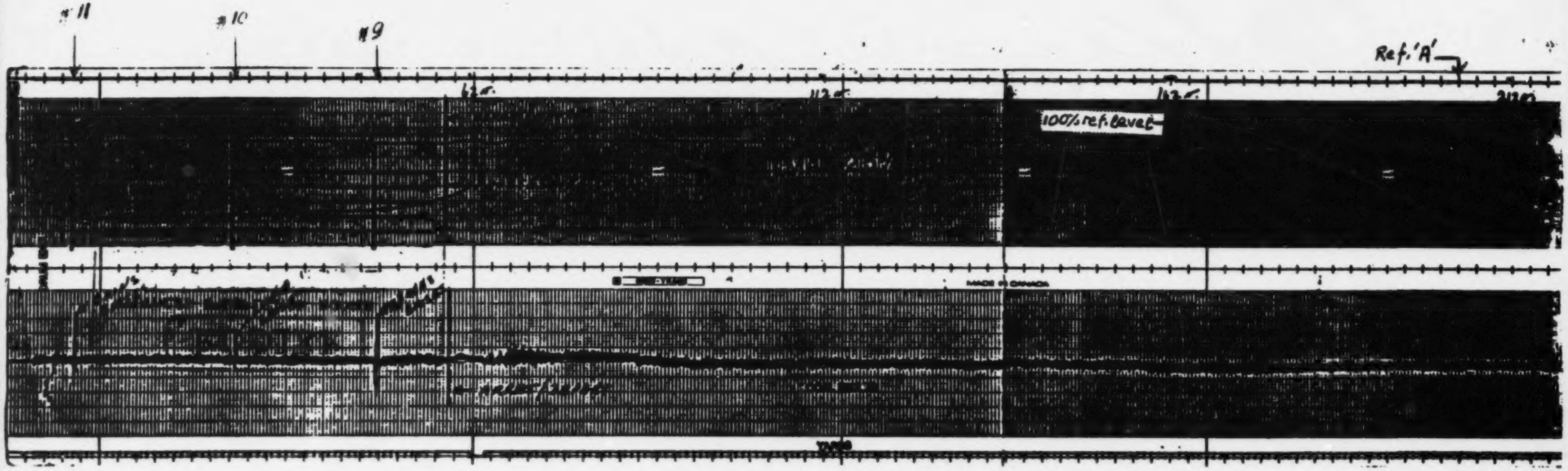

Fig. 1e — 18.1.89 shop-floor Magnograph test

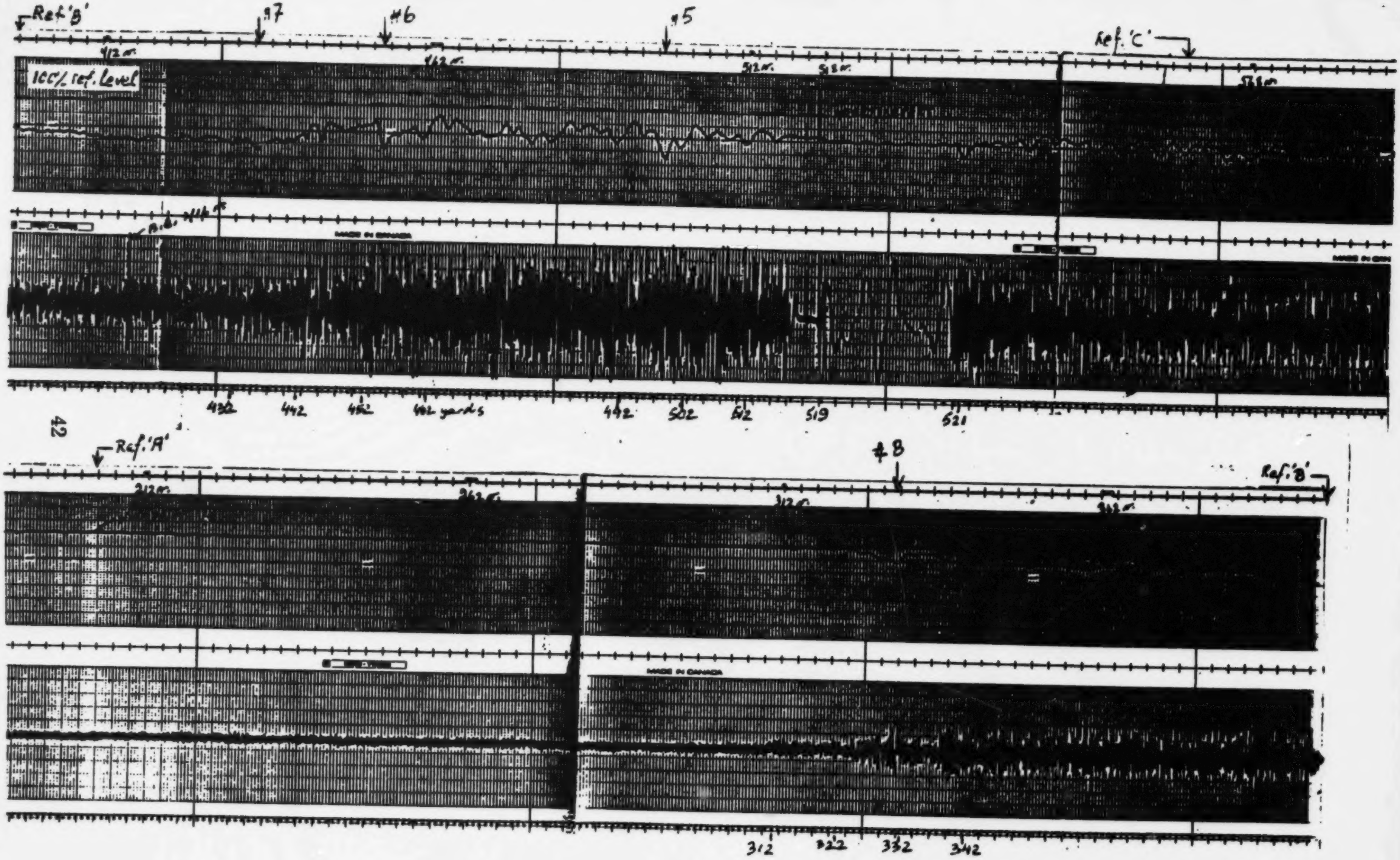

Fig. 1e (continued) — 18.1.89 shop-floor Magnograph test

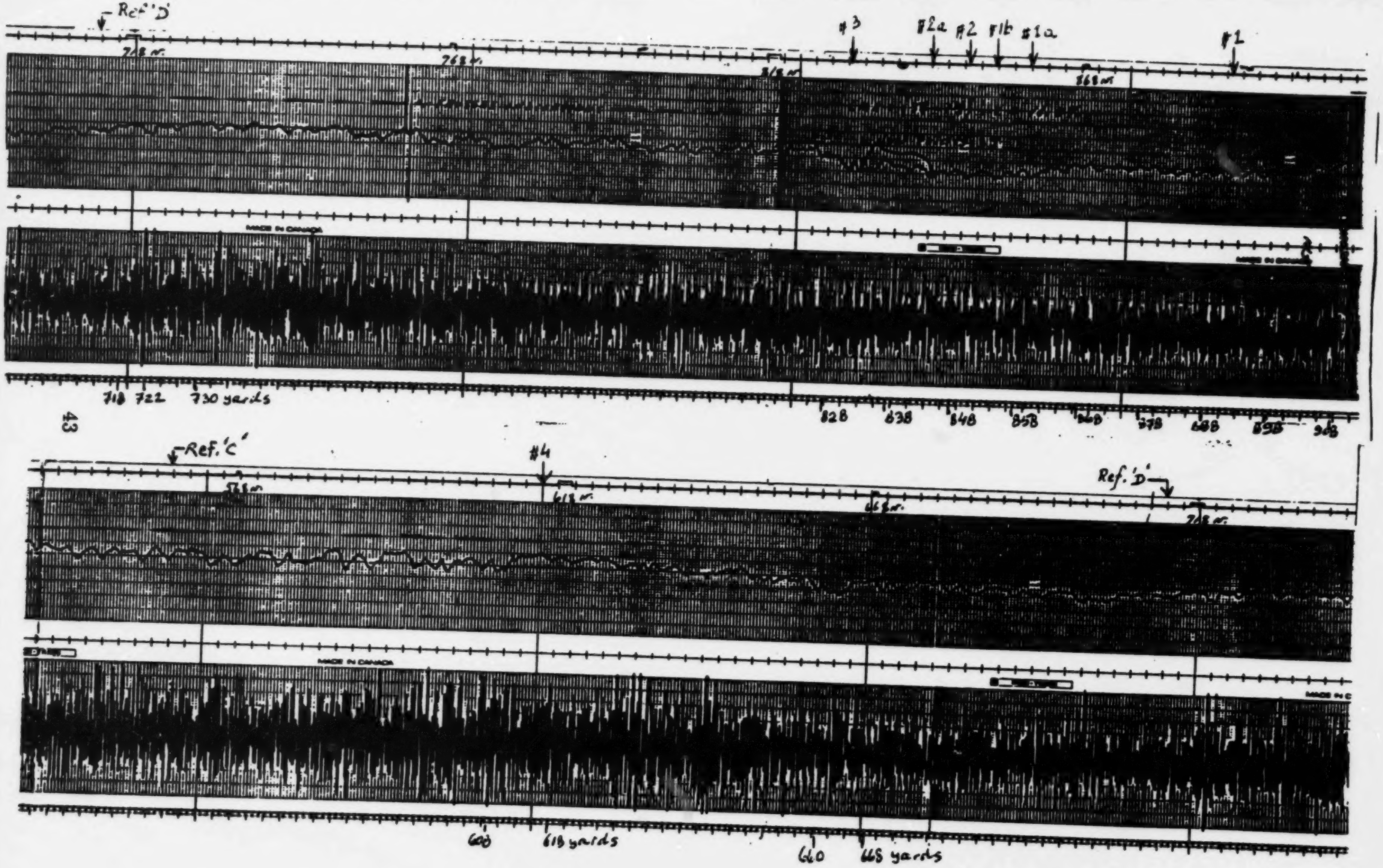

Fig. 1e (continued) — 18.1.89 shop-floor Magnograph test

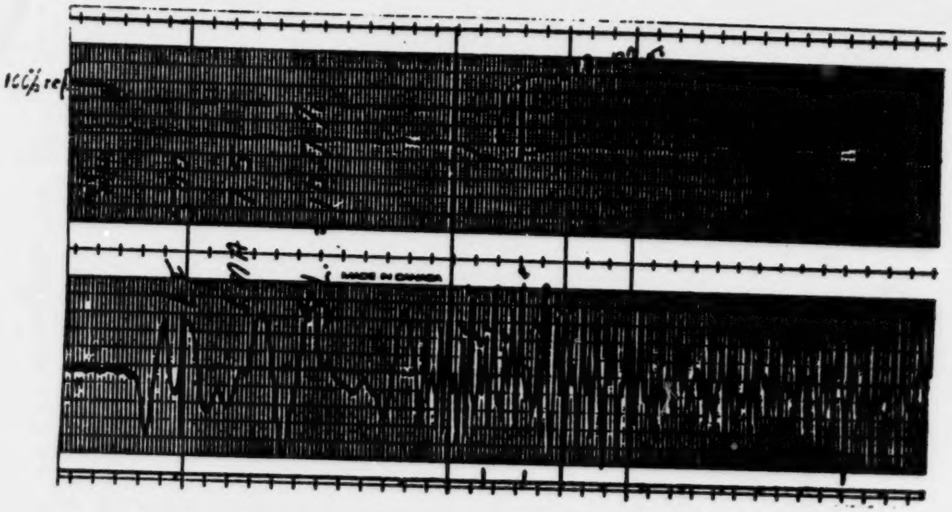

Fig. $1e_2$ — 18.1.89 shop-floor Magnograph test:

for LBS calculation of 521 yard chart- segment

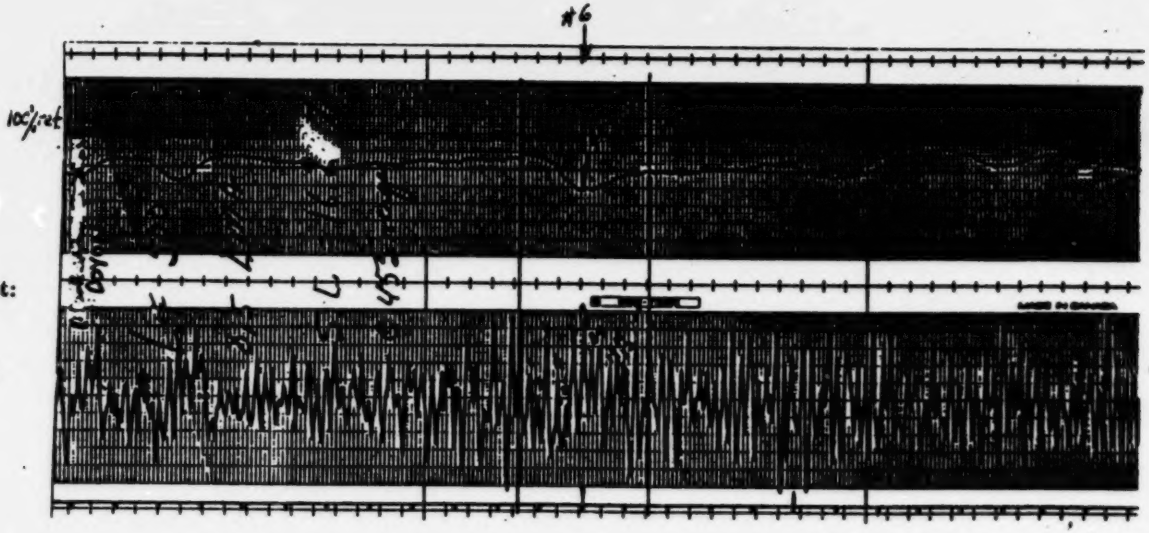

Fig. $1e_1$ — 18.1.89 shop-floor Magnograph test:

for LBS calculation of 455 yard chart- segment

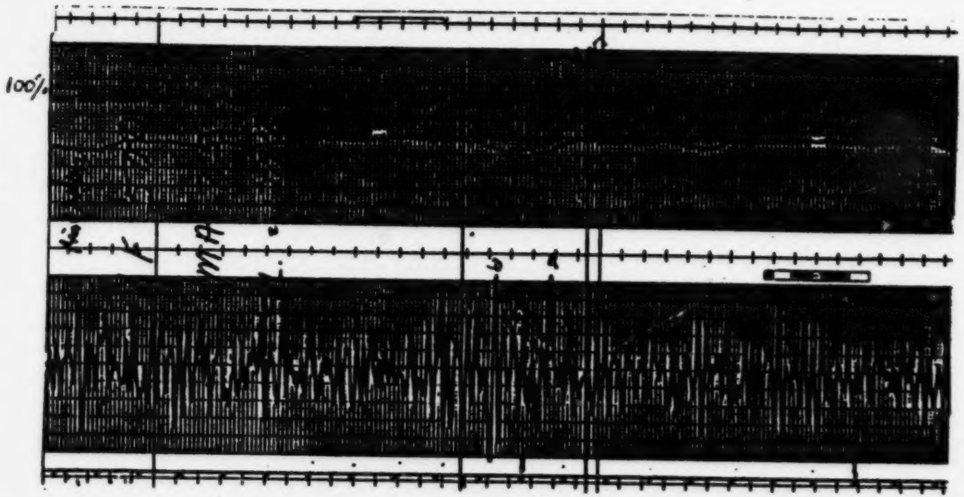

Fig. $1e_4$ — 18.1.89 shop-floor Magnograph test:

for LBS calculation of 722 yard chart- segment

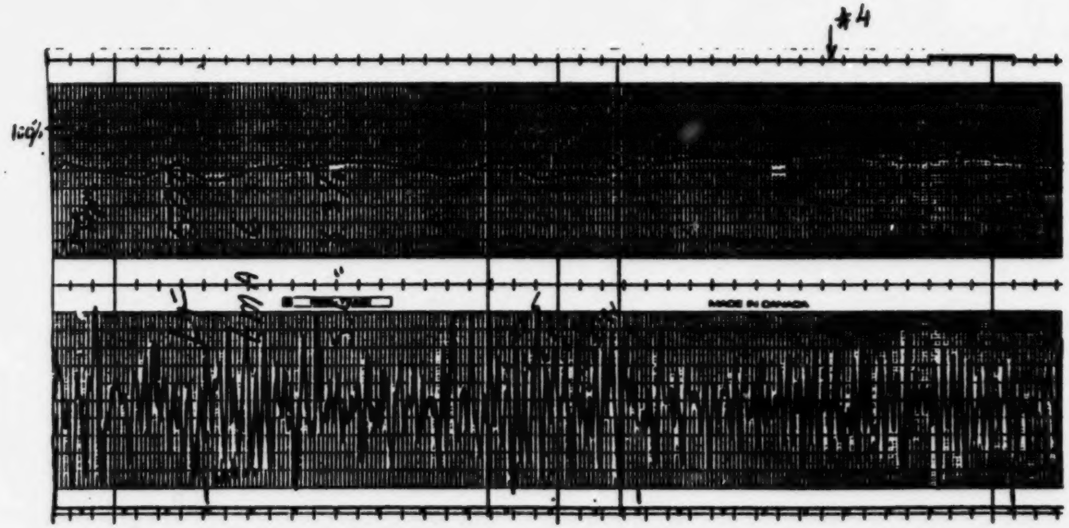

Fig. $1e_3$ — 18.1.89 shop-floor Magnograph test:

for LBS calculation of 609 yard chart- segment

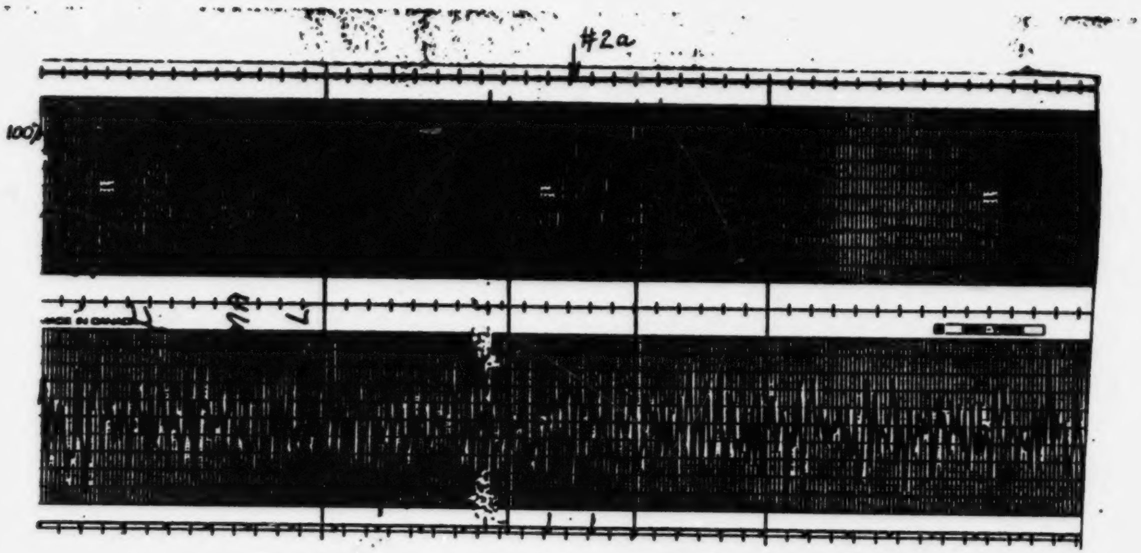

Fig. $1e_5$ — 18.1.89 shop-floor Magnograph test: for LBS calculation of 844 yard chart- segment

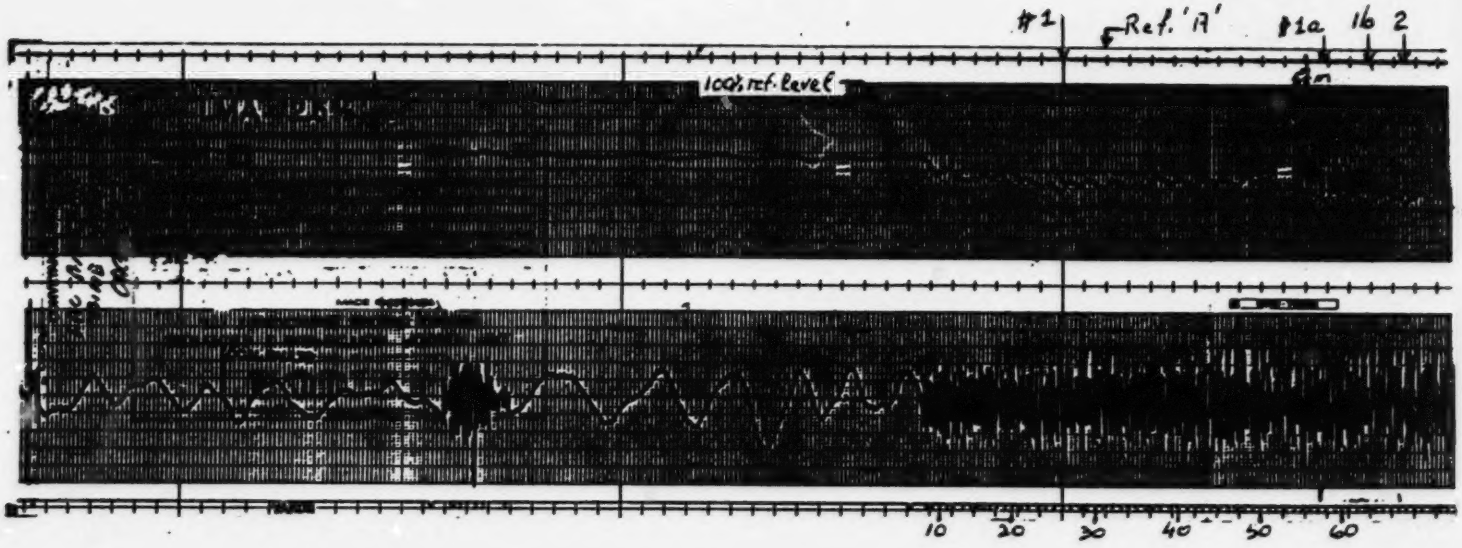

Fig. 1f — 4.4.89 shop-floor Magnograph test

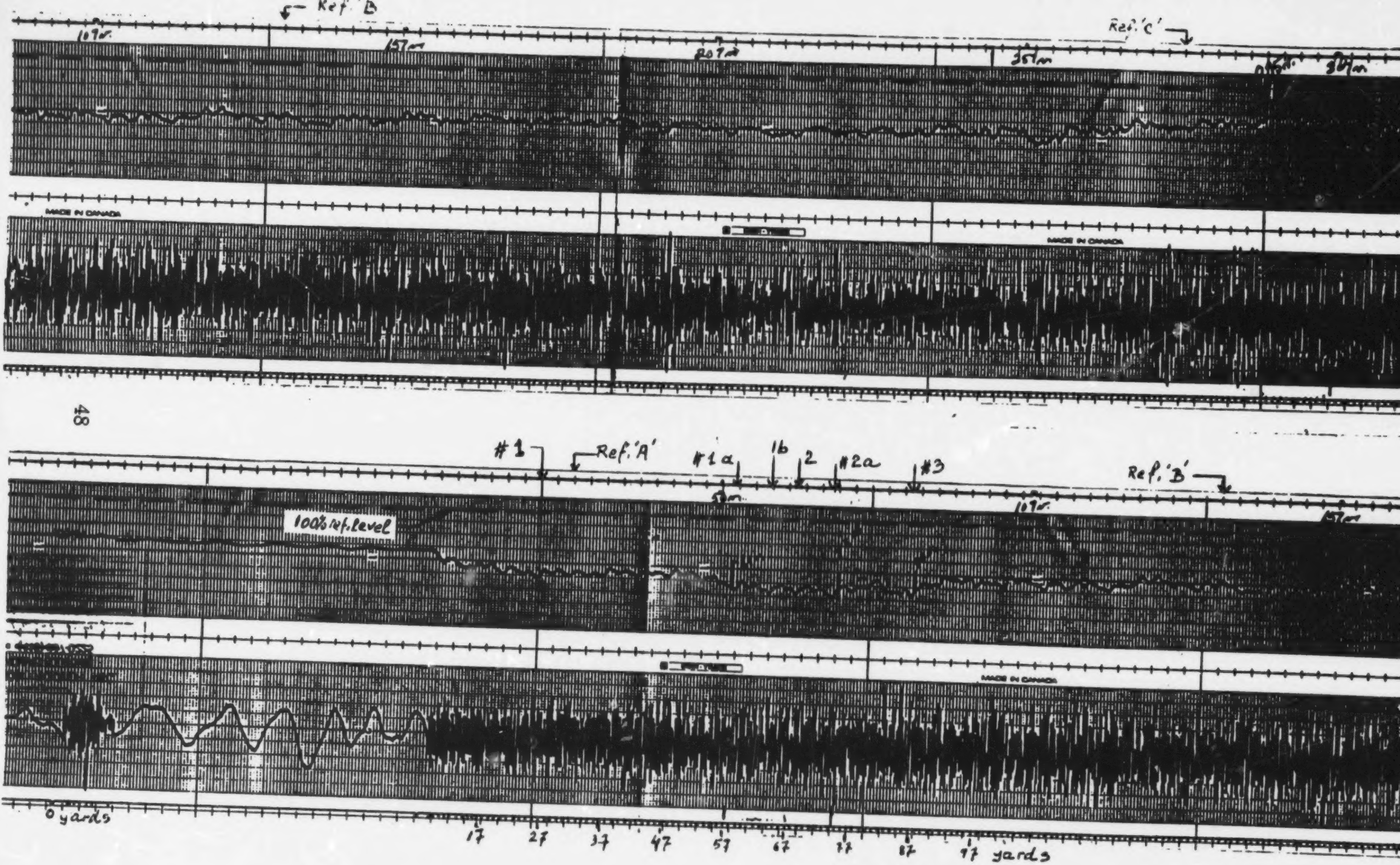

Fig. 1f (continued) — 4.4.89 shop-floor Magnograph test

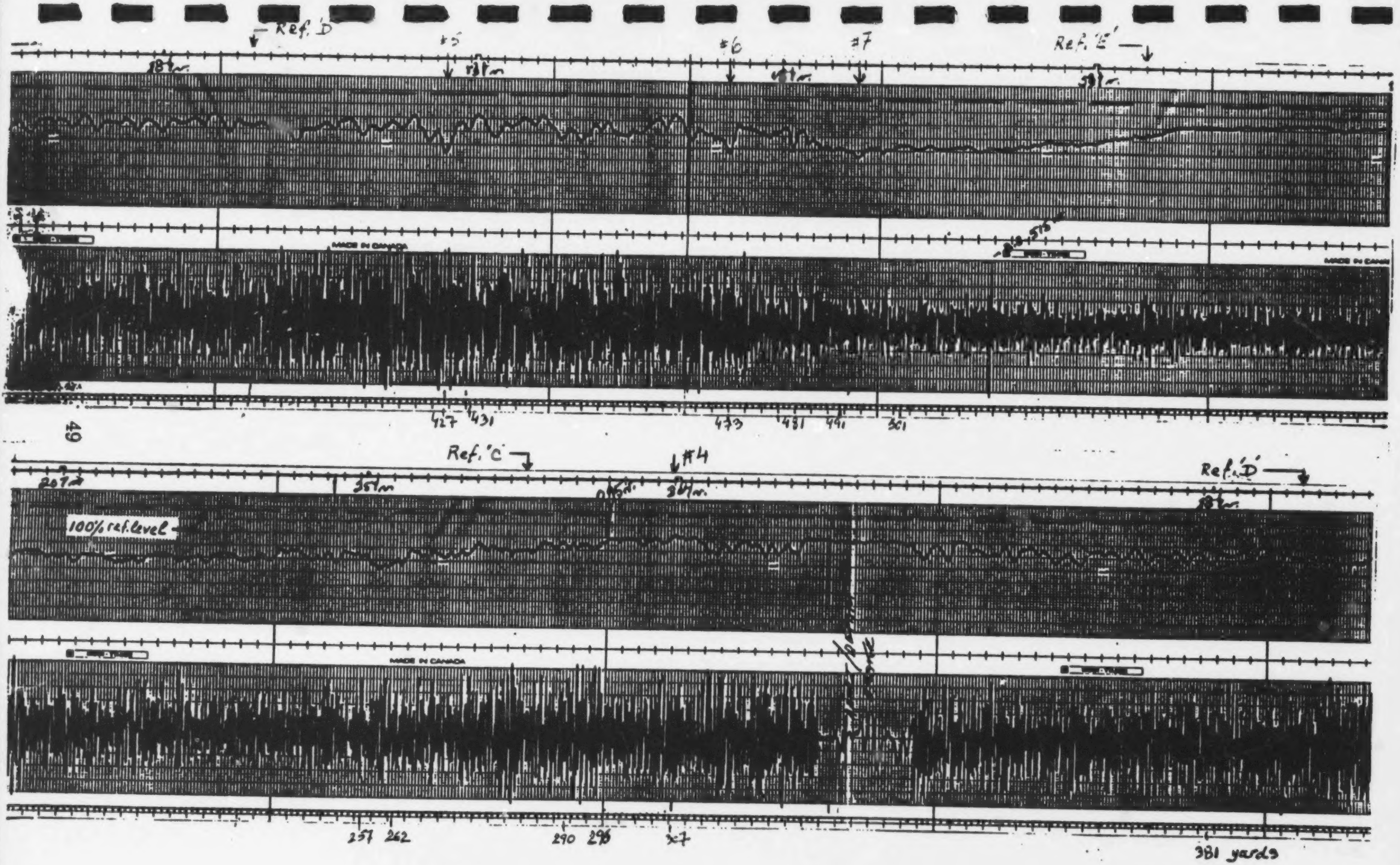

Fig. 1f (continued) — 4.4.89 shop-floor Magnograph test

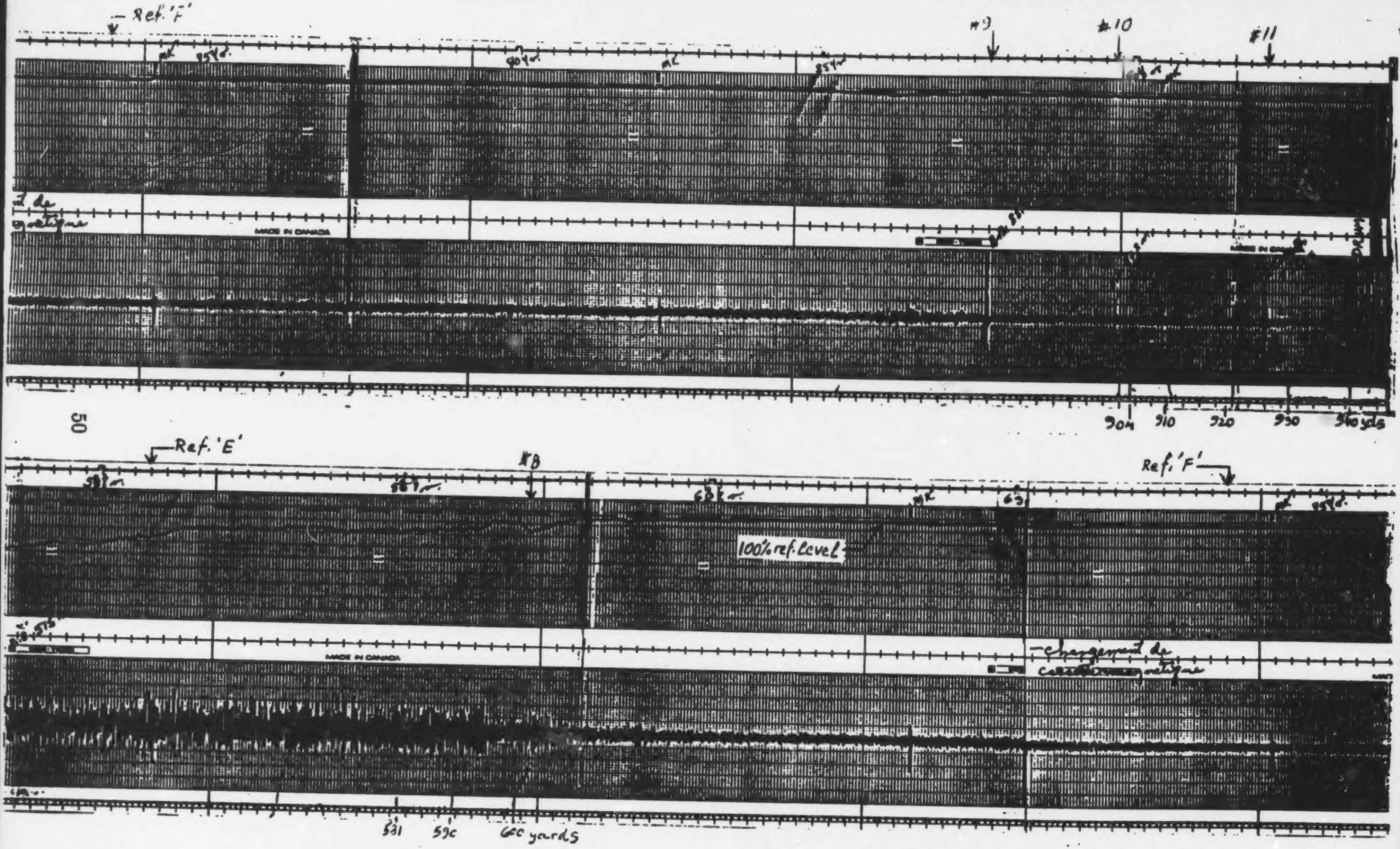

Fig. 1f (continued) — 4.4.89 shop-floor Magnograph test

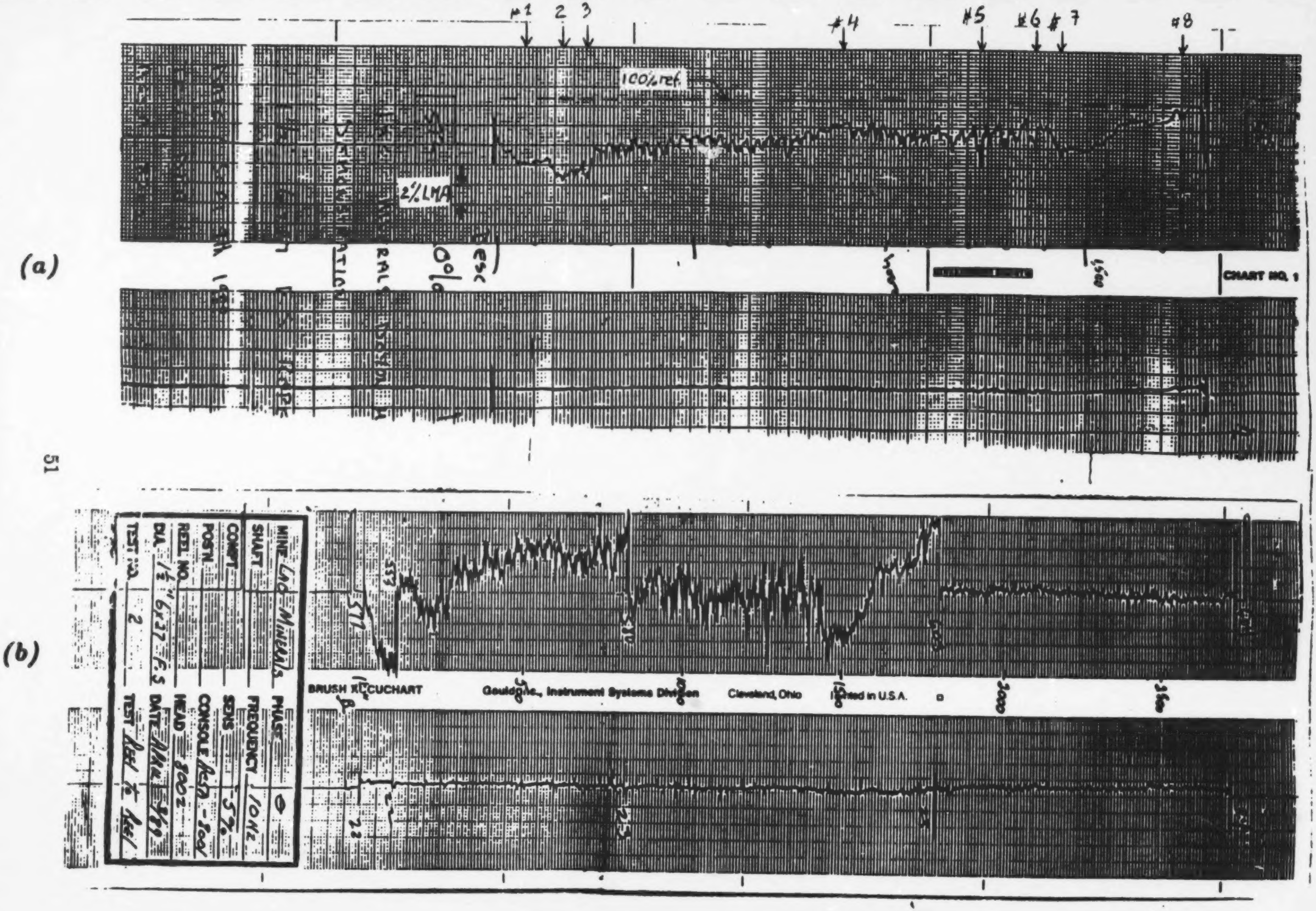

MINE	Lac Minerals	PHASE	0
SHAFT		FREQUENCY	10 Hz
COMPT		SENS	5%
POS'N		CONSOLE	Acsa - 8001
REEL NO.		HEAD	8002
DIA.	1½" 6x37 F.S	DATE	April 3/89
TEST NO.	2	TEST	Reel to Reel

Fig. 2 — Rotesco AC tests: (a) 9.9.88 in situ, and (b) 3.4.89 shop-floor

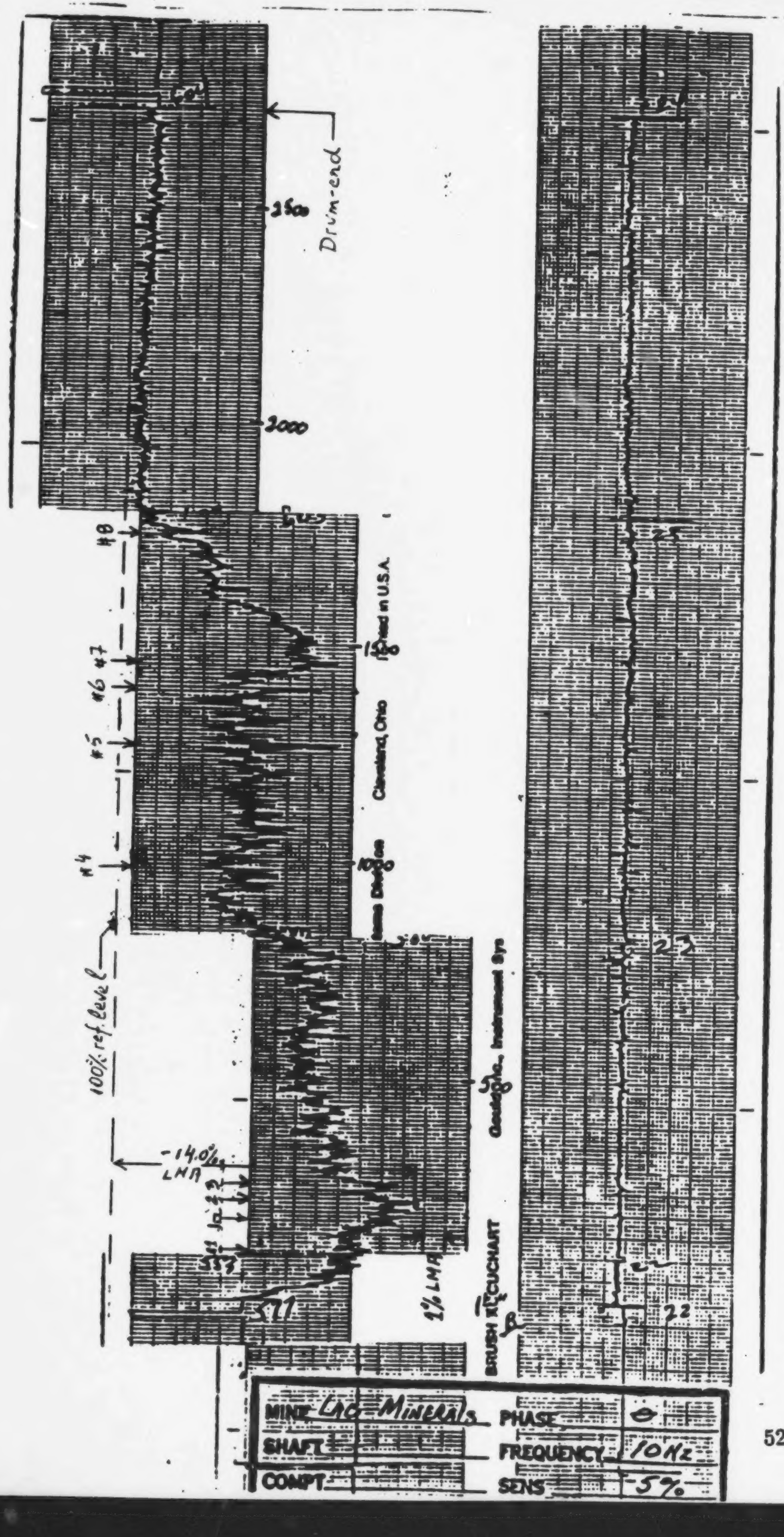

MINE Lac Minerals
SHAFT
COMPT
PHASE 0
FREQUENCY 10 Hz
SENS 5%

Fig. 2c — 3.4.89 shop-floor Rotesco AC test: as realigned and marked by authors

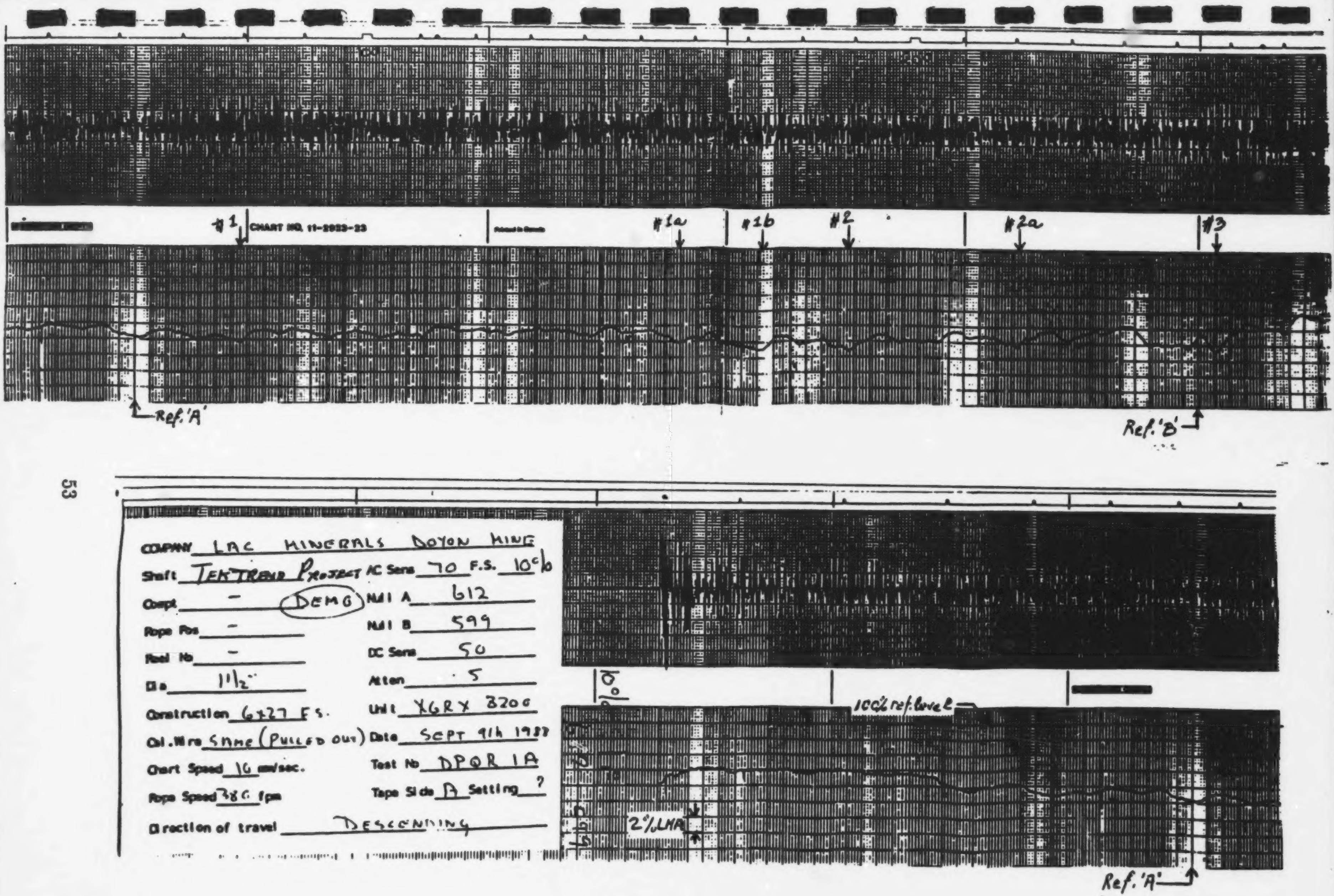

COMPANY LAC MINERALS DOYON MINE
Shaft TEKTREND PROJECT AC Sens 70 F.S. 10%
Compt - (DEMO)
NMI A 612
Rope Pos -
NMI B 599
Reel No -
DC Sens 50
Dia 1½"
Atten .5
Construction 6x27 F.S.
Unit XGRX 3200
Ol. Wire SAME (PULLED OUT)
Date SEPT 9th 1989
Chart Speed 16 mm/sec.
Test No DPOR 1A
Rope Speed 386 fpm
Tape Side B Setting ?
Direction of travel DESCENDING

Fig. 3a — 9.9.89 in situ Rotescograph test

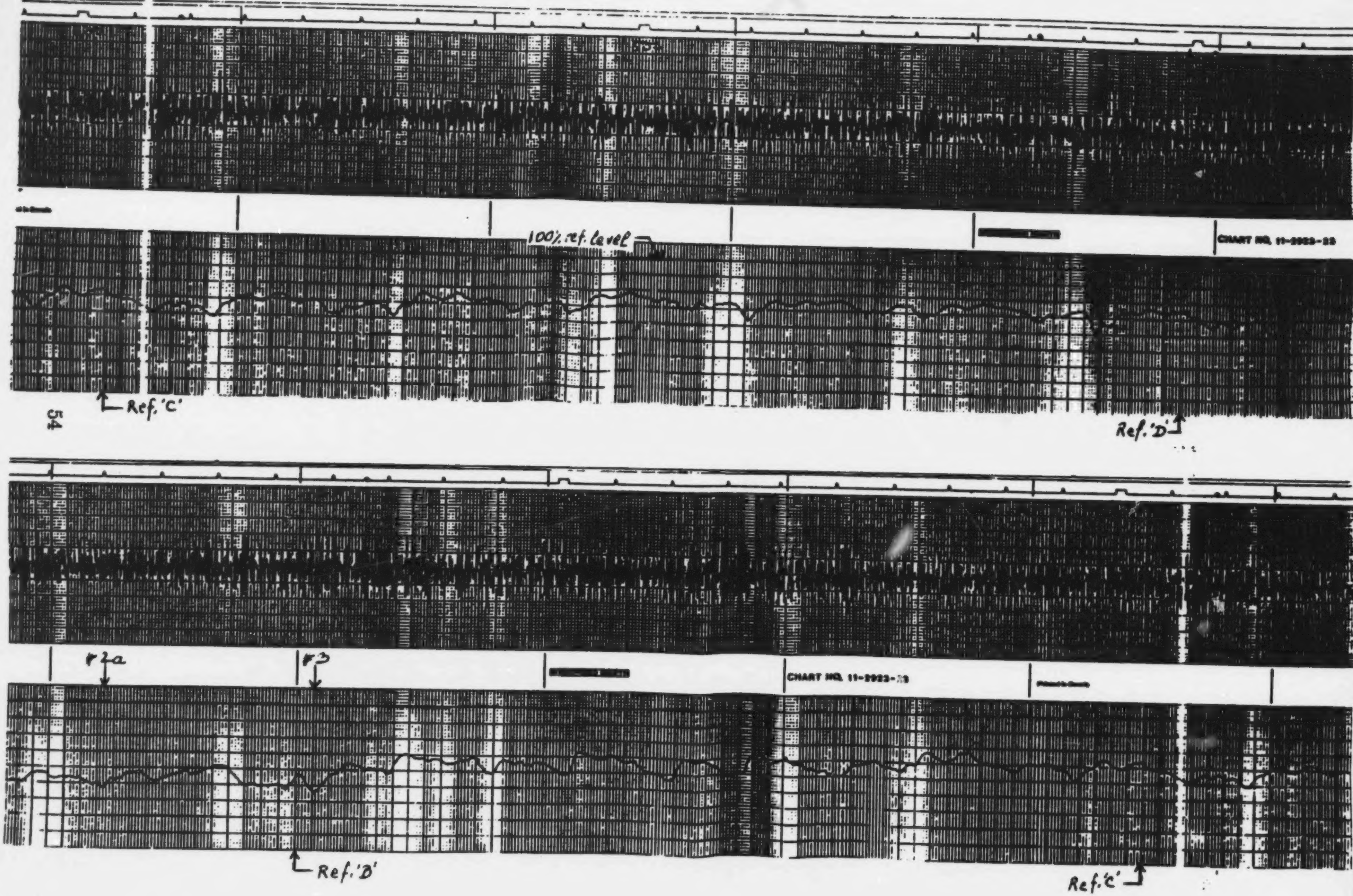

Fig. 3a (continued) — 9.9.89 in situ Rotescograph test

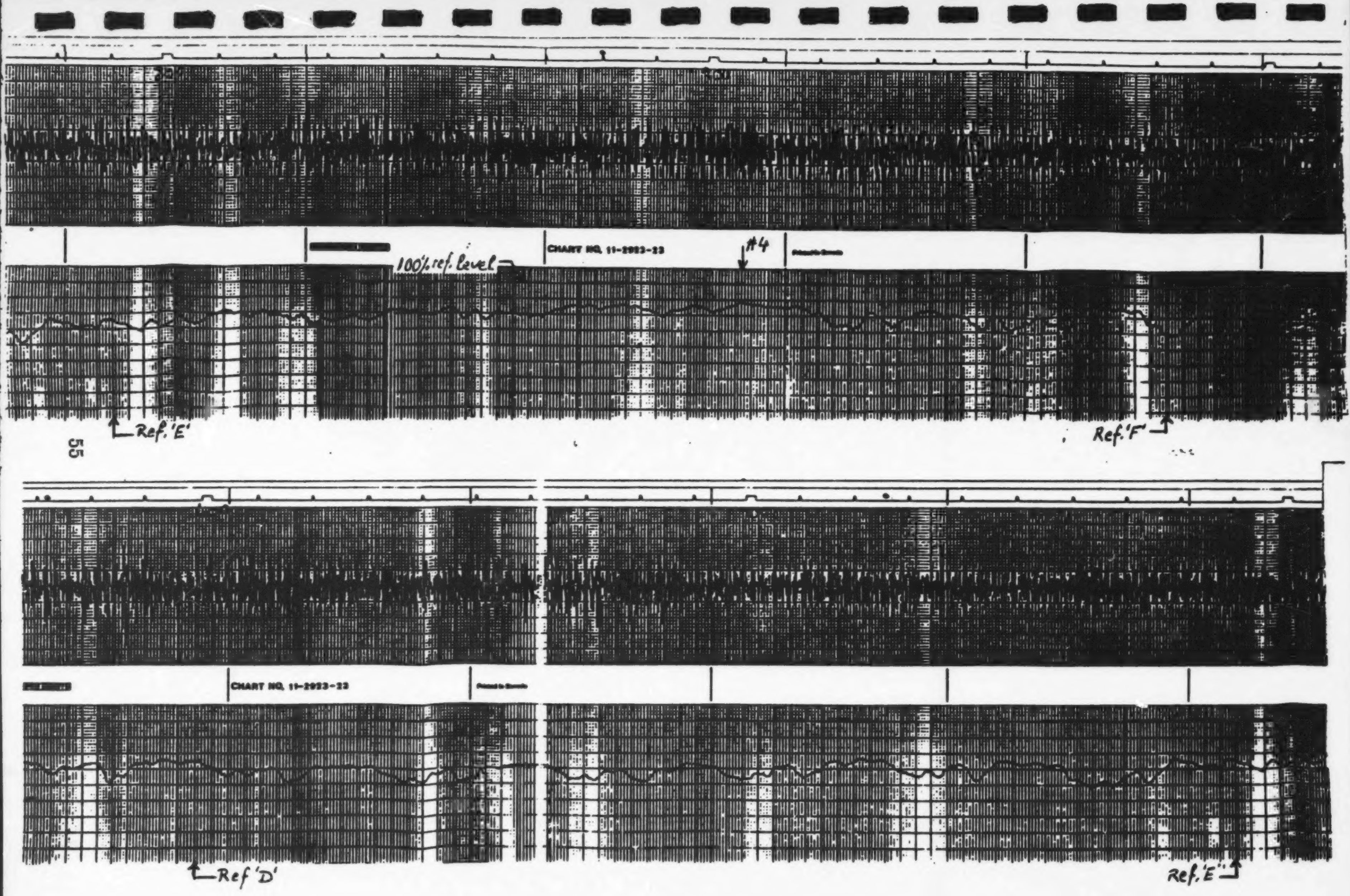

Fig. 3a (continued) — 9.9.89 in situ Rotescograph test

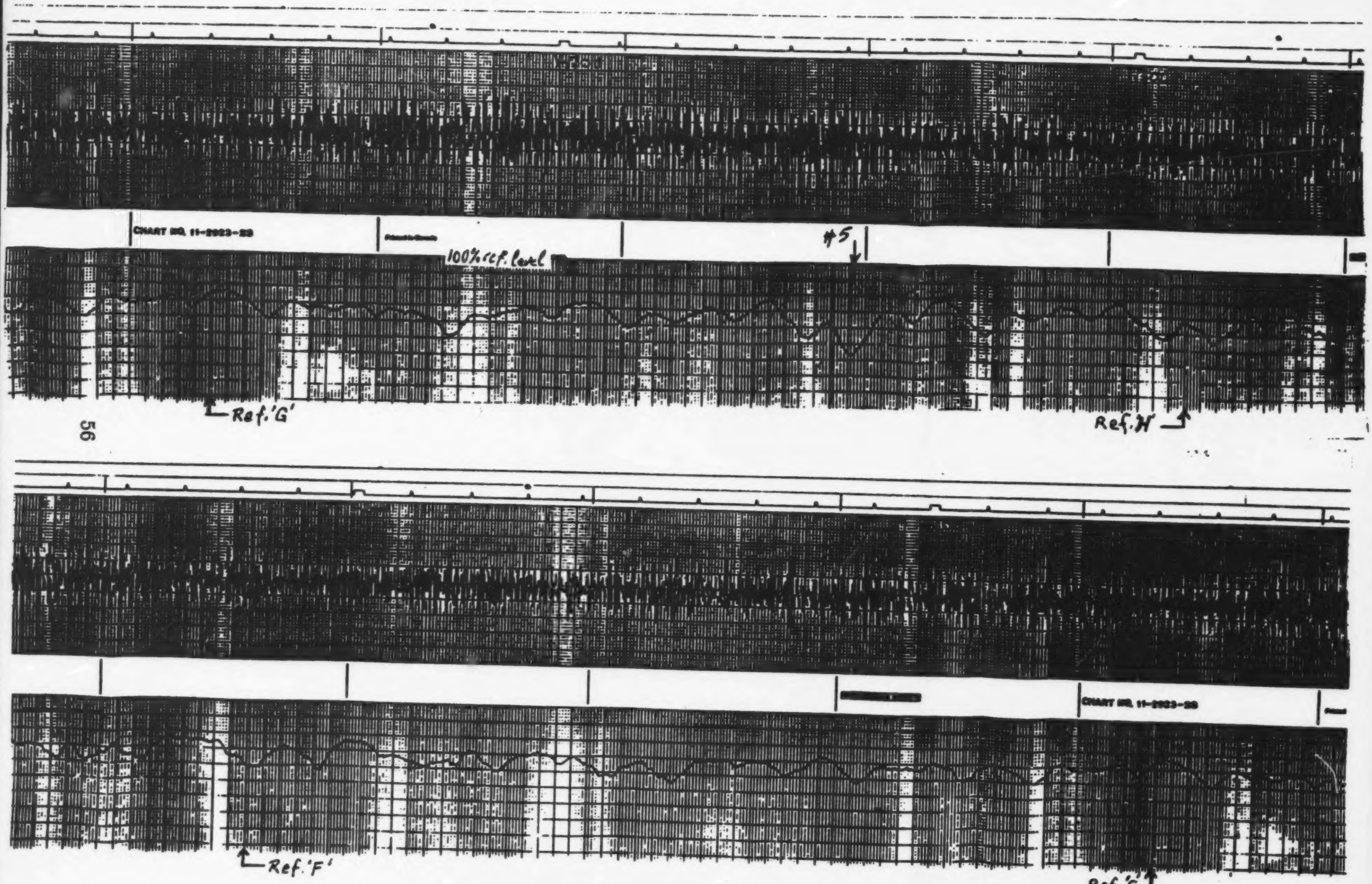

Fig. 3a (continued) — 9.9.89 in situ Rotescograph test

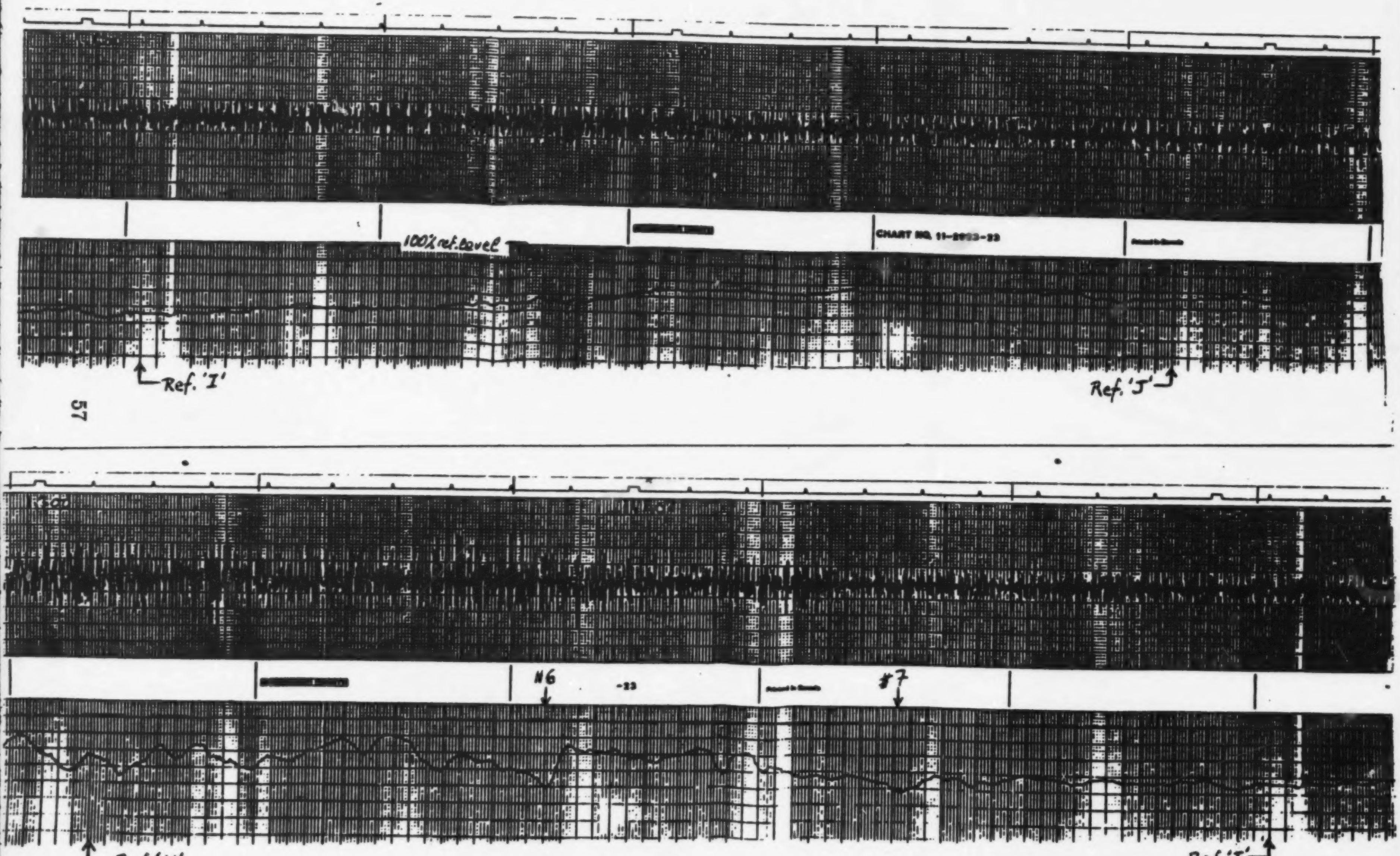

Fig. 3a (continued) — 9.9.89 in situ Rotescograph test

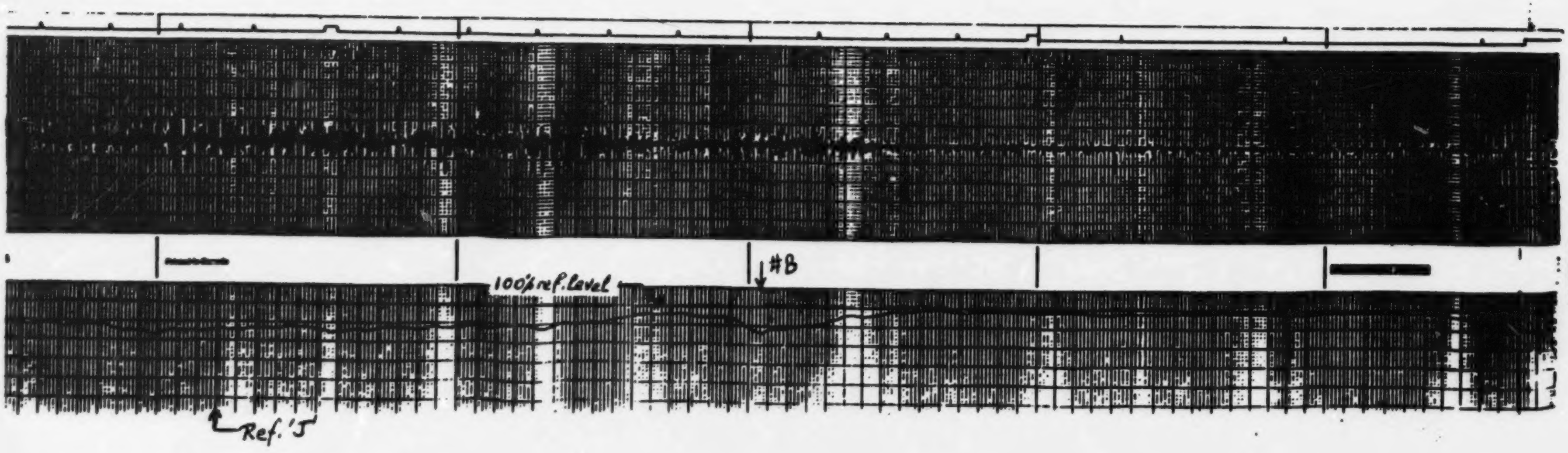

Fig. 3a (continued) — 9.9.89 in situ Rotescograph test

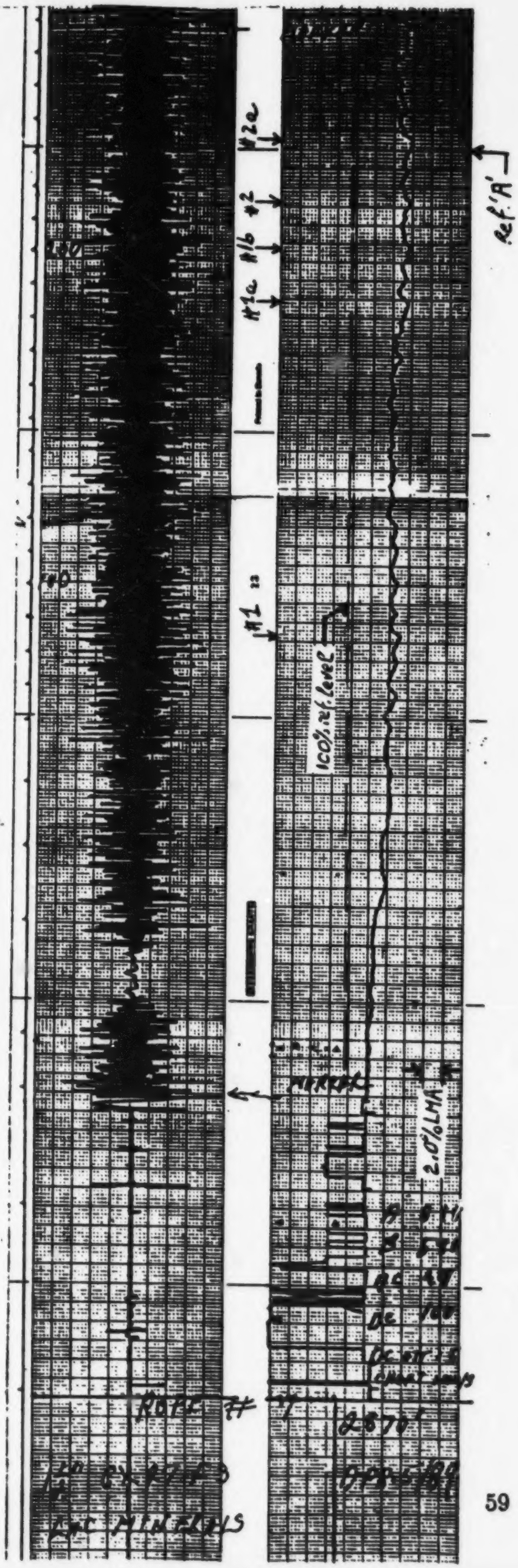

Fig. 3b — 5.4.89 shop-floor Rotescograph test: as marked by authors

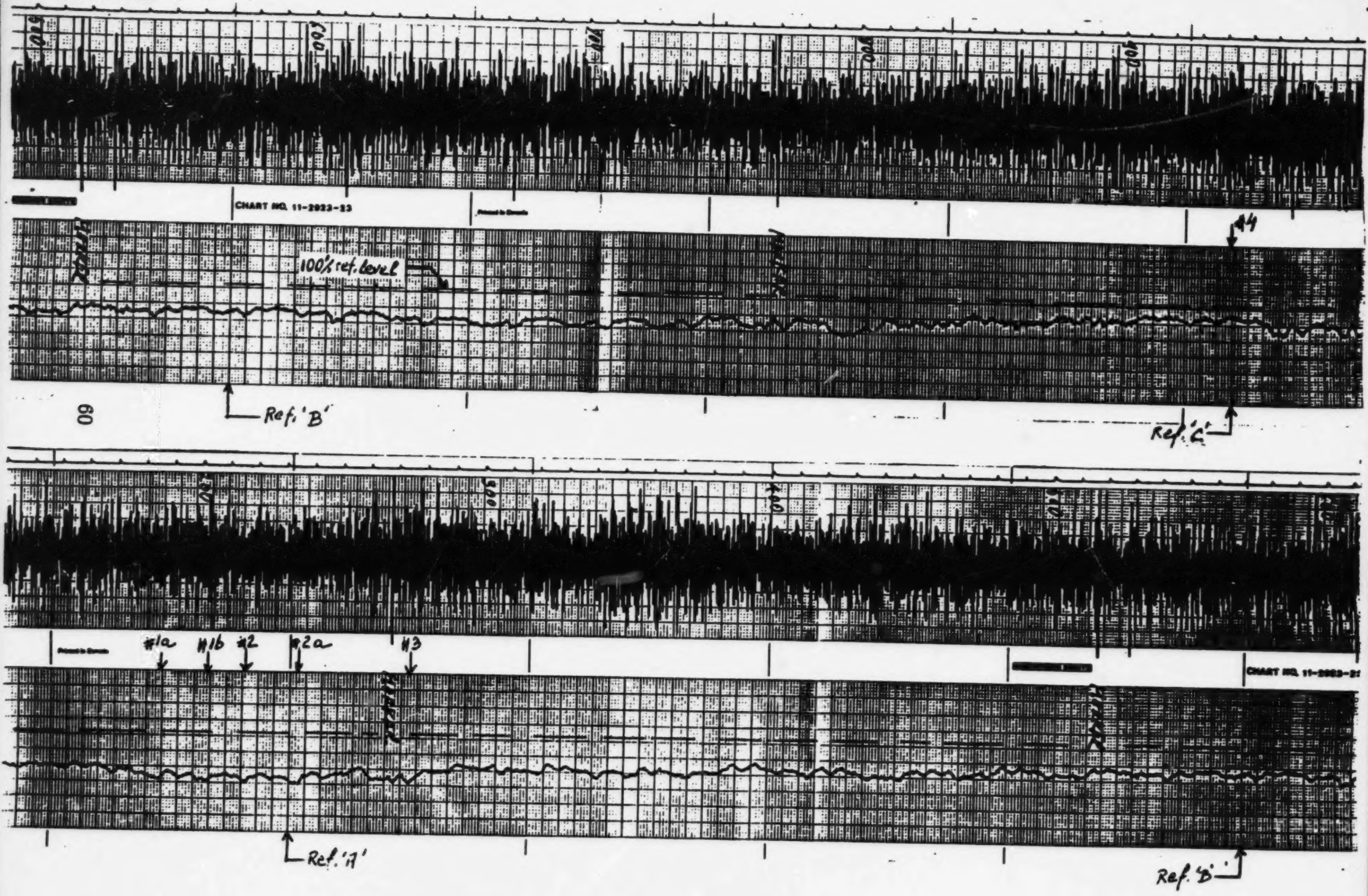

Fig. 3b (continued) — 5.4.89 shop-floor Rotescograph test: as marked by authors

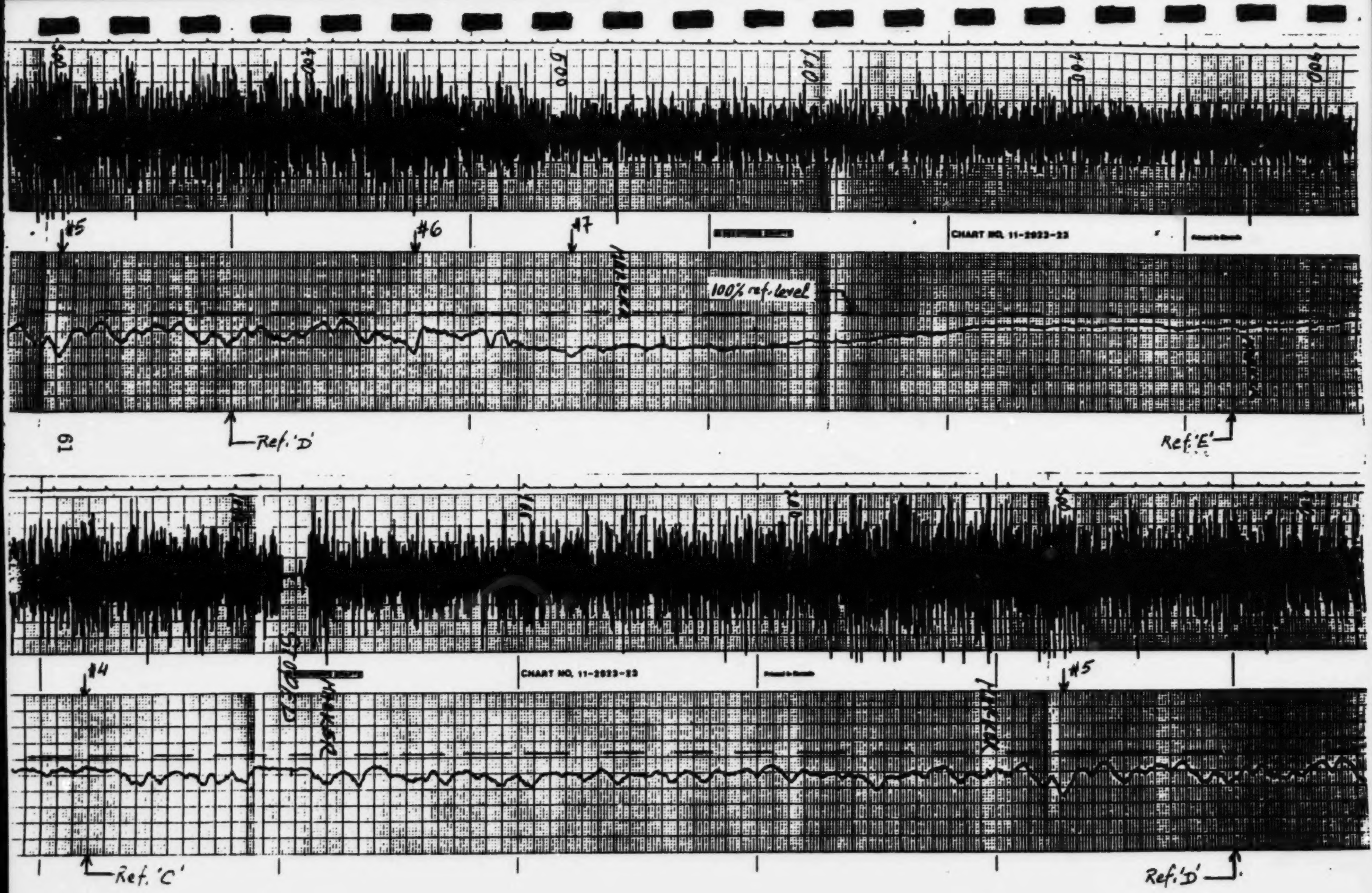

Fig. 3b (continued) — 5.4.89 shop-floor Rotescograph test:- as marked by authors

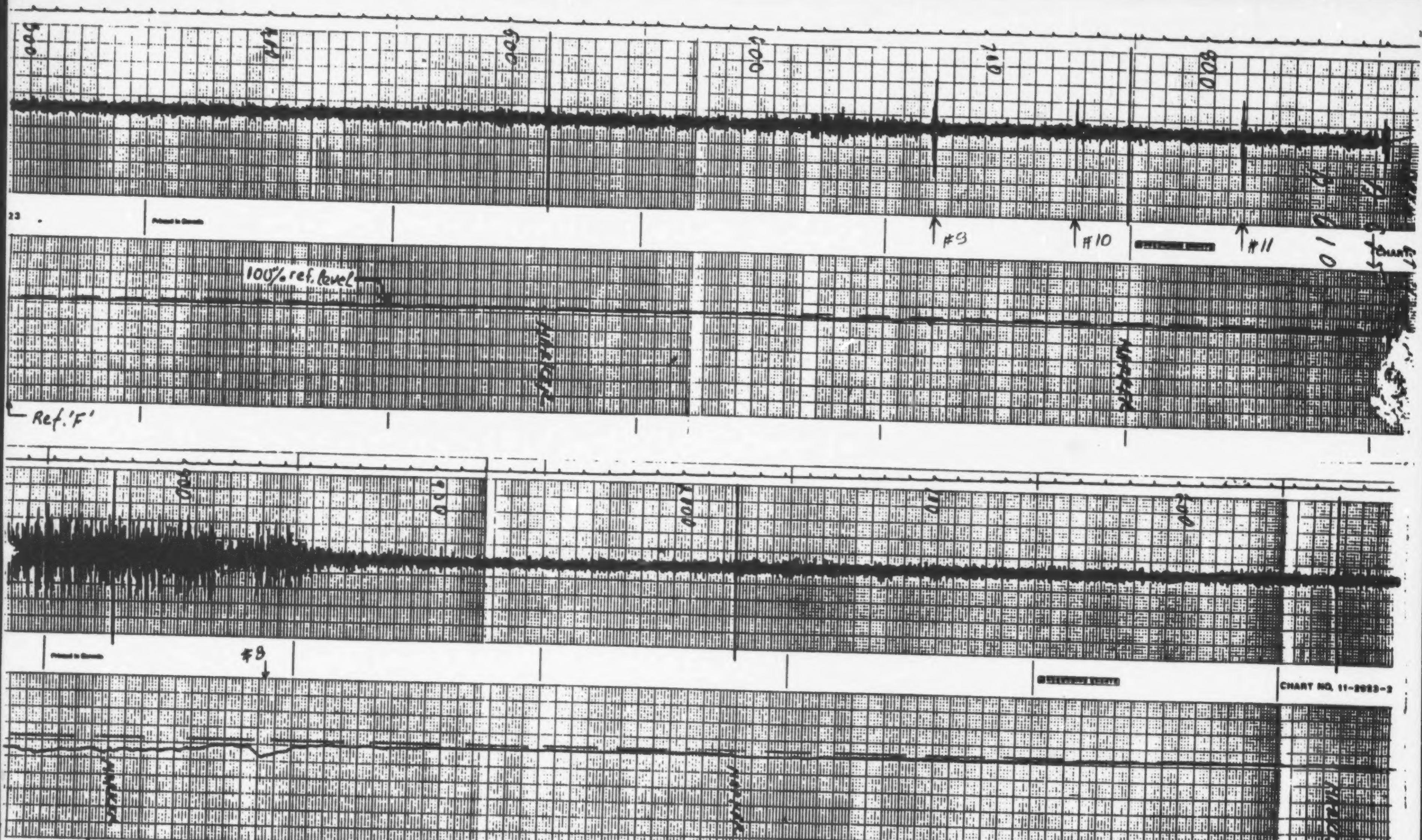

Fig. 3b (continued) — 5.4.89 shop-floor Rotescograph test: as marked by authors

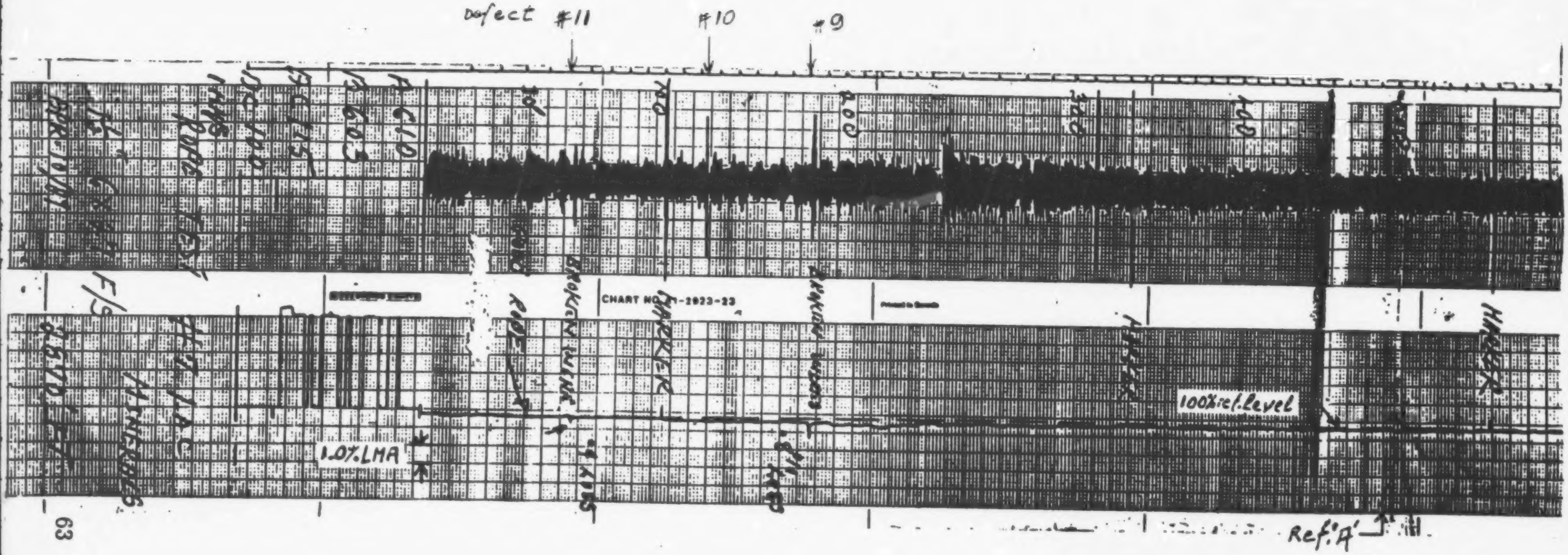

Fig. 3c — 10.4.89 shop-floor Rotescograph test: as submitted by operator and additionally marked by authors

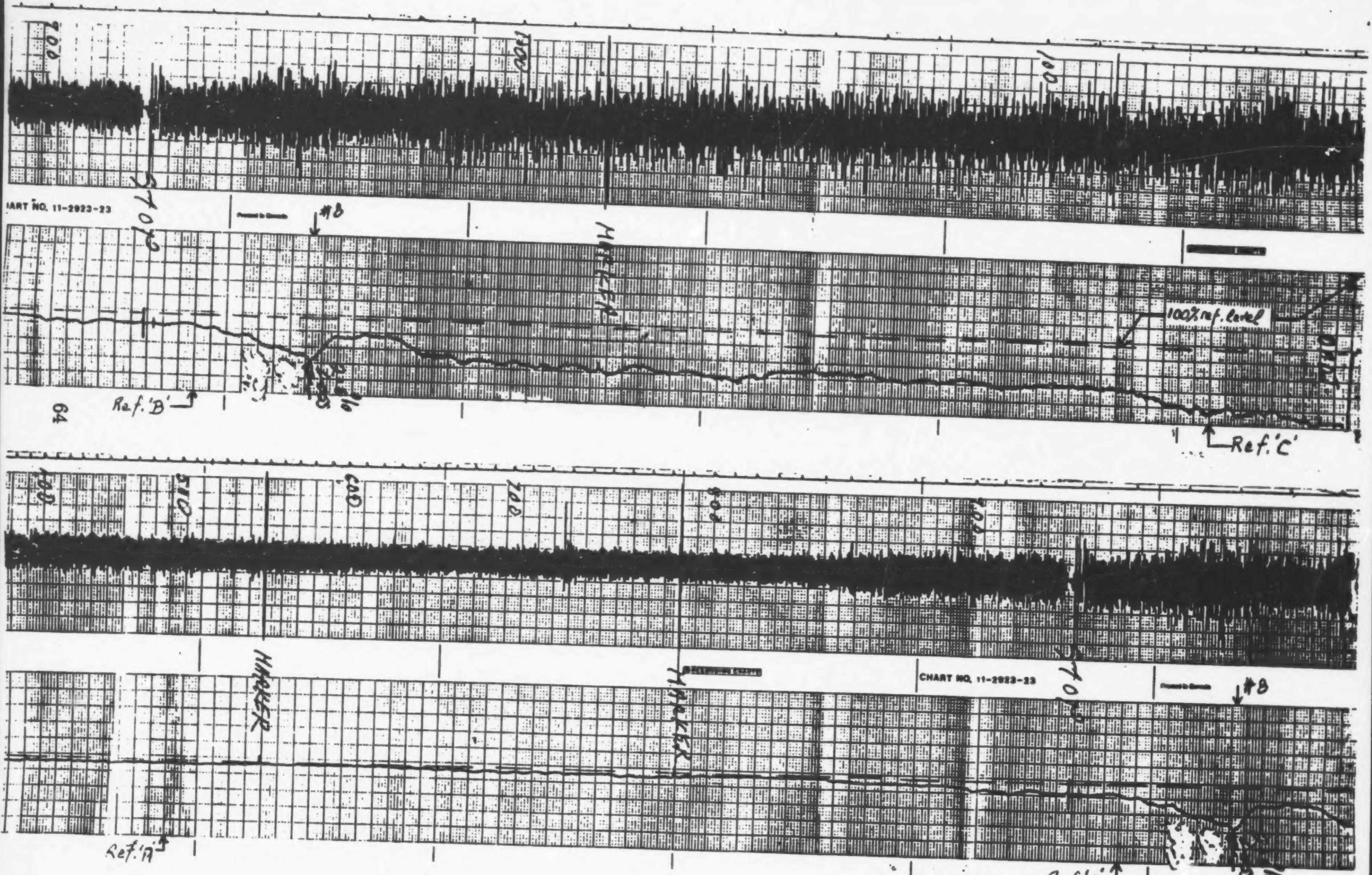

Fig. 3c (continued) — 10.4.89 shop-floor Rotescograph test: as submitted by operator and additionally marked by authors

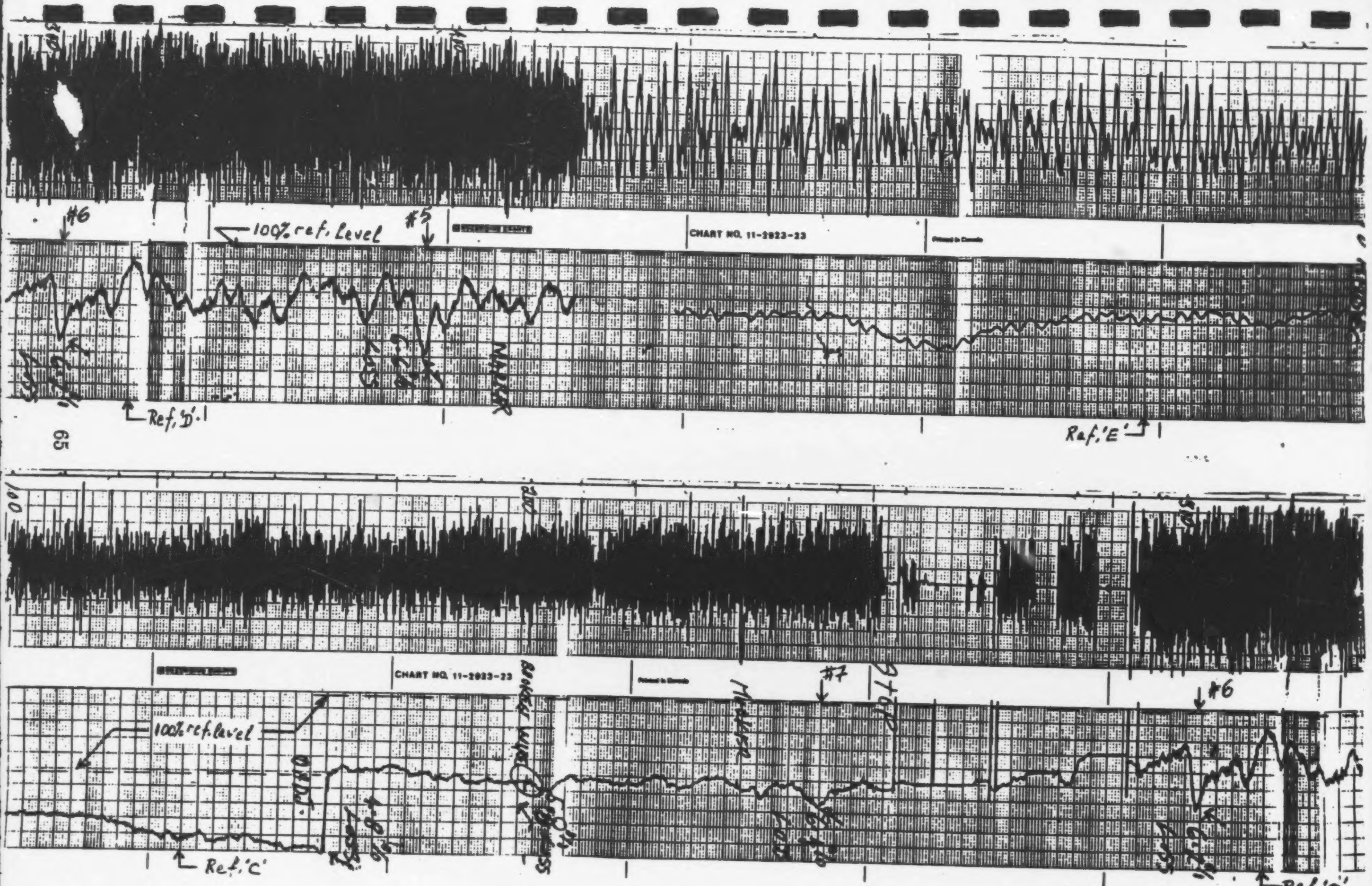

Fig. 3c (continued) — 10.4.89 shop-floor Rotescograph test: as submitted by operator and additionally marked by authors

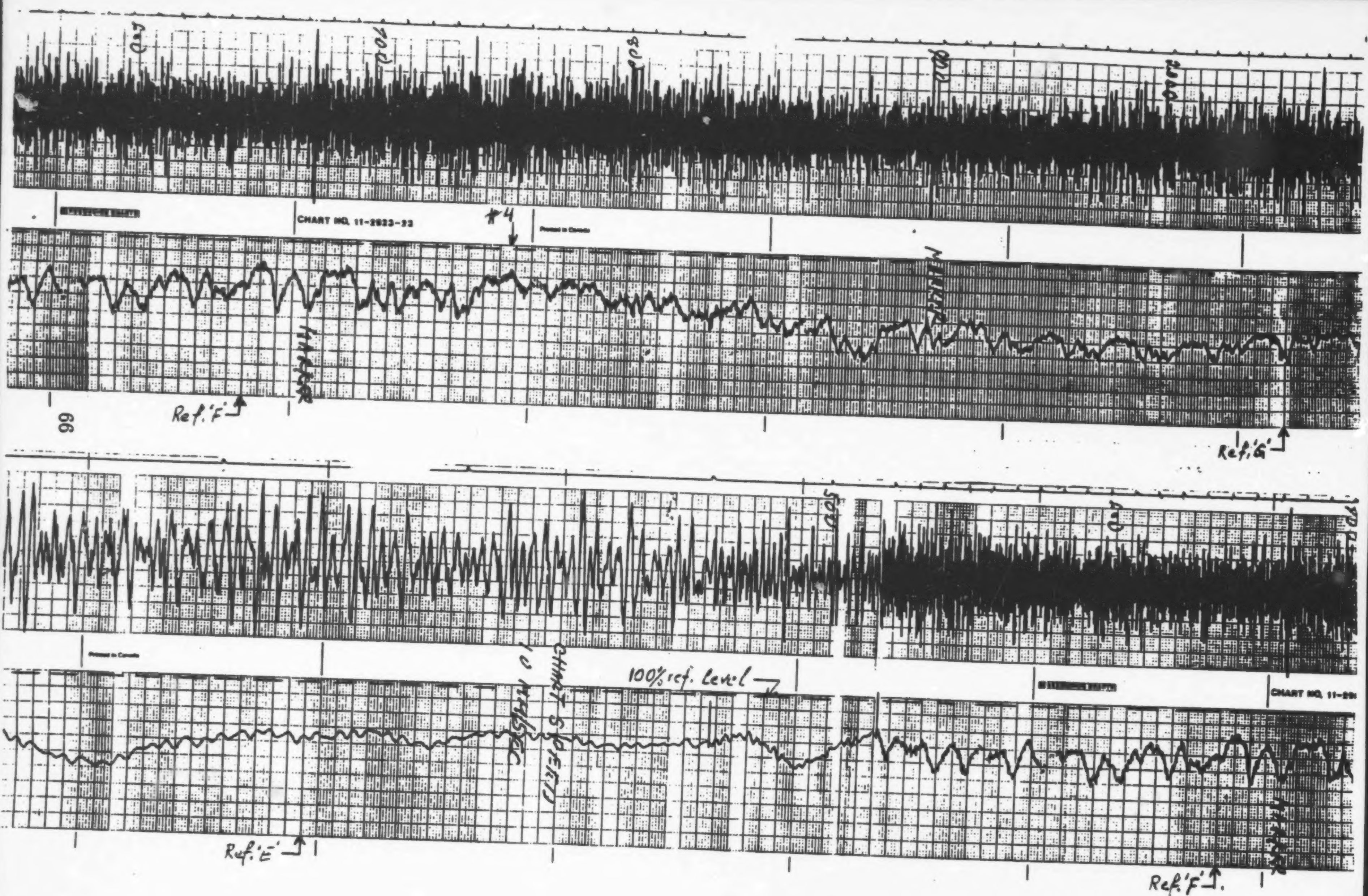

Fig. 3c (continued) — 10.4.89 shop-floor Rotescograph test: as submitted by operator and additionally marked by authors

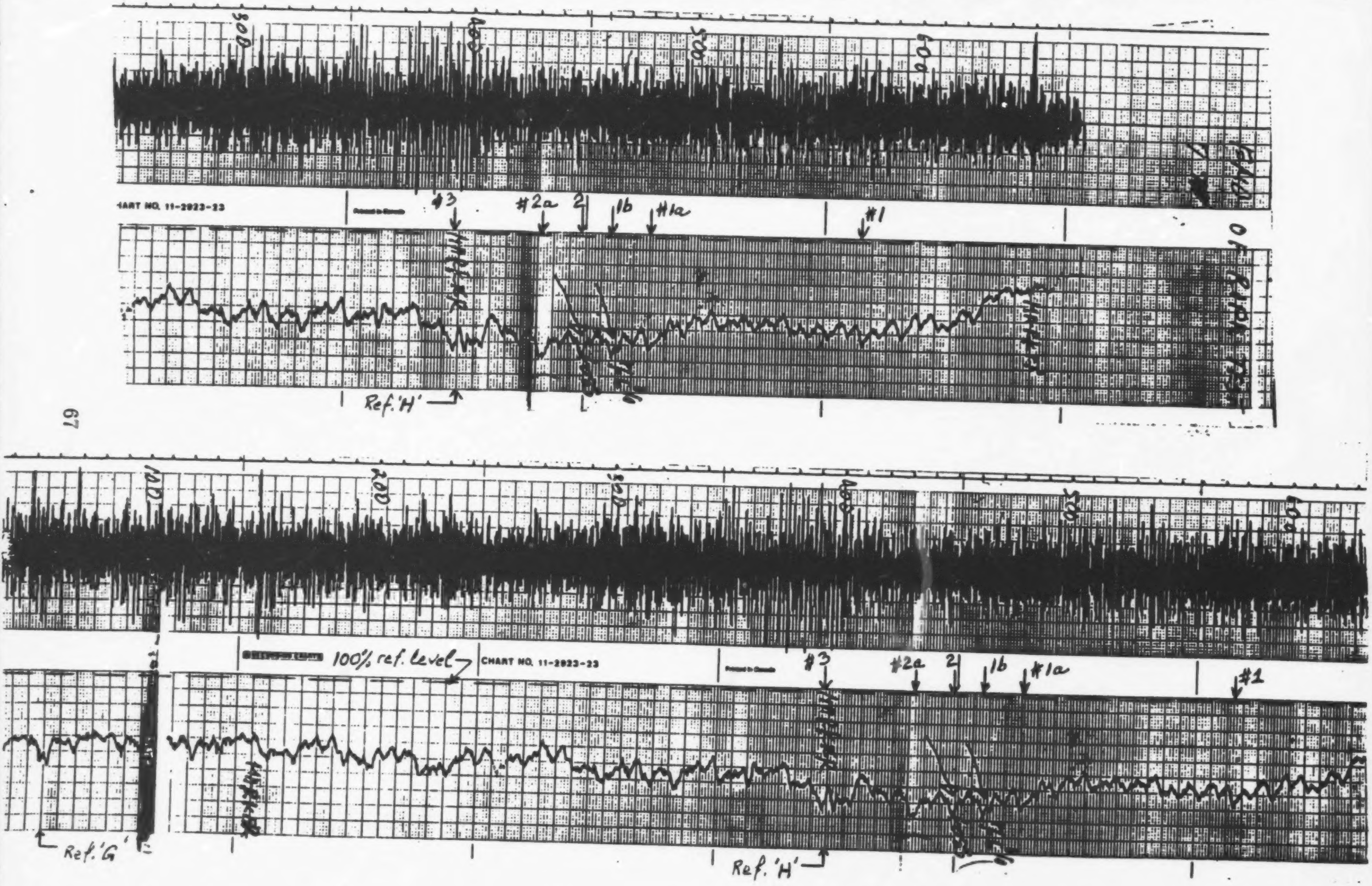

Fig. 3c (continued) — 10.4.89 shop-floor Rotescograph test: as submitted by operator and additionally marked by authors

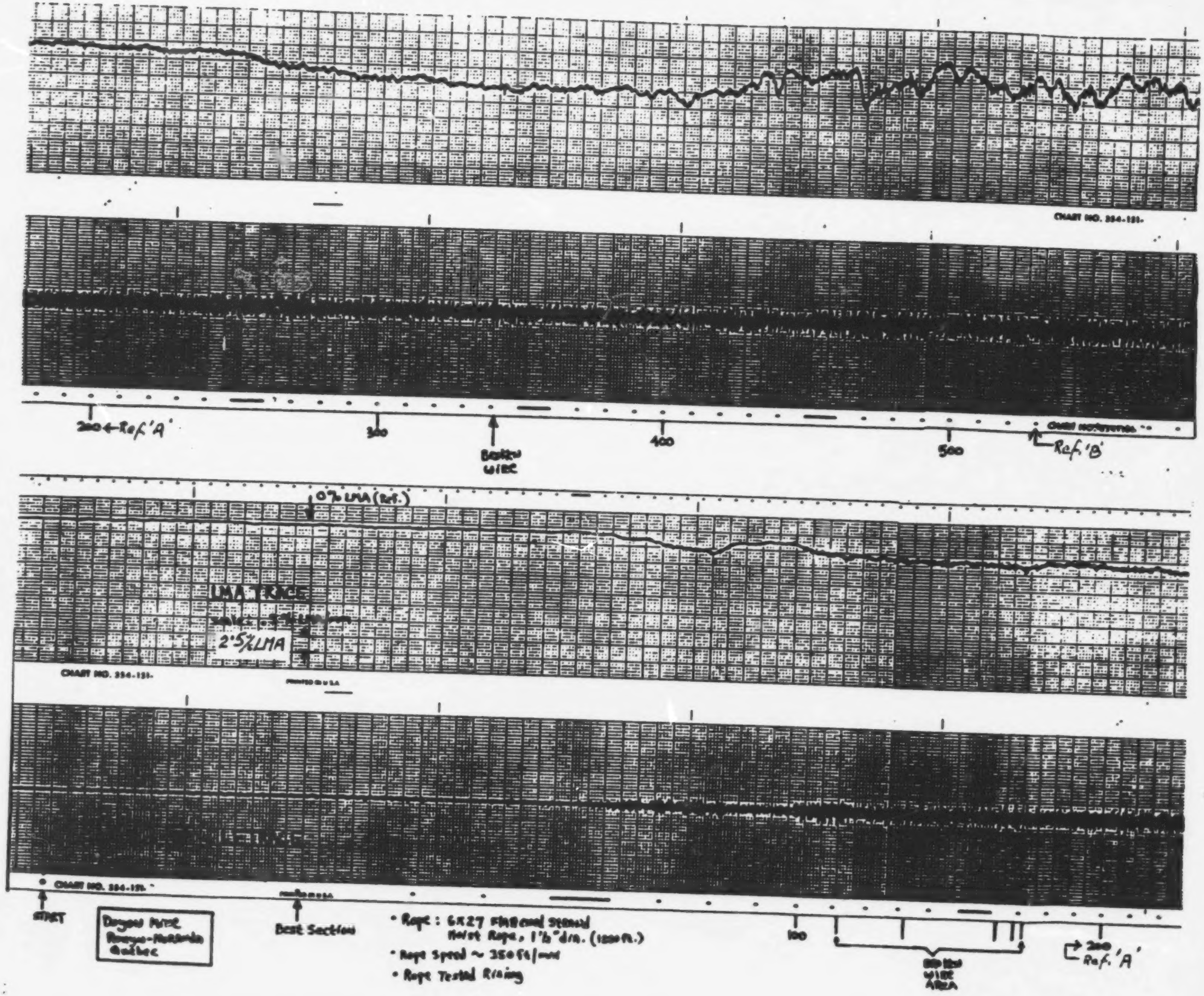

Fig. $4a_1$ — 9.9.88 in situ LMA-250 test; as submitted to authors, w[illegible] ope[illegible]ng'

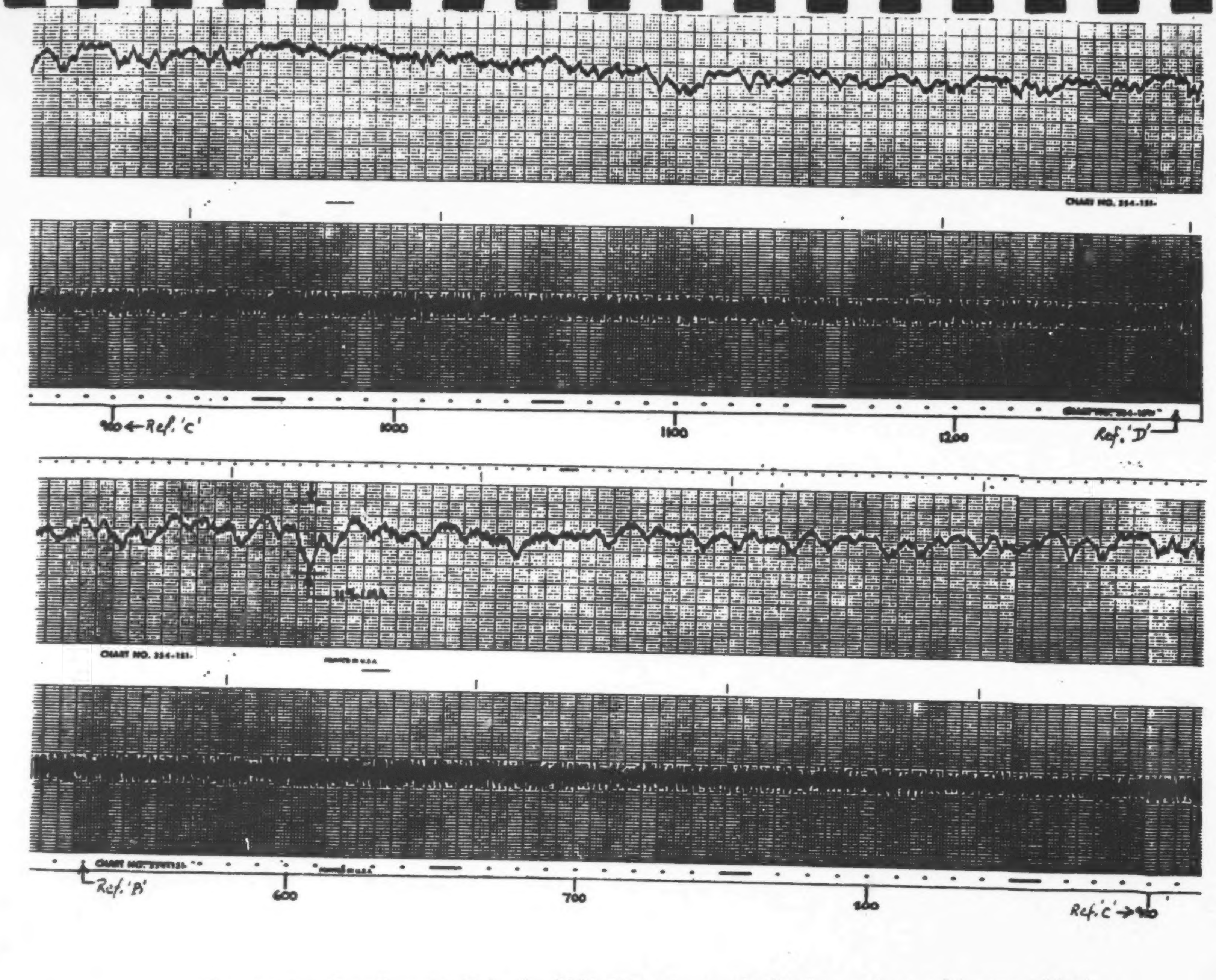

Fig. 4a$_1$ (continued) — 9.9.88 in situ LMA-250 test: as submitted to authors, with rope 'rising'

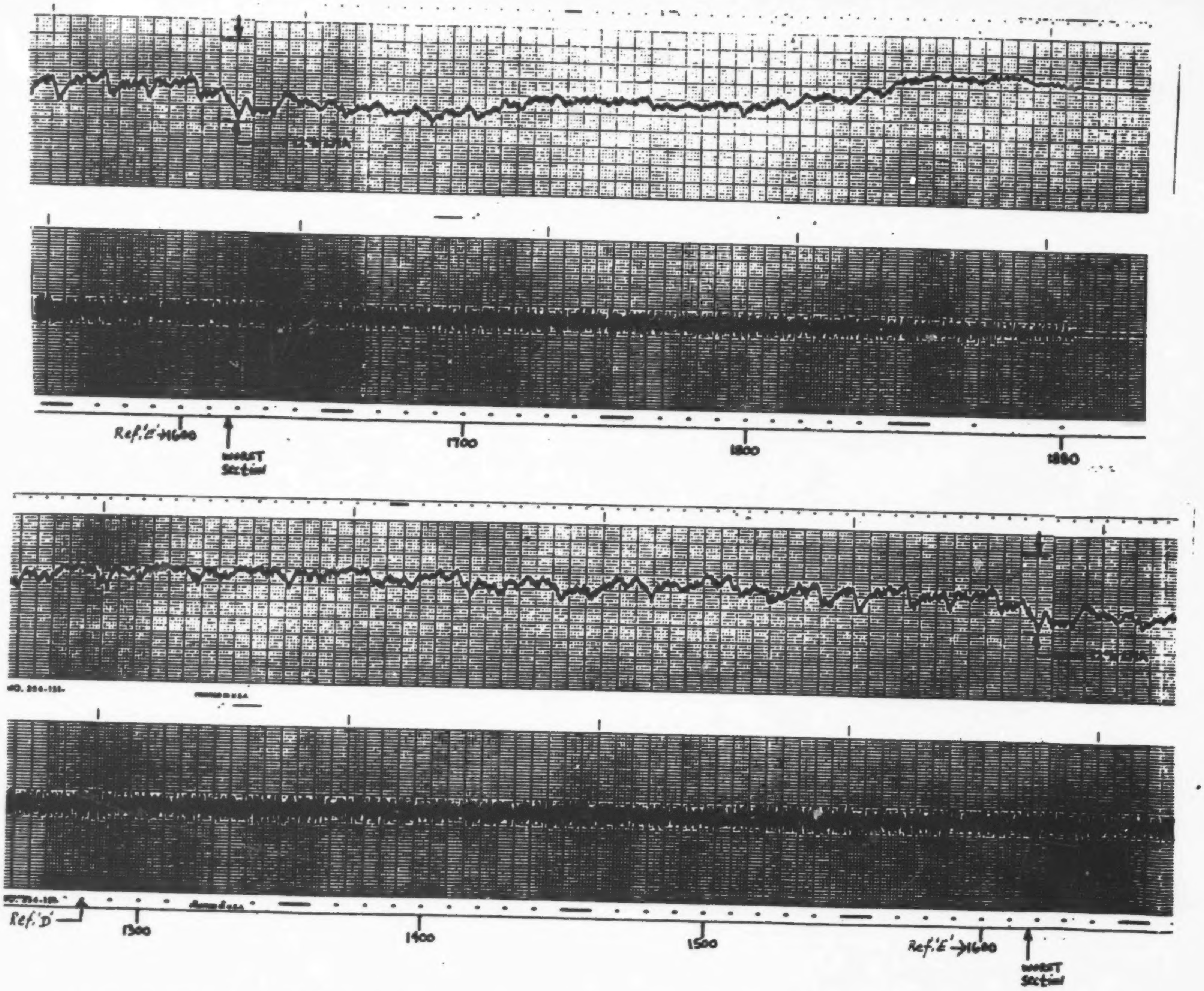

Fig. 4a$_1$ (continued) — 9.9.88 in situ LMA-250 test: as submitted to authors, with rope 'rising'

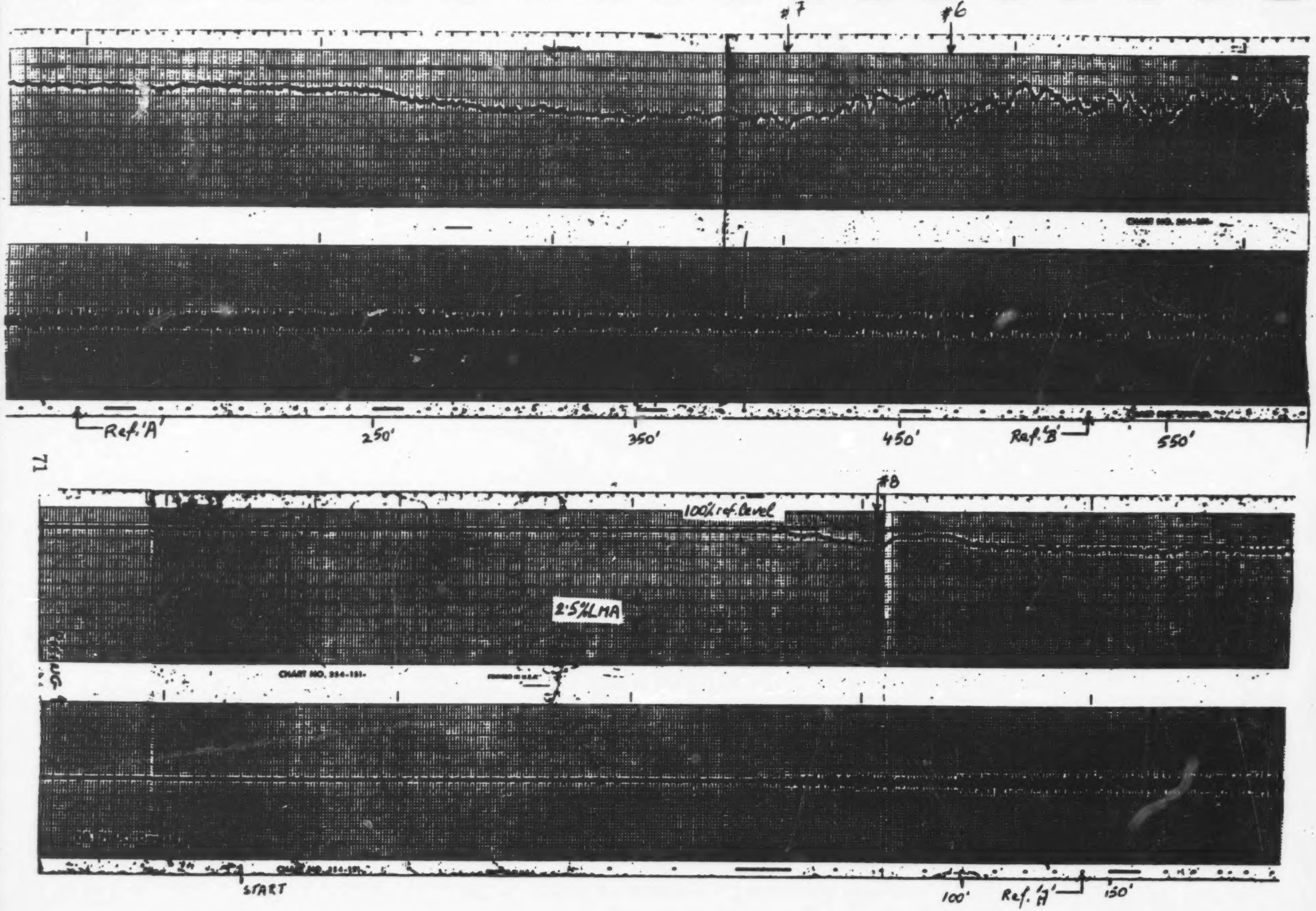

Fig. $4a_2$ — 9.9.88 in situ LMA-250 test: as marked by authors, with rope 'rising'

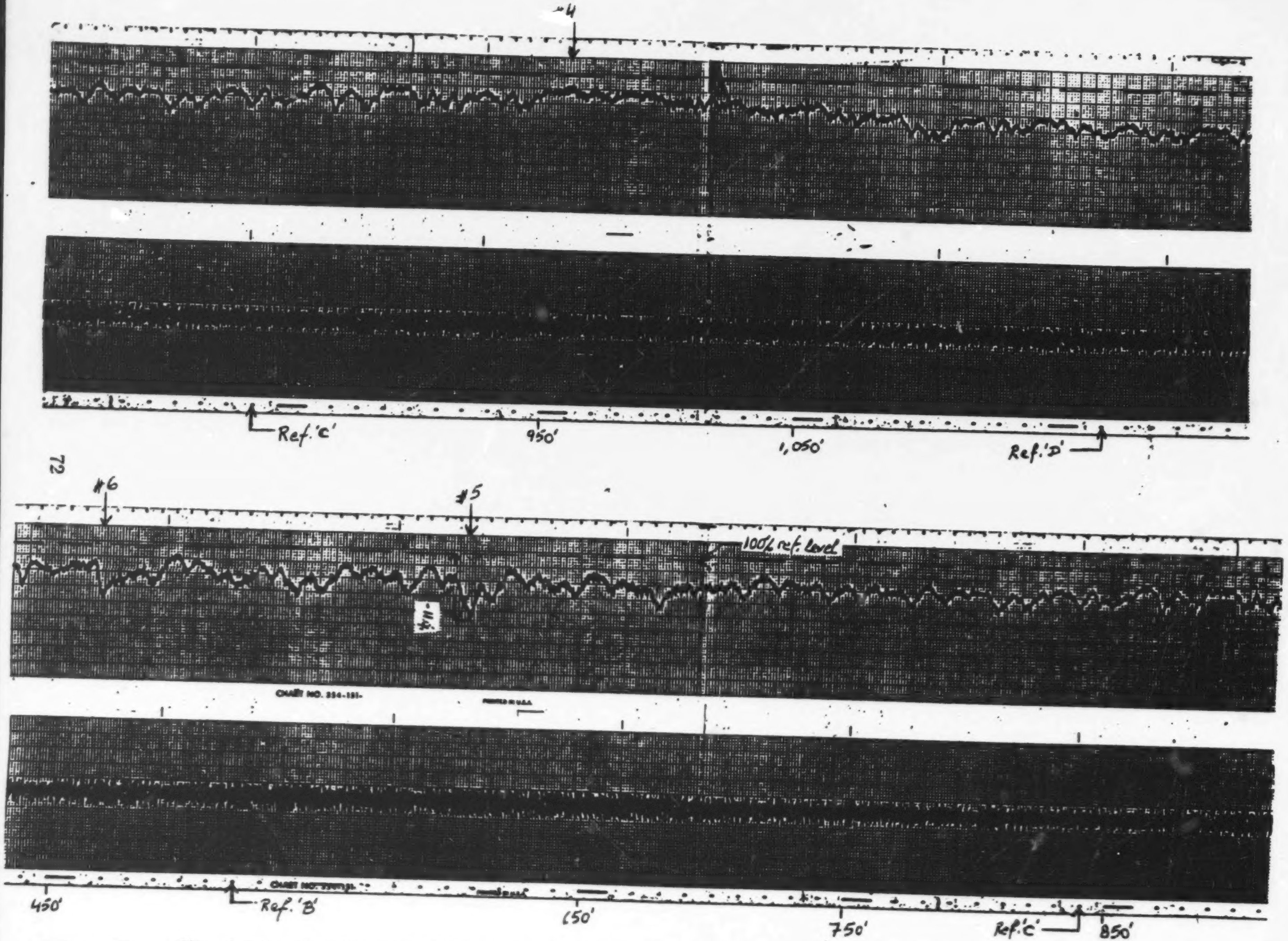

Fig. 4 (continued) — [illegible]9.88 [illegible]itu[illegible] A-2[illegible] test: [illegible]nar[illegible] by [illegible]ors, [illegible]n ro[illegible] rising

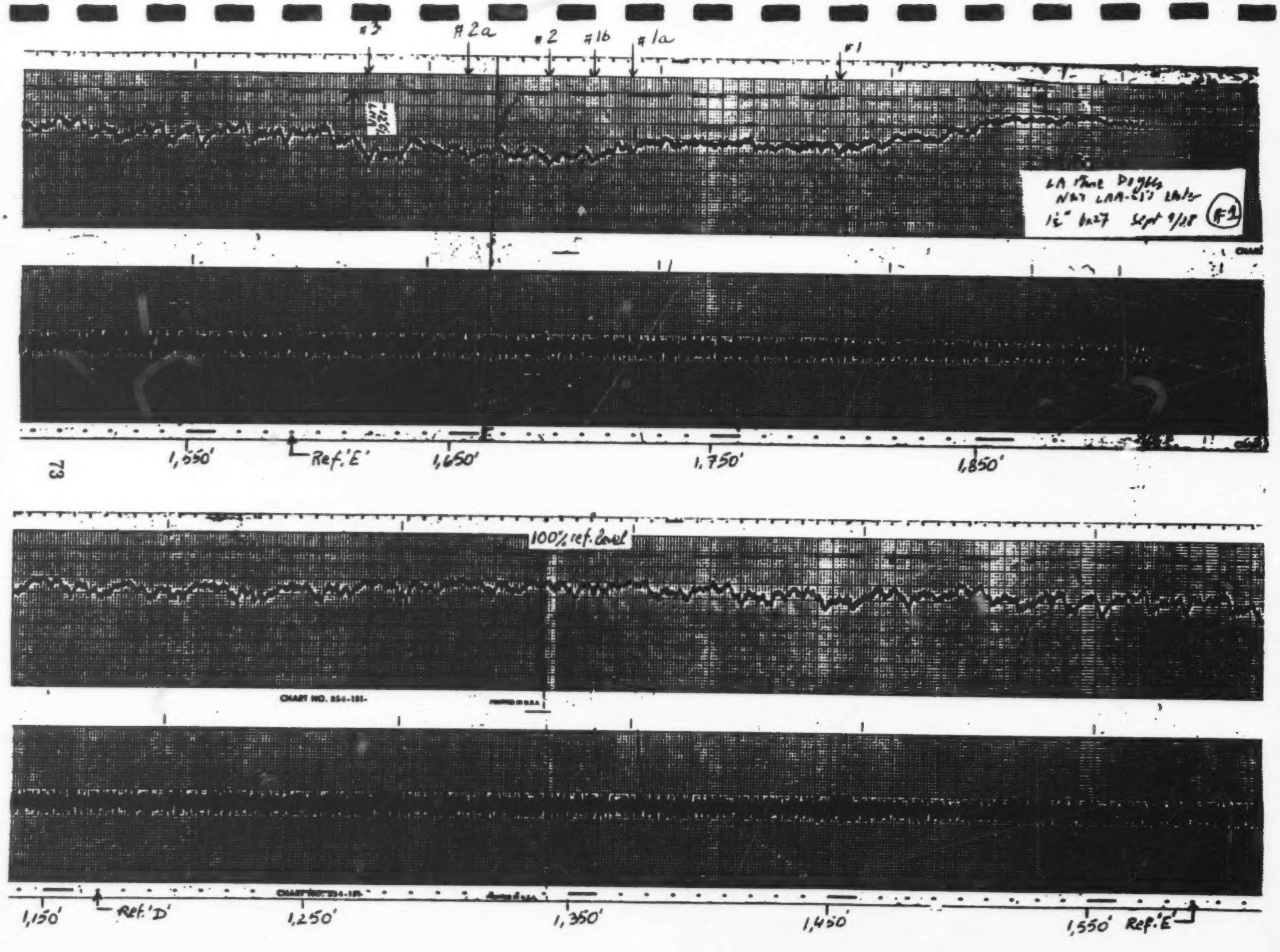

Fig. 4a$_2$ (continued) — 9.9.88 in situ LMA-250 test: as marked by authors, with rope 'rising'

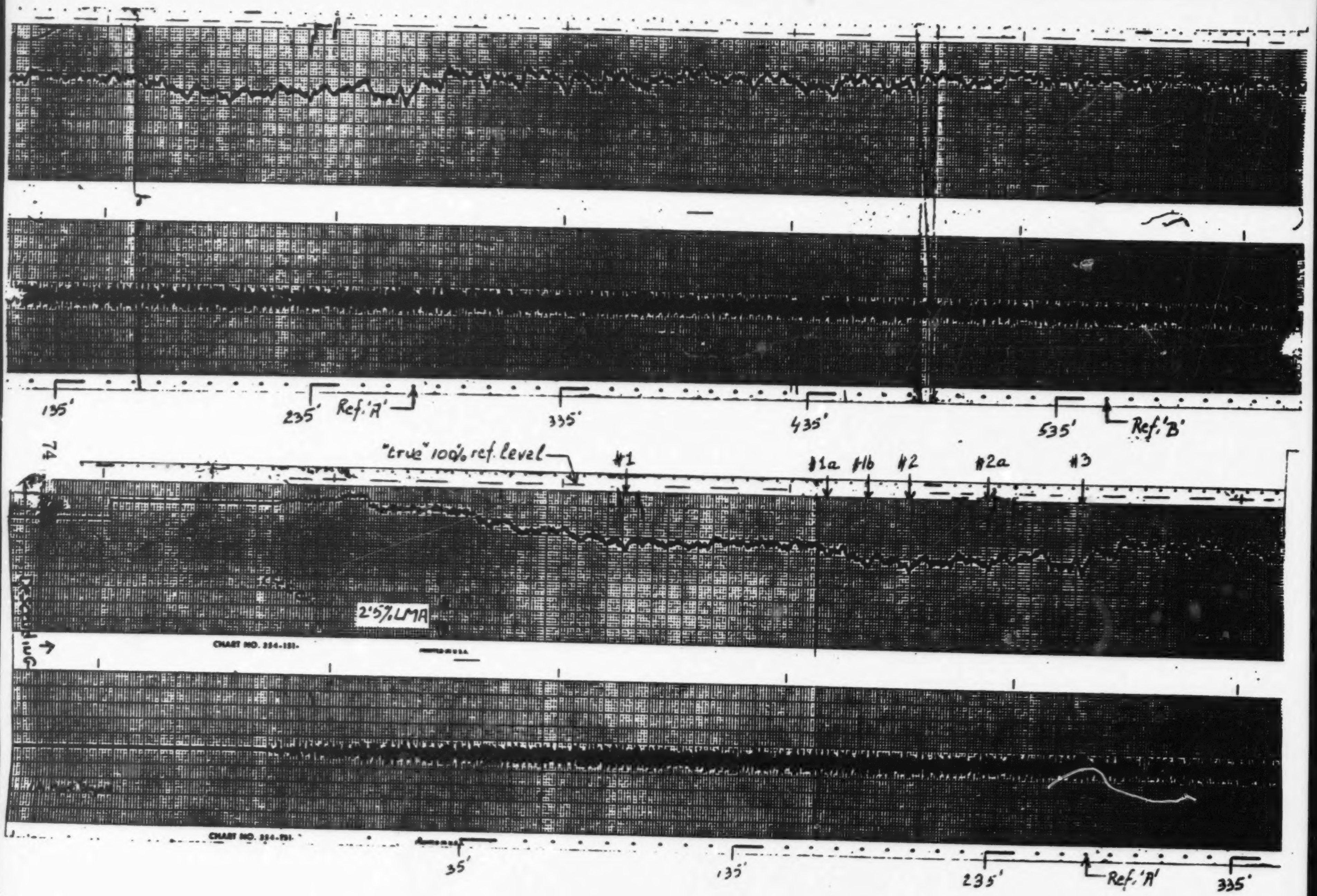

Fig. 4b — 9.9.88 in situ LMA-250 test: as marked by authors, with rope 'descending'

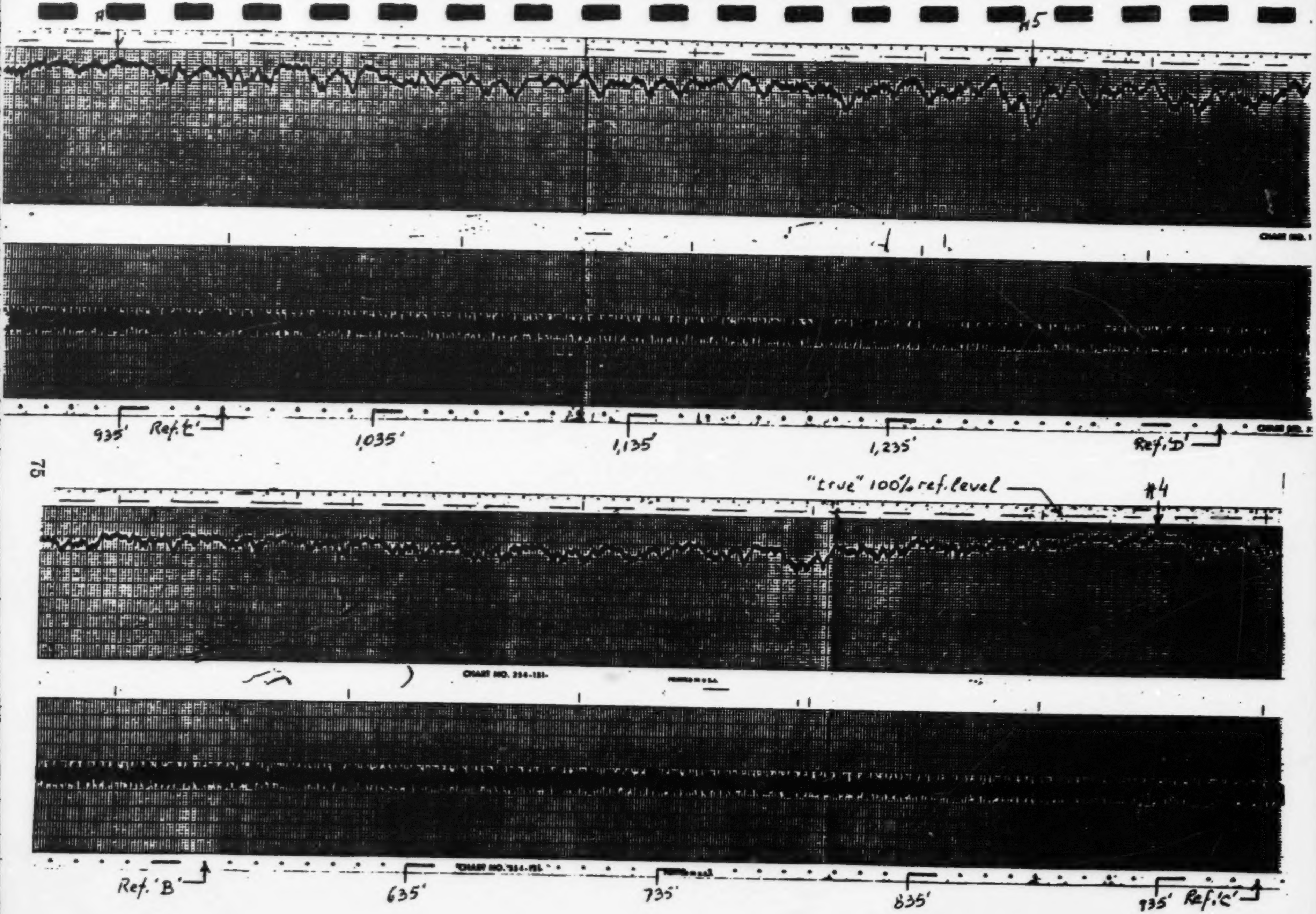

Fig. 4b (continued) — 9.9.88 in situ LMA-250 test: as marked by authors, with rope 'descending'

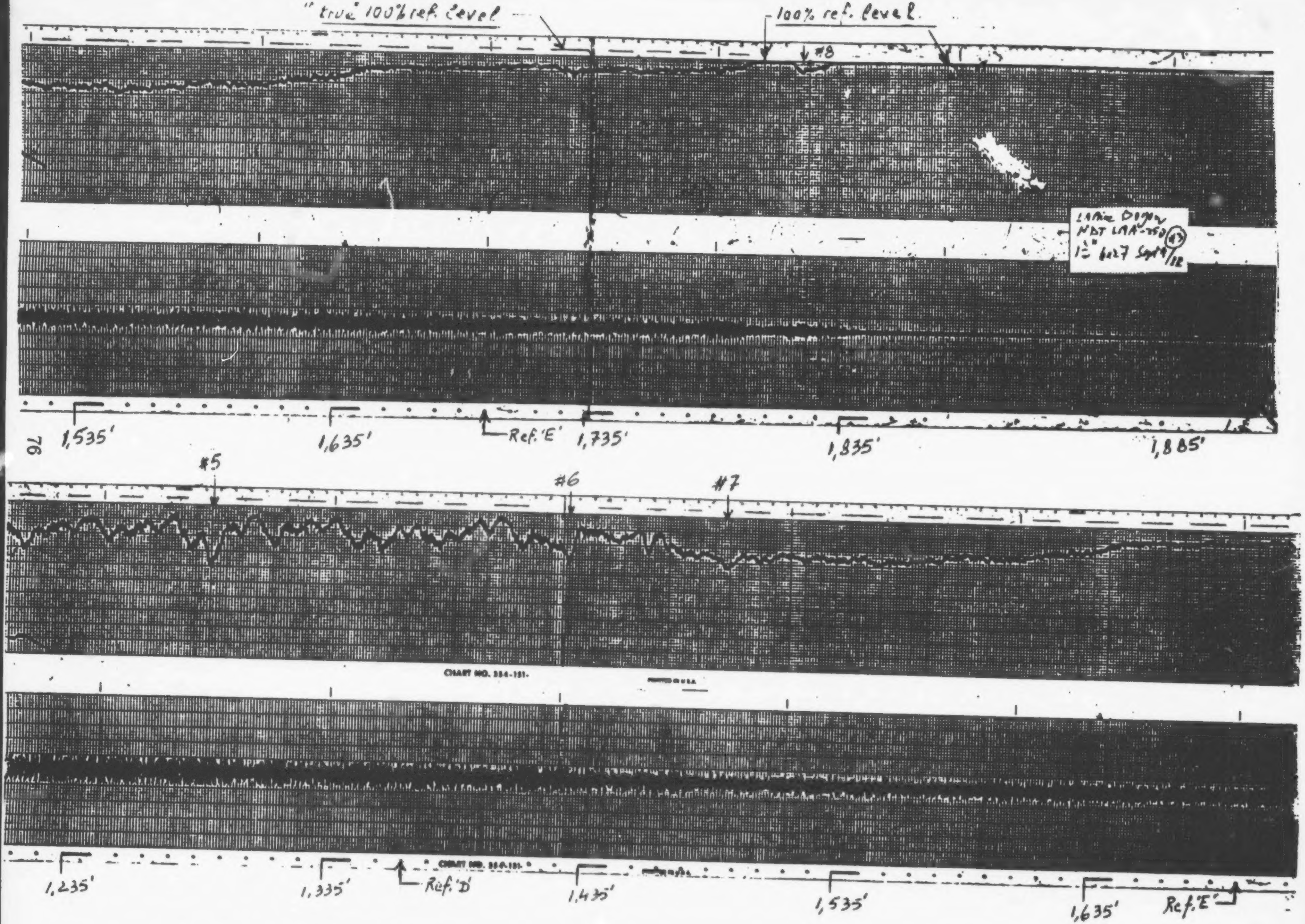

Fig. 4b (continued) — 9.9.88 in situ LMA-250 test; as marked by authors, with rope 'descending'

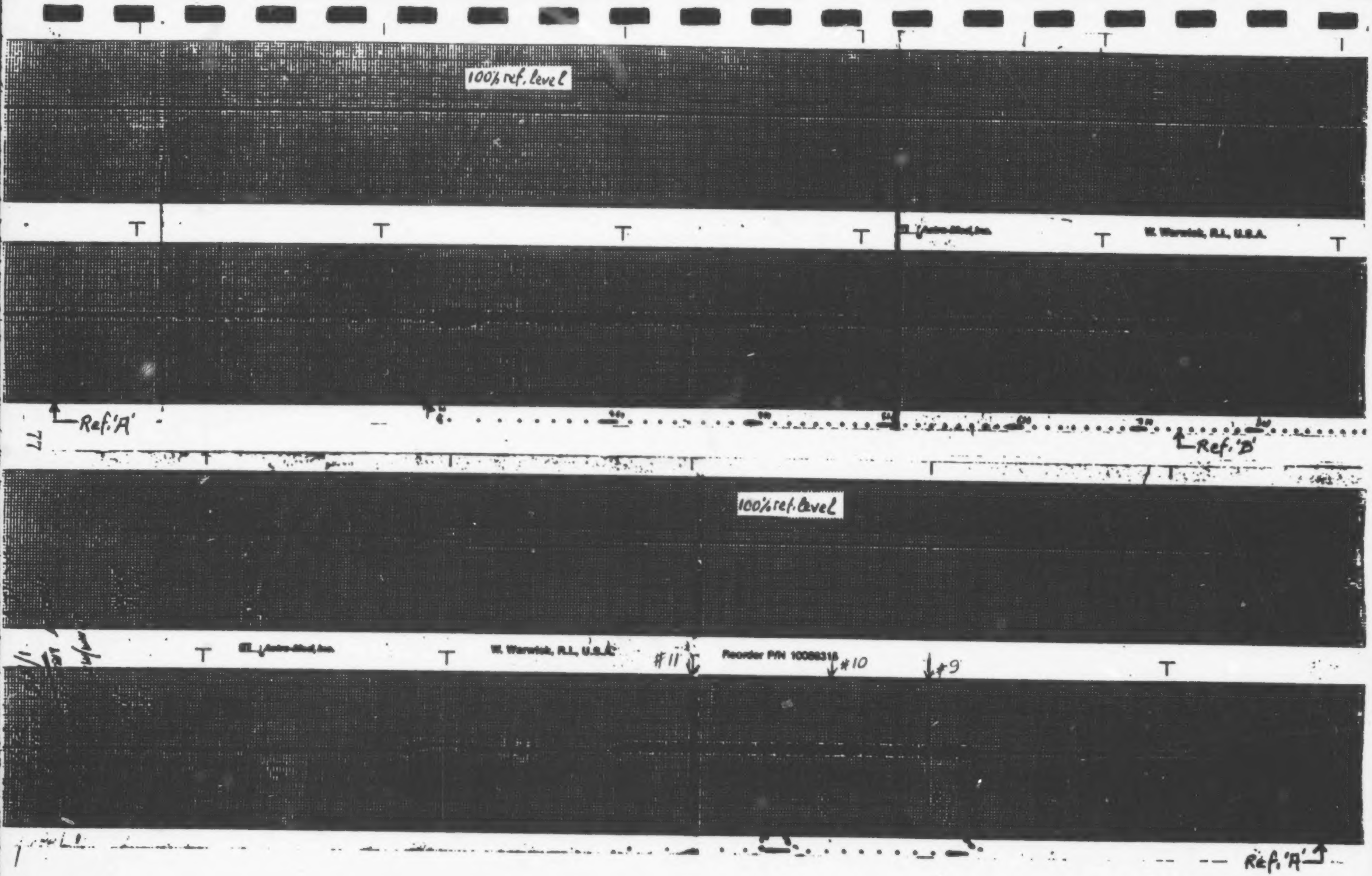

Fig. 4c — 18.1.89 shop-floor LMA-250 test: as marked by authors

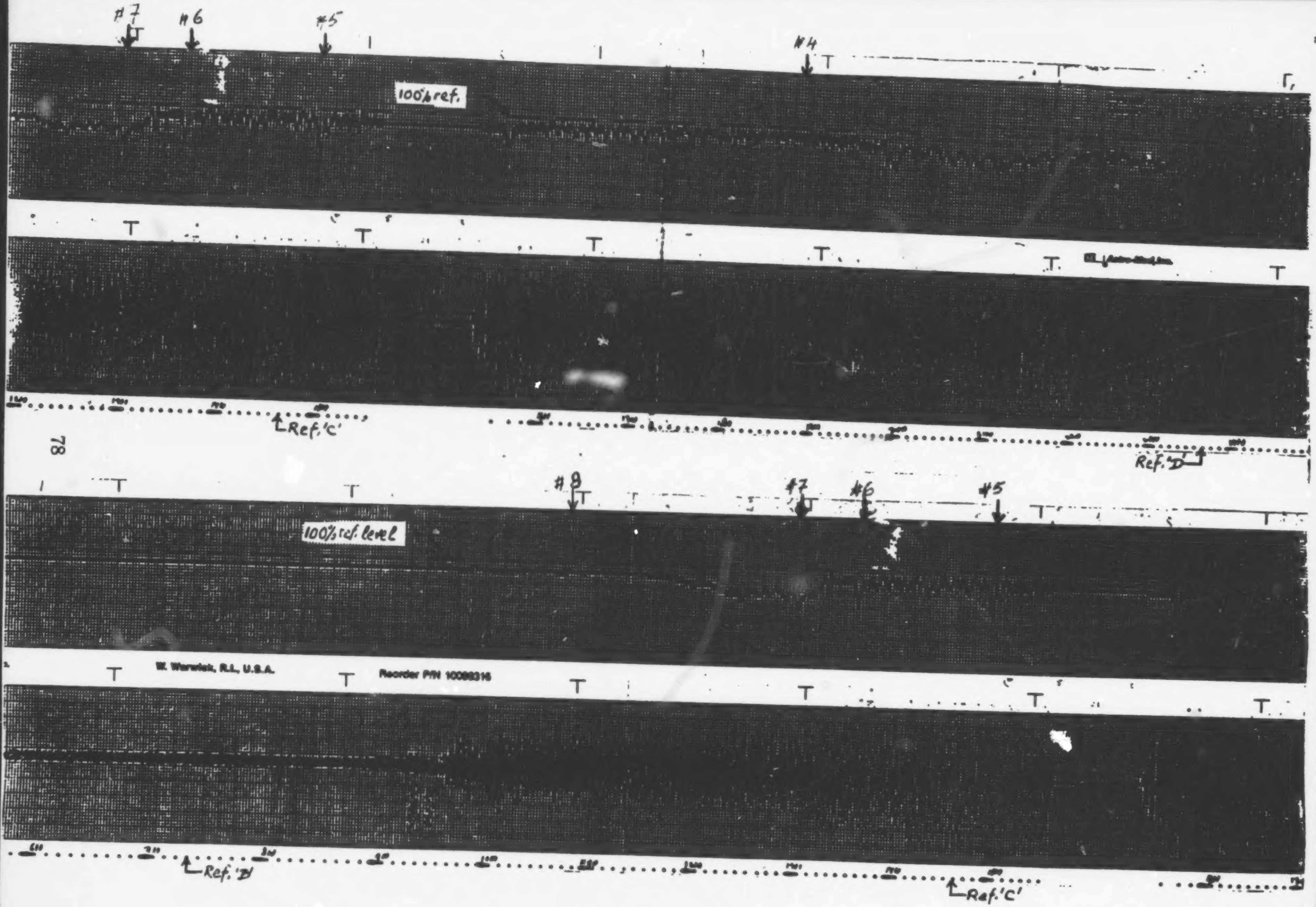

Fig. 4c (continued) — 18.1.89 shop-floor LMA-250 test: as marked by authors

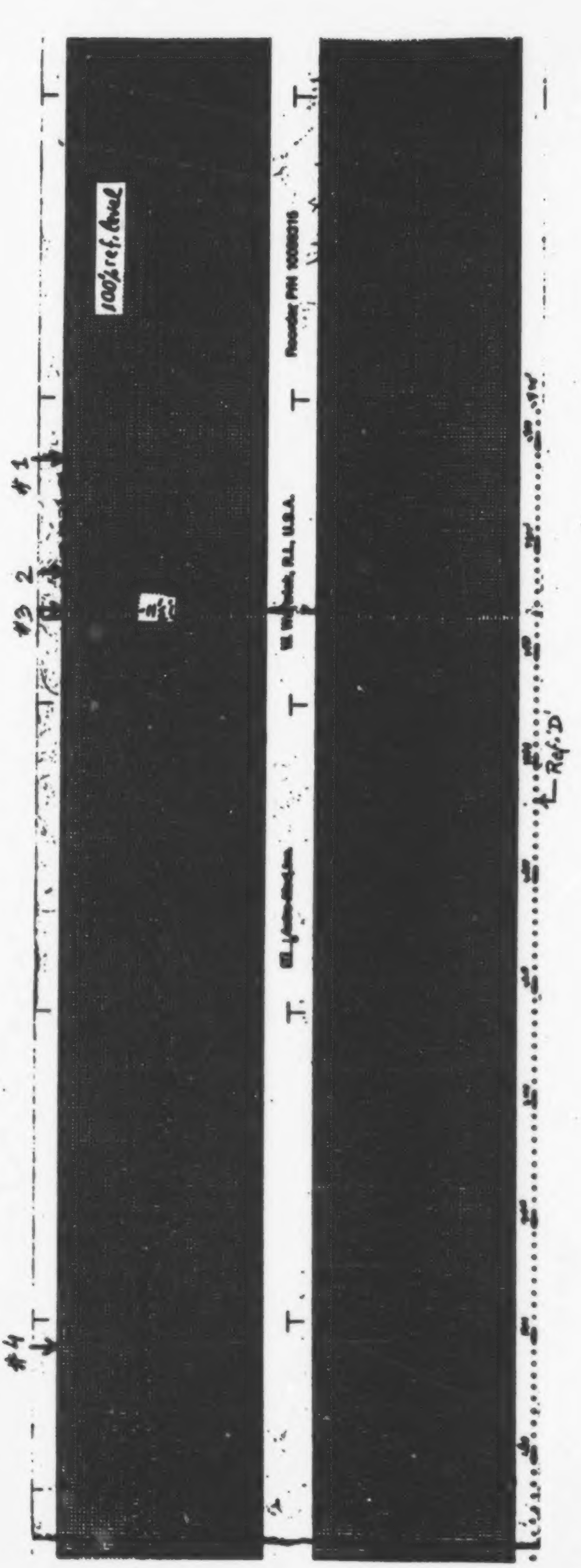

Fig. 4c (continued) — 18.1.89 shop-floor LMA-250 test: as marked by authors

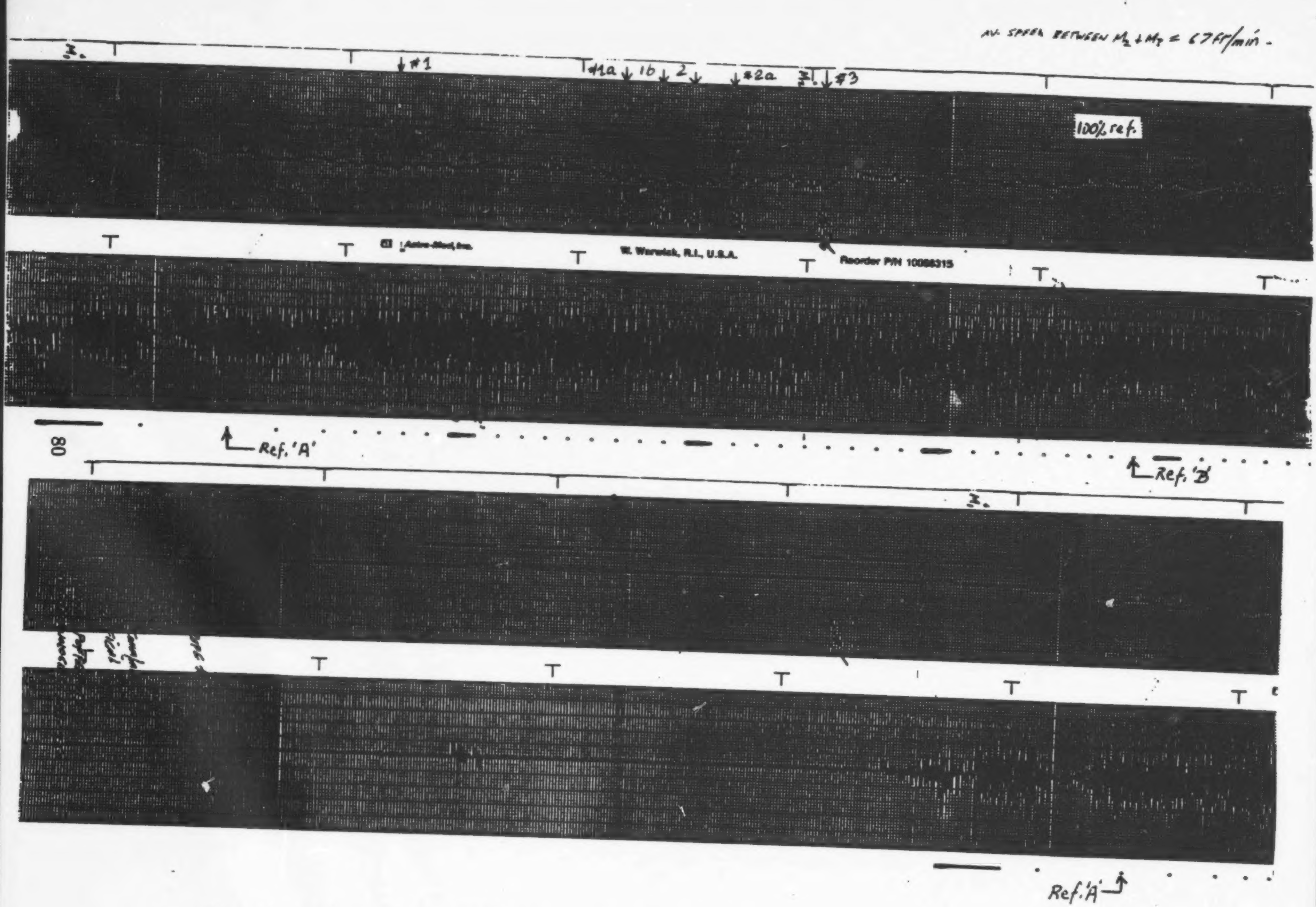

Fig. 4d — 4.4.89 shop-floor LMA-250 test: as submitted by operator and additionally marked by authors

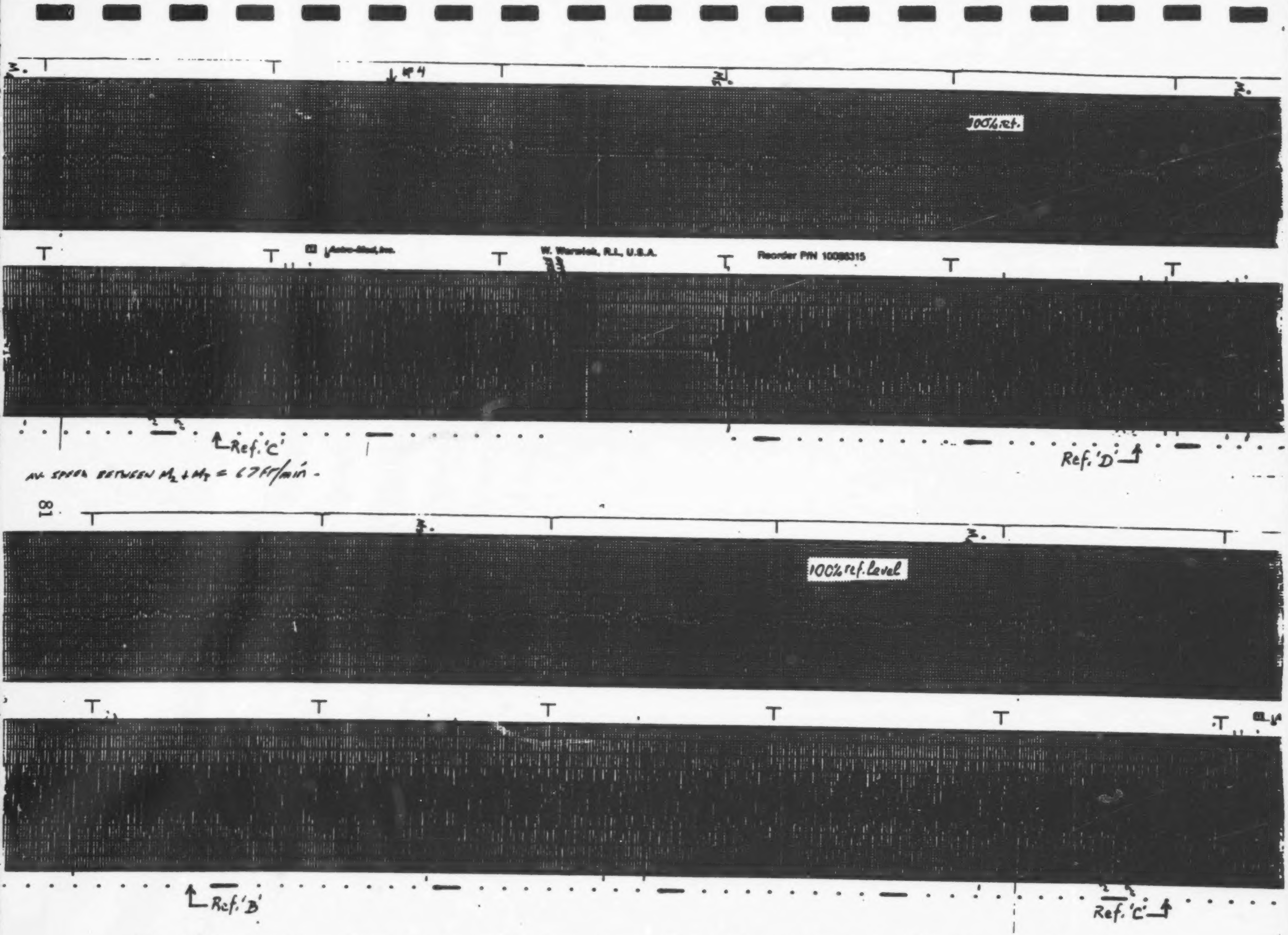

Fig. 4d (continued) — 4.4.89 shop-floor LMA-250 test: as submitted by operator and additionally marked by authors

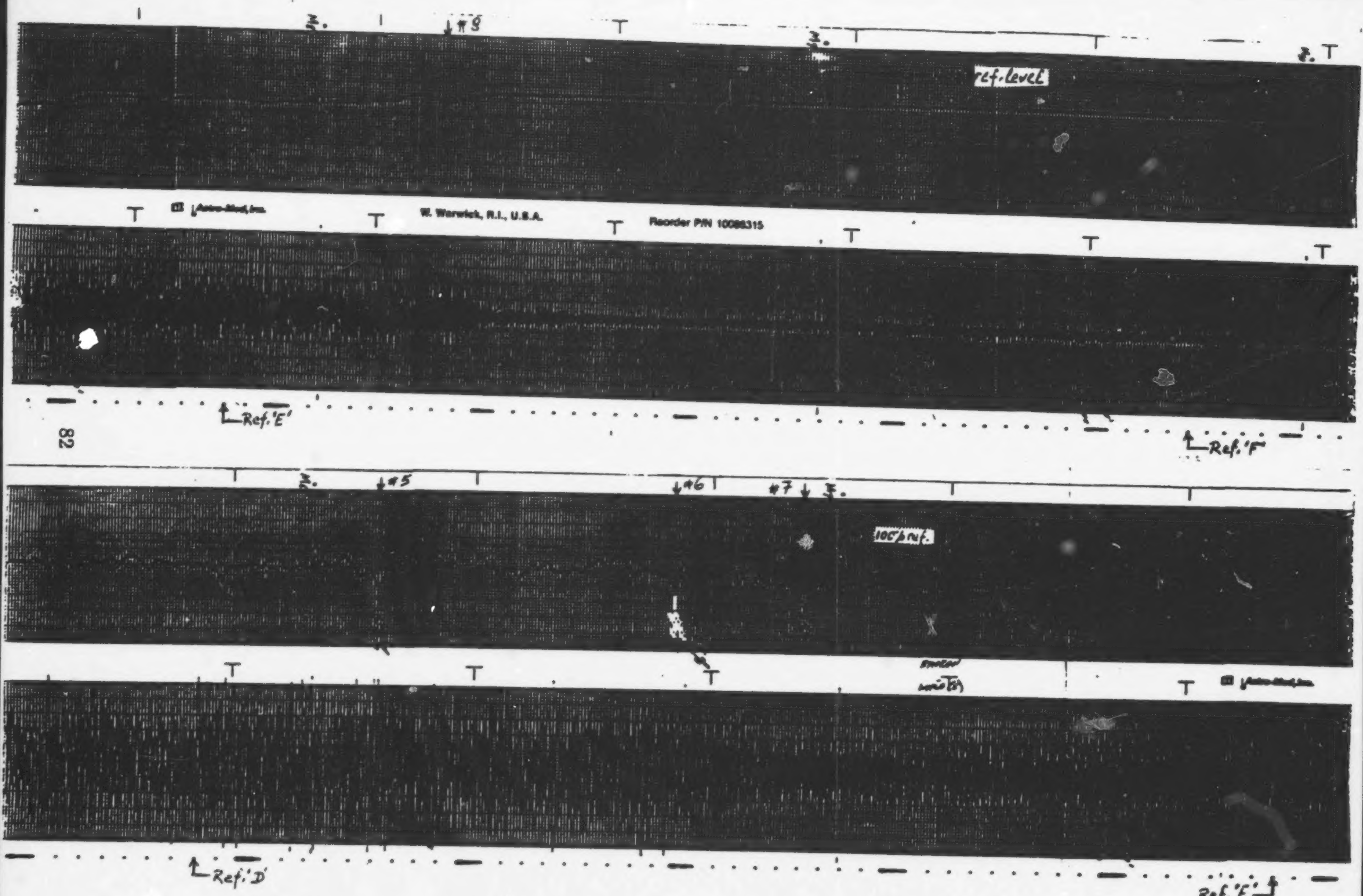

Fig. 4d (continued) — 4.4.89 shop-floor LMA-250 test: as submitted by operator and additionally marked by authors

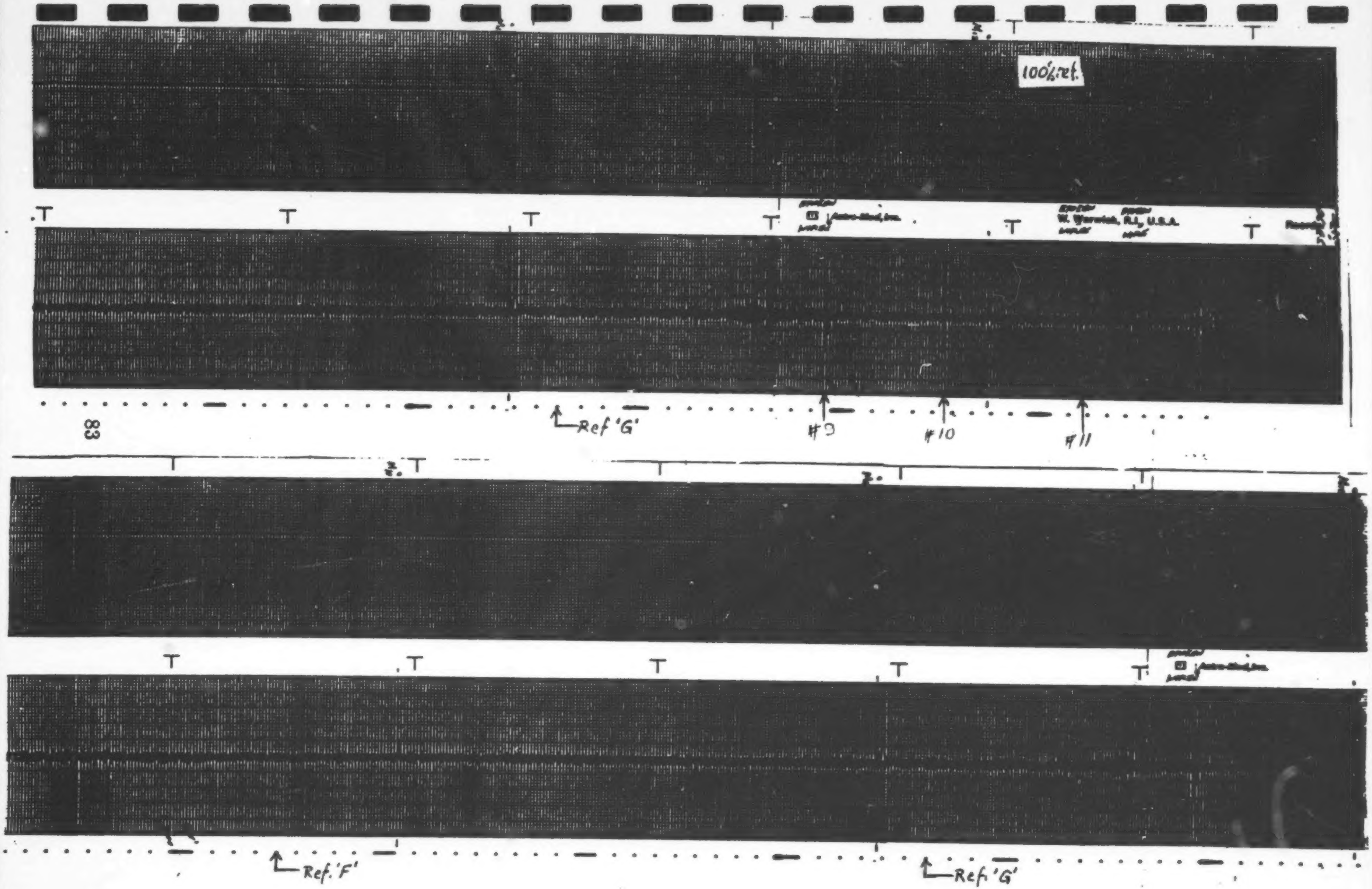

Fig. 4d (continued) — 4.4.89 shop-floor LMA-250 test: as submitted by operator and additionally marked by authors

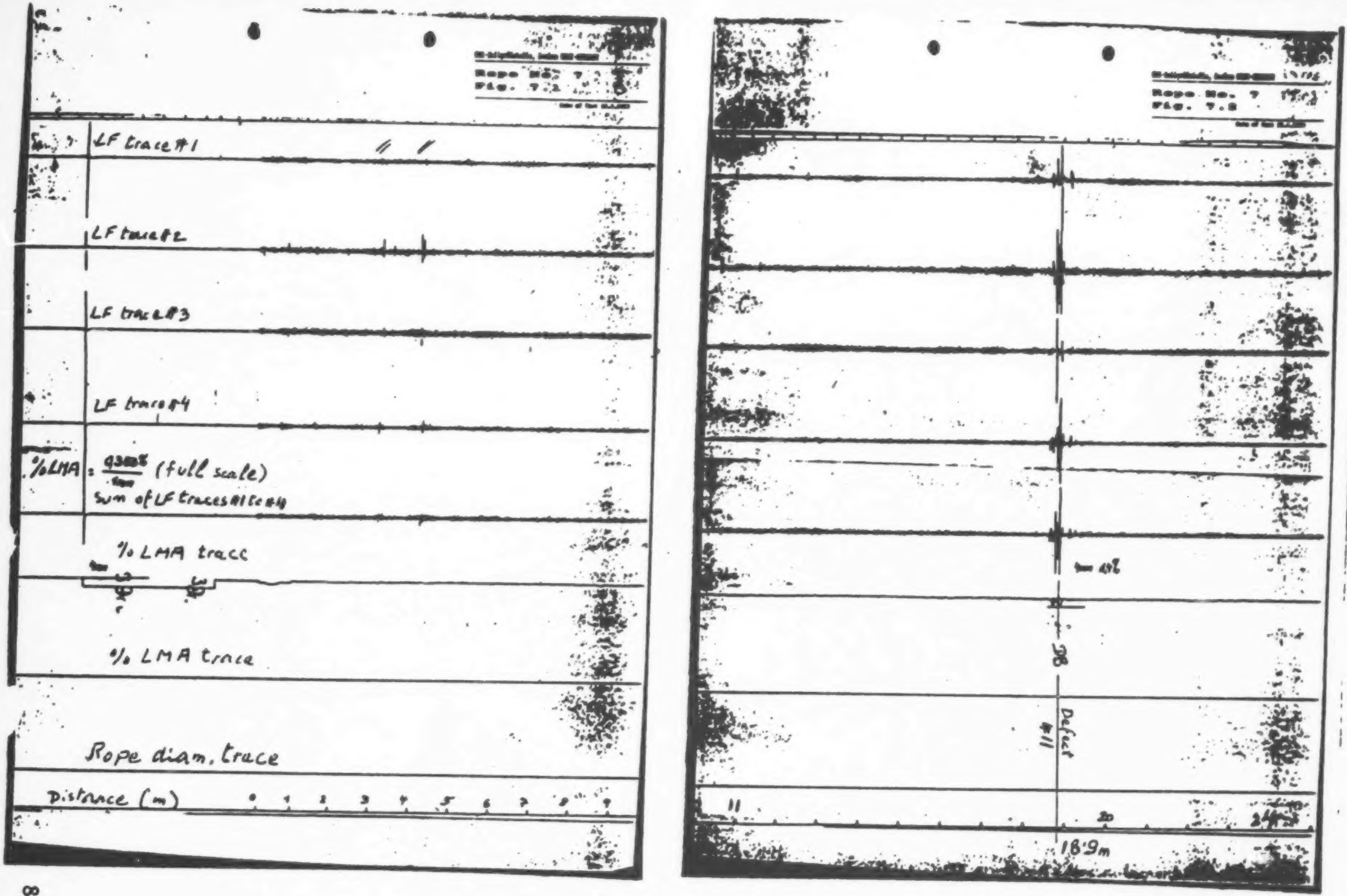

Fig. 5 — 10.4.89 shop-floor WBK test: as submitted by the operators and additionally marked by authors

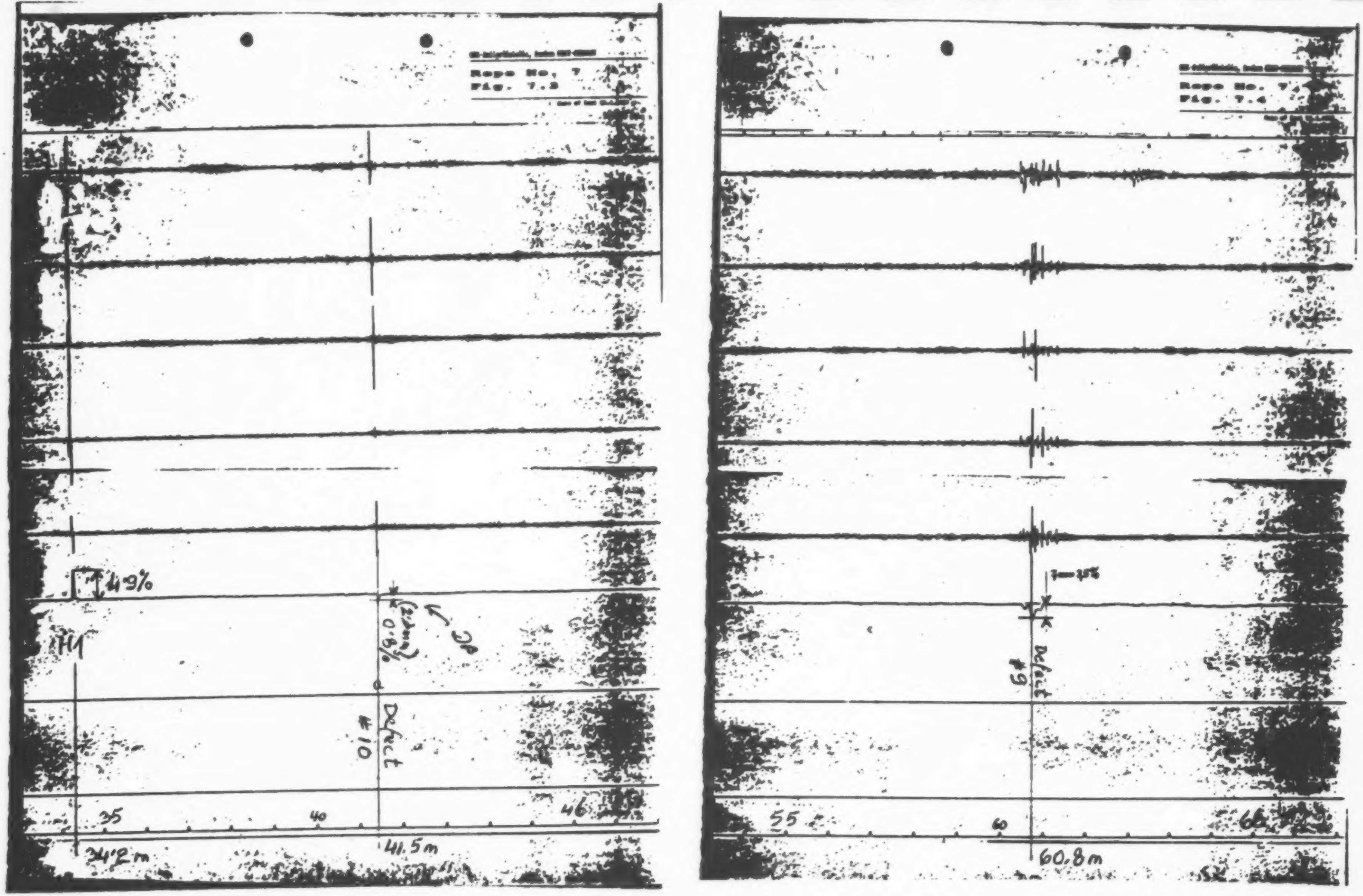

Fig. 5 (continued) — 10.4.89 shop-floor WBK test: as submitted by the operators and additionally marked by authors

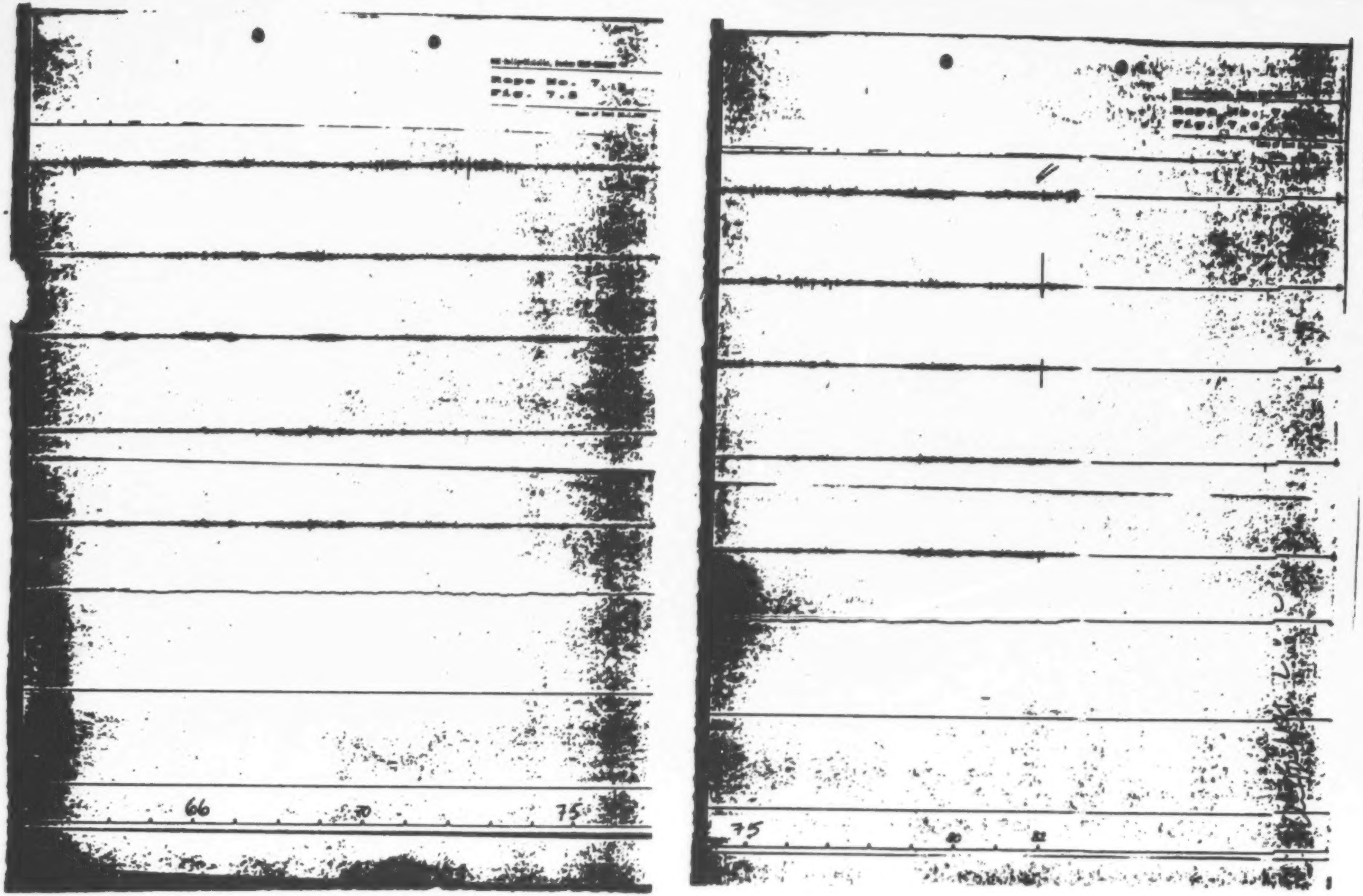

Fig. 5 (continued) — 10.4.89 shop-floor WBK test: as submitted by the operators and additionally marked by authors

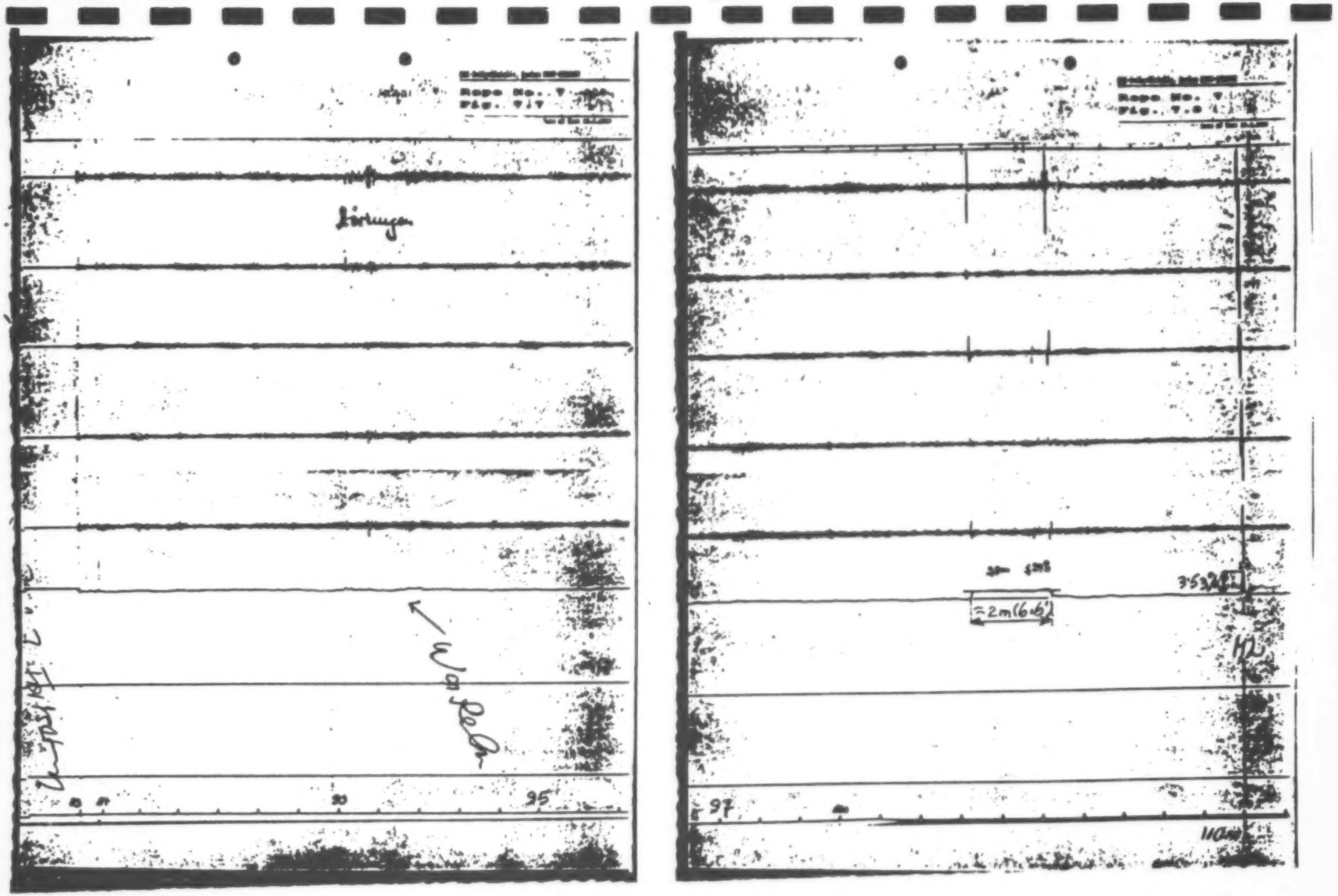

Fig. 5 (continued) — 10.4.89 shop-floor WBK test: as submitted by the operators and additionally marked by authors

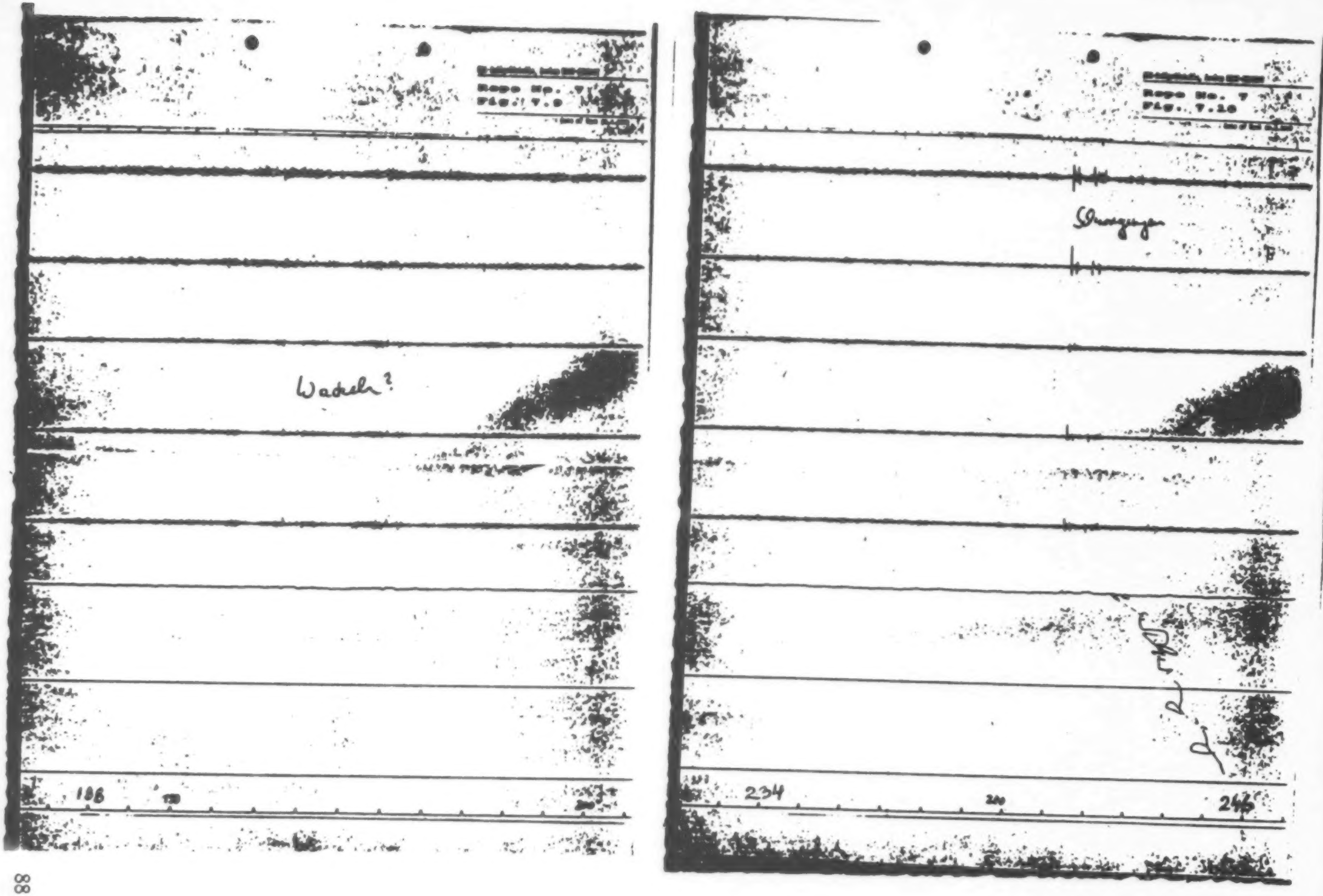

Fig. 5 (continued) — 10.4.89 shop-floor WBK test: as submitted by the operators and additionally marked by authors

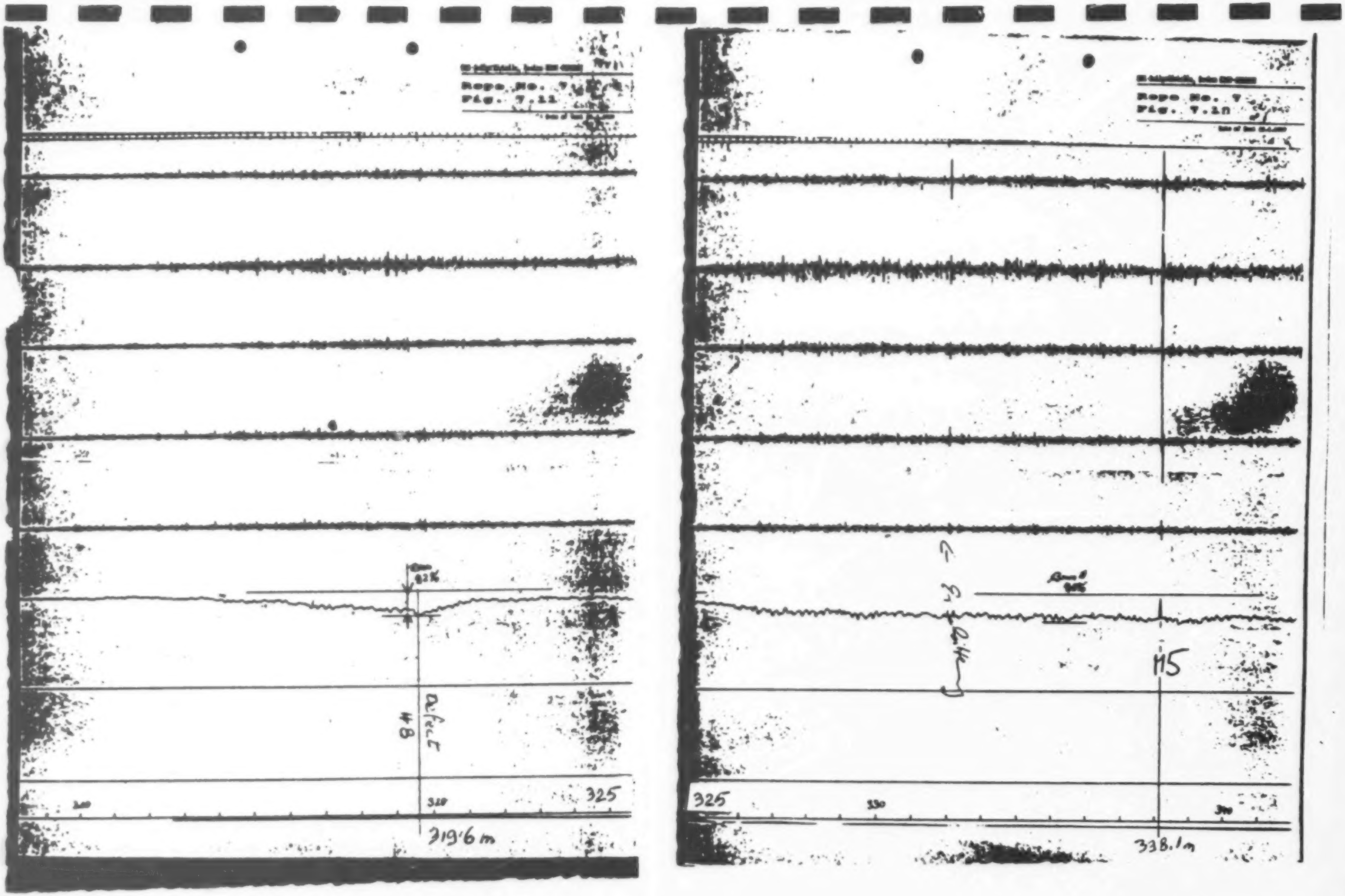

Fig. 5 (continued) — 10.4.89 shop-floor WBK test: as submitted by the operators and additionally marked by authors

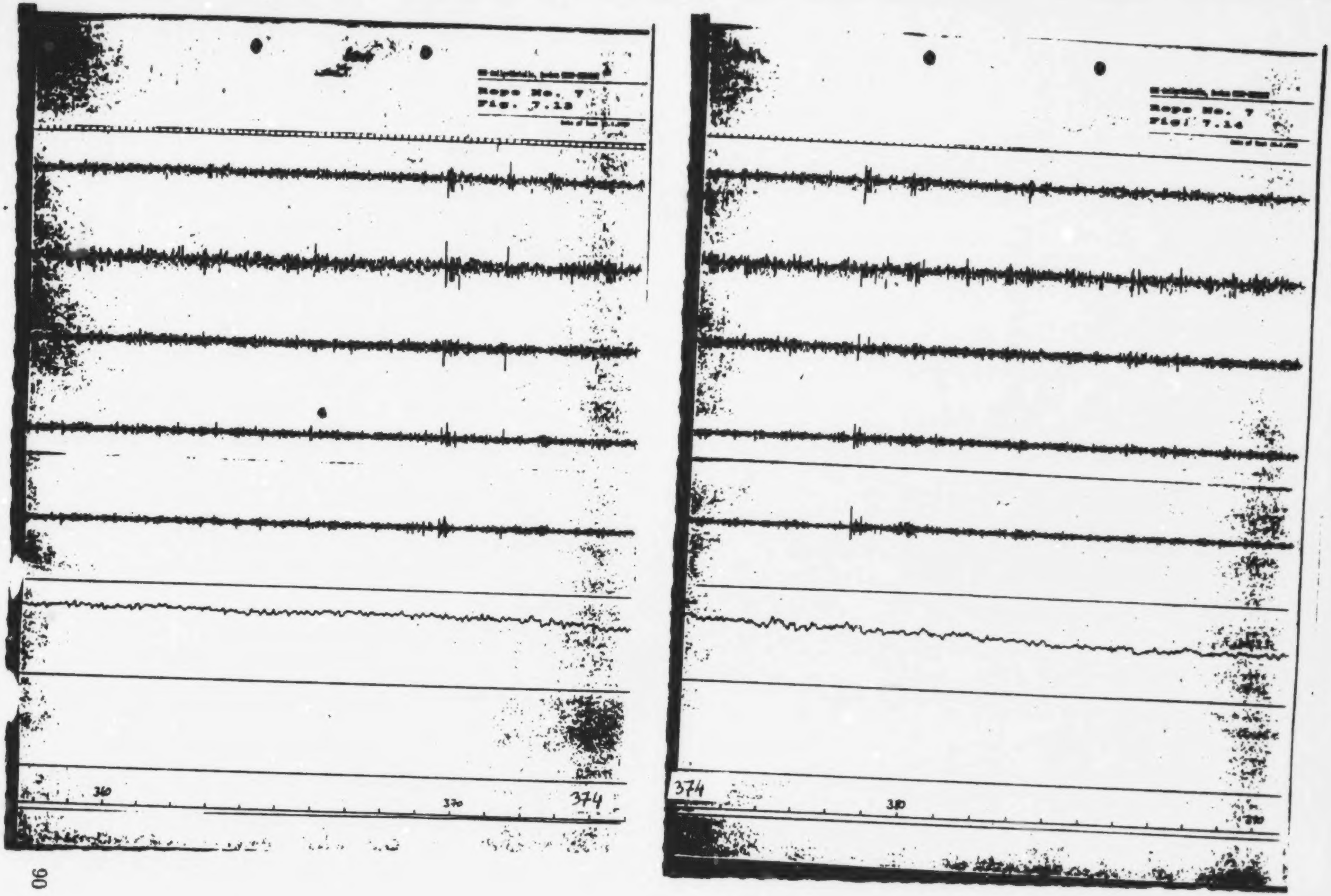

Fig. 5 (continued) — 10.4.89 shop-floor WBK test: as submitted by the operators and additionally marked by authors

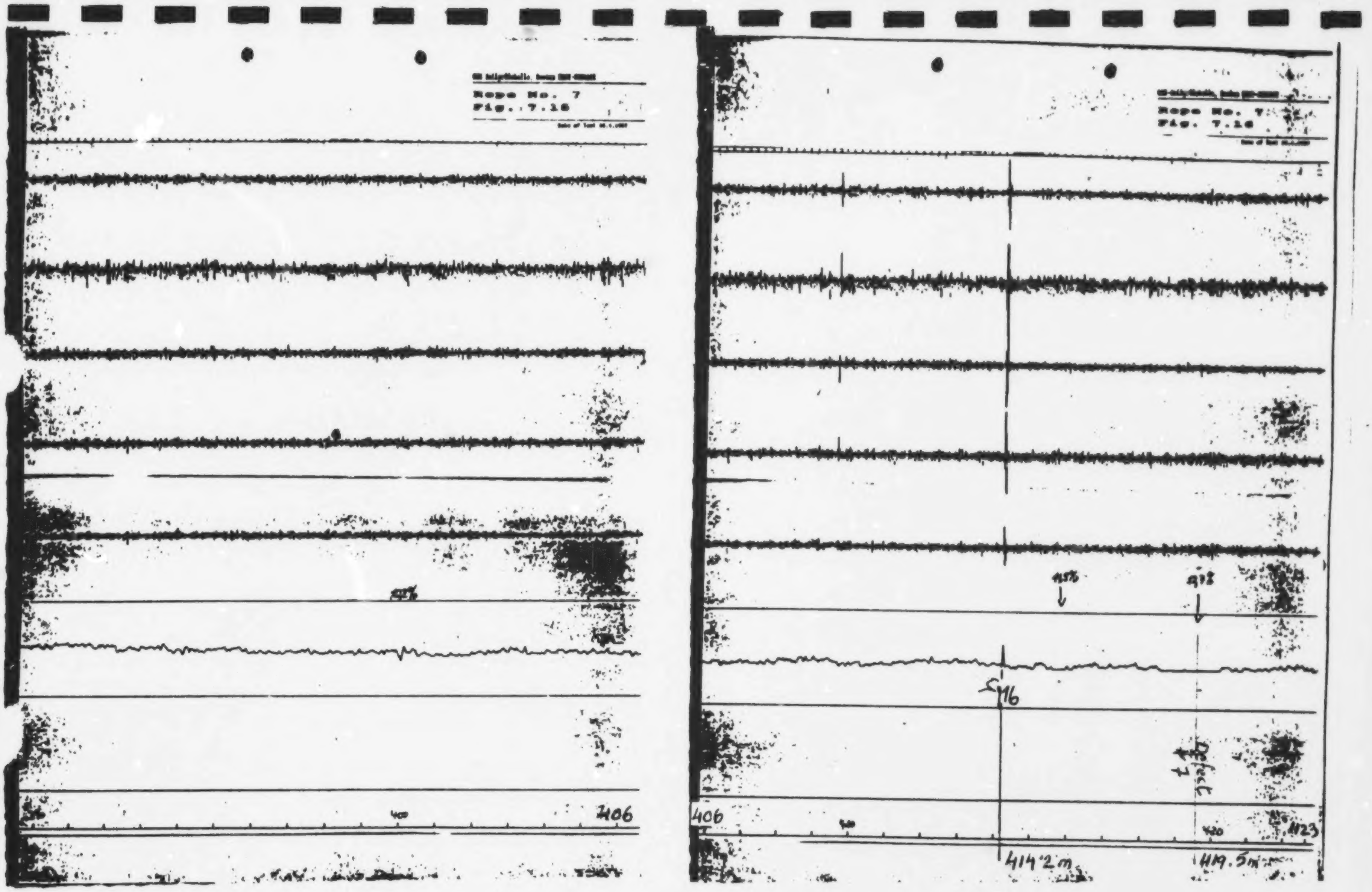

Fig. 5 (continued) — 10.4.89 shop-floor WBK test: as submitted by the operators and additionally marked by authors

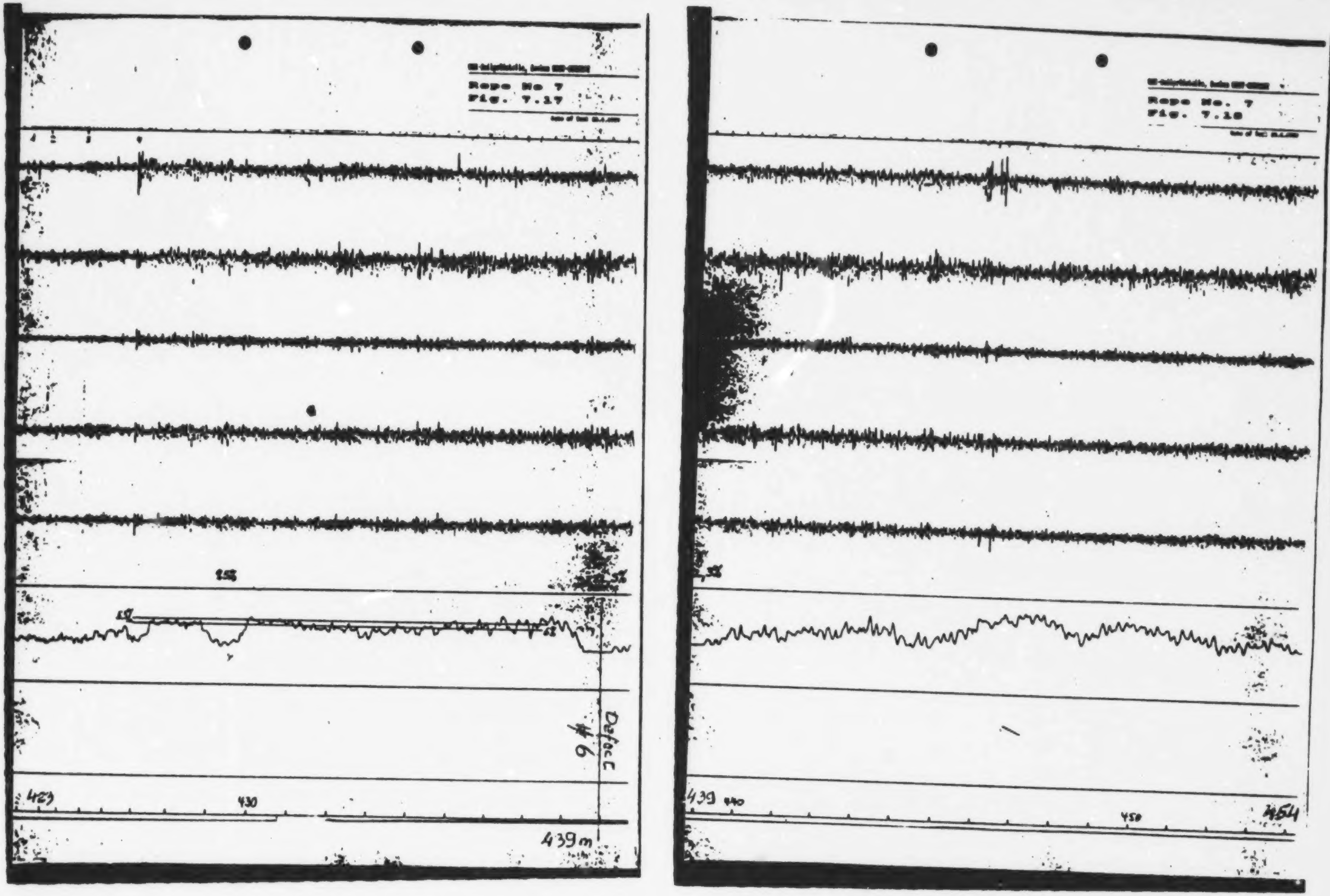

Fig. 5 (continued) — 10.4.89 shop-floor WBK test: as submitted by the operators and additionally marked by authors

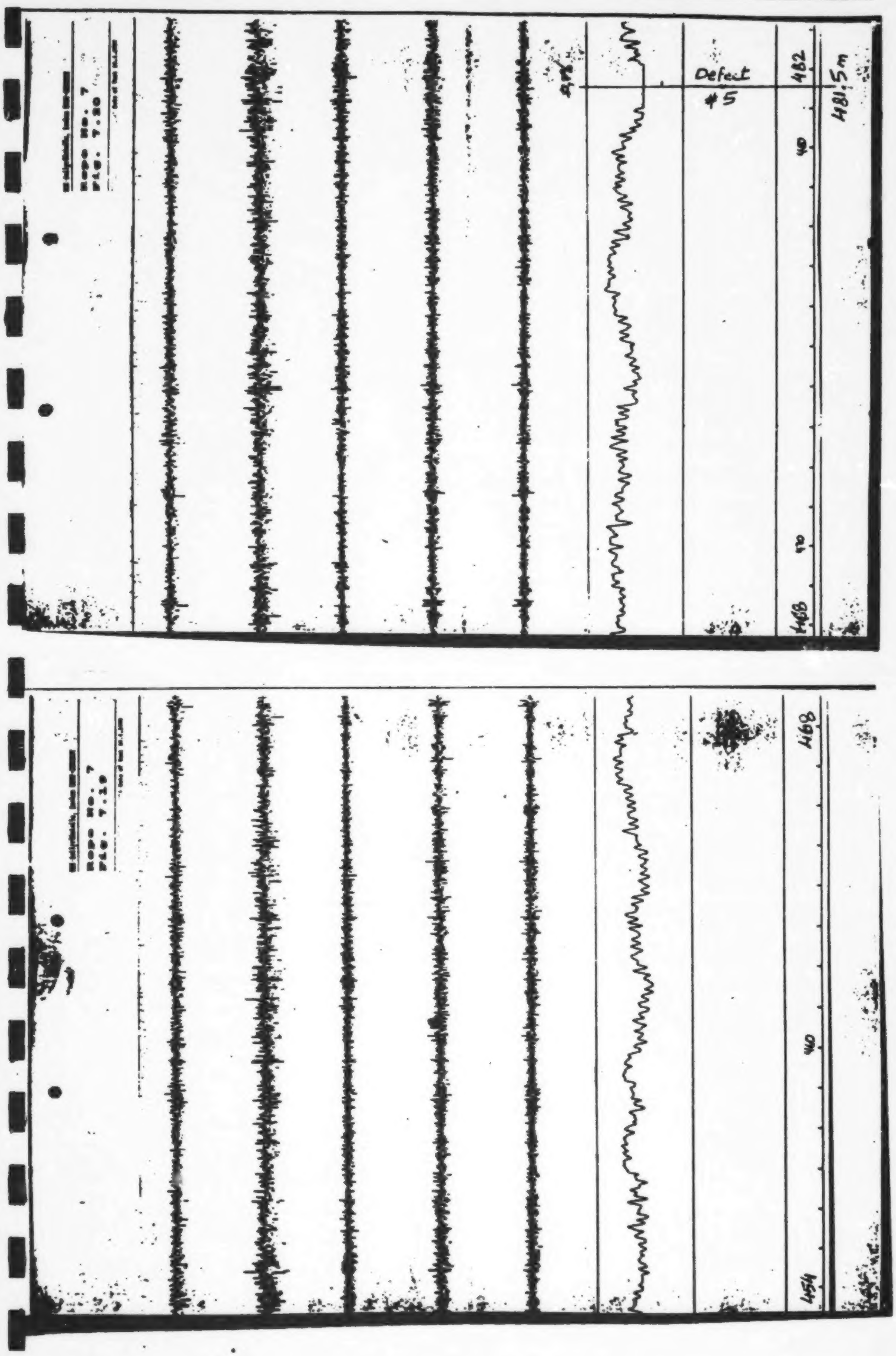

Fig. 5 (continued) — 10.4.89 shop-floor WBK test: as submitted by the operators and additionally marked by authors

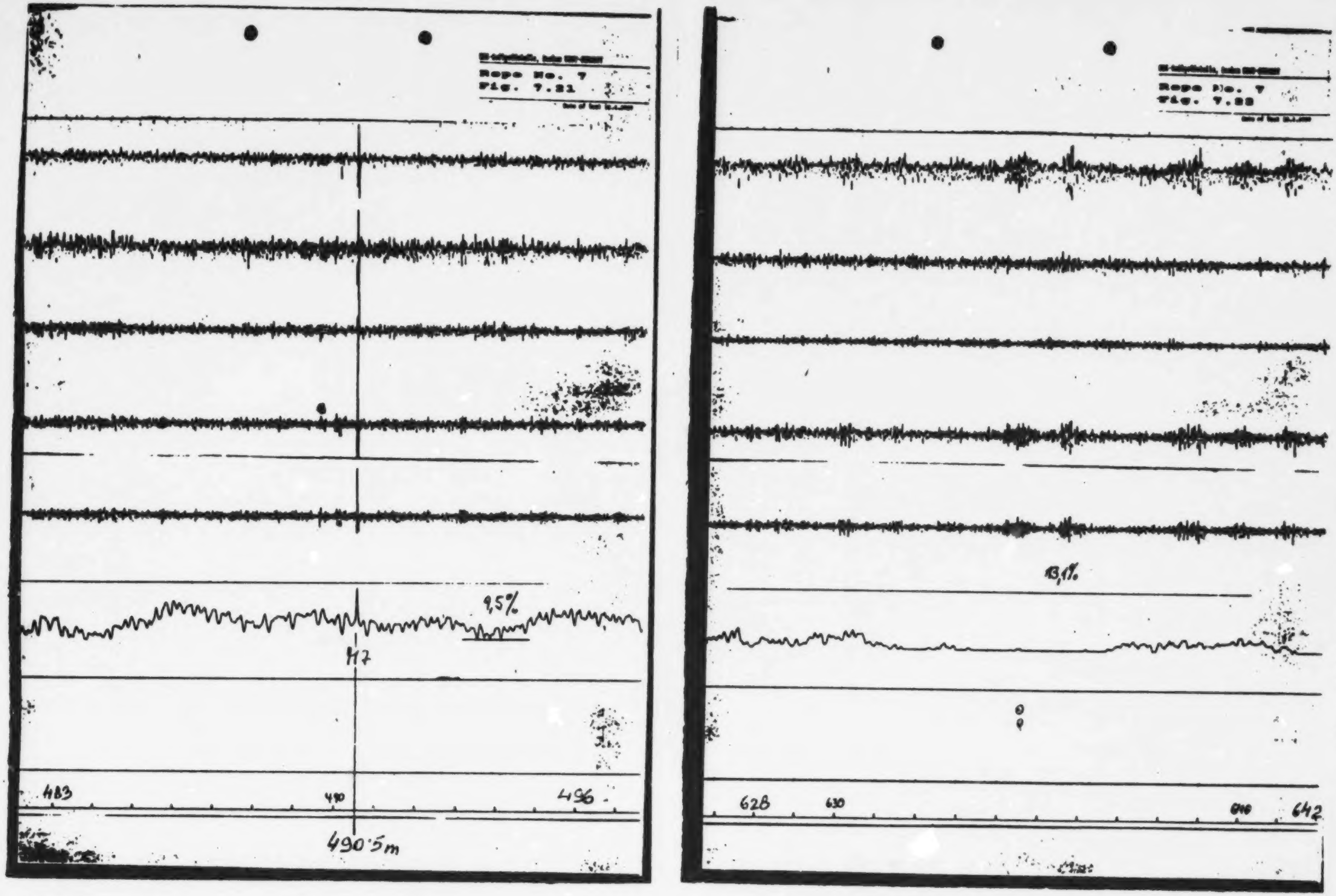

Fig. 5 (continued) — 10.4.89 shop-floor WBK test: as submitted by the operators and additionally marked by authors

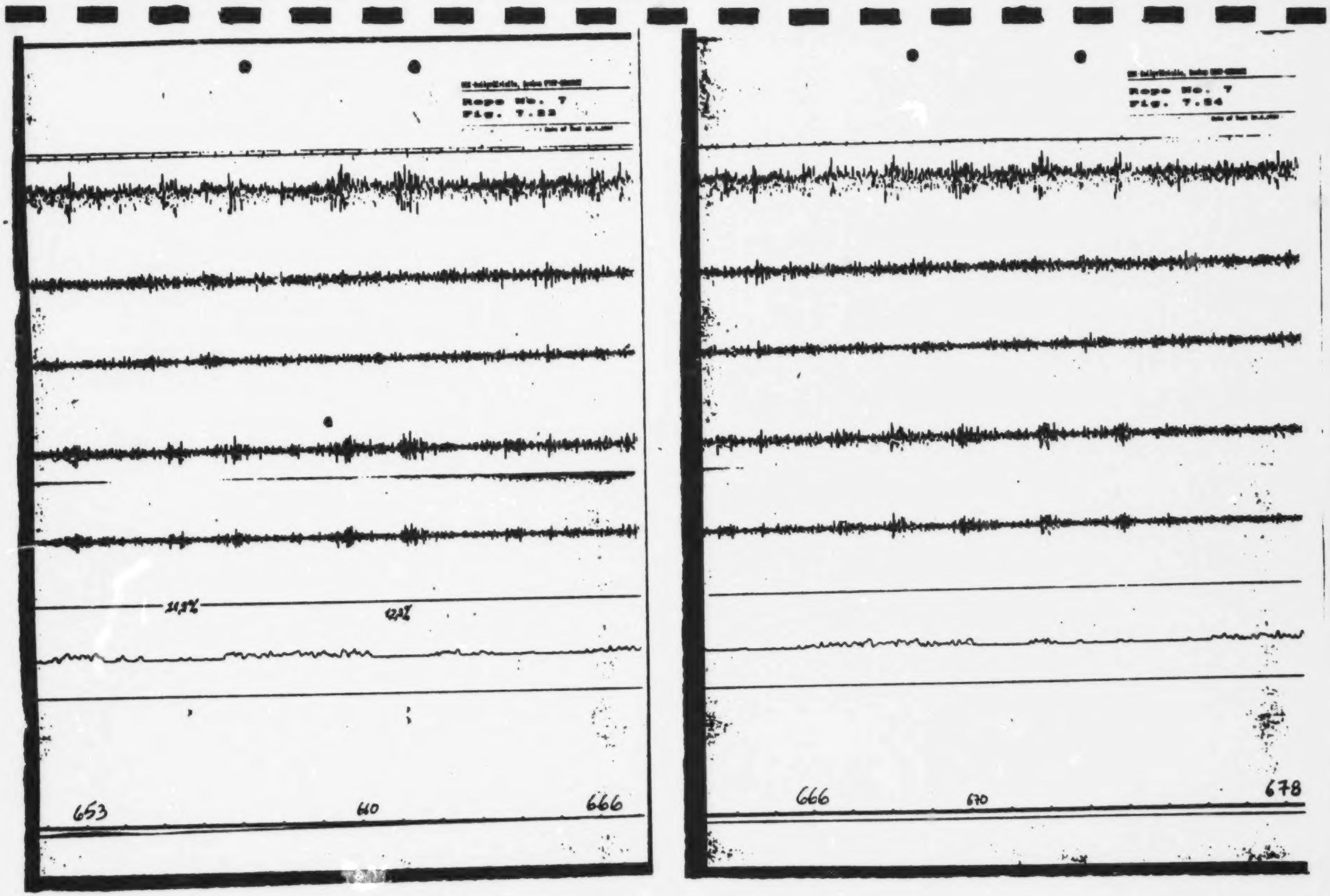

Fig. 5 (continued) — 10.4.89 shop-floor WBK test: as submitted by the operators and additionally marked by authors

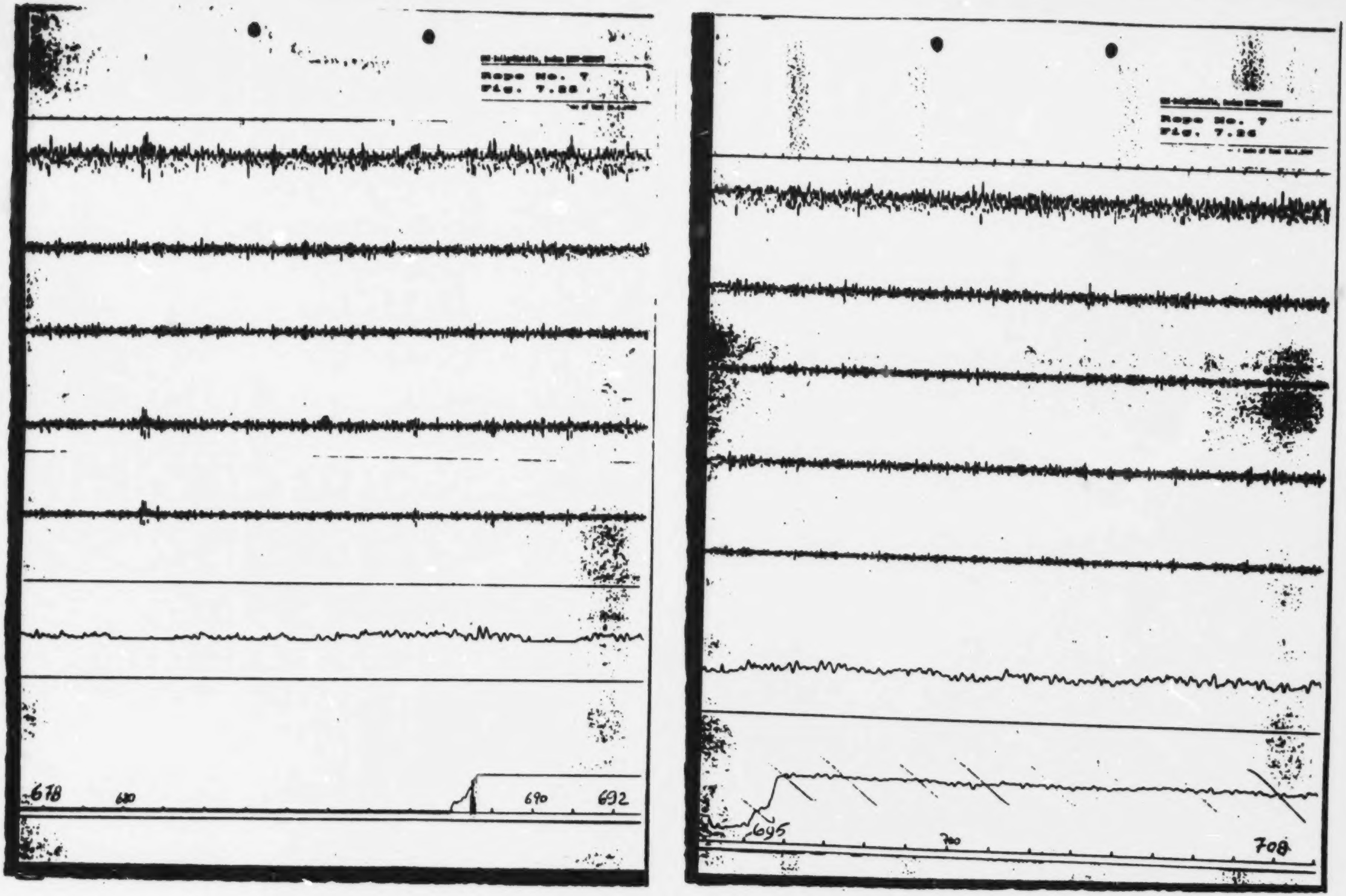

Fig. 5 (continued) — 10.4.89 shop-floor WBK test: as submitted by the operators and additionally marked by authors

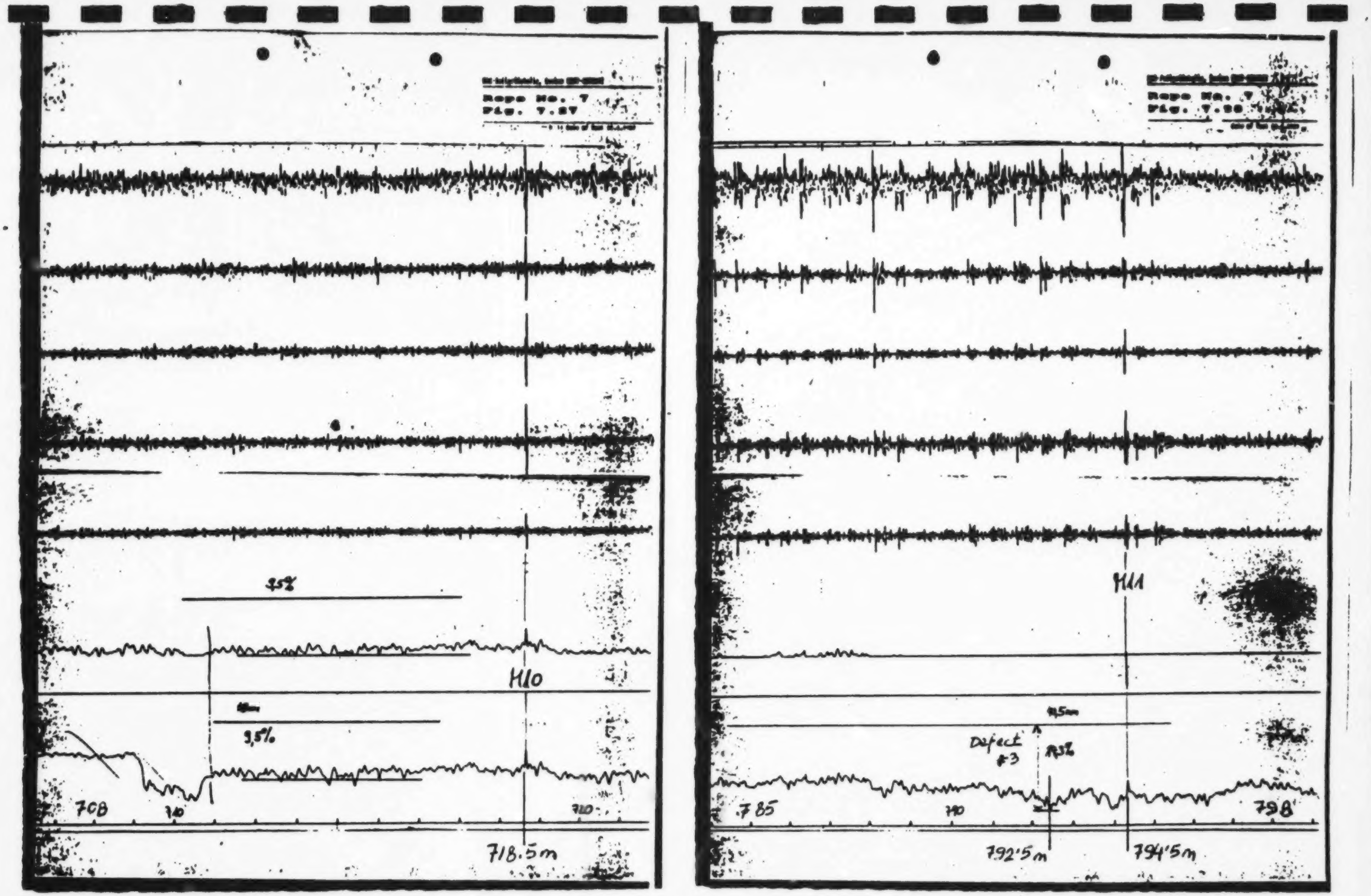

Fig. 5 (continued) — 10.4.89 shop-floor WBK test: as submitted by the operators and additionally marked by authors

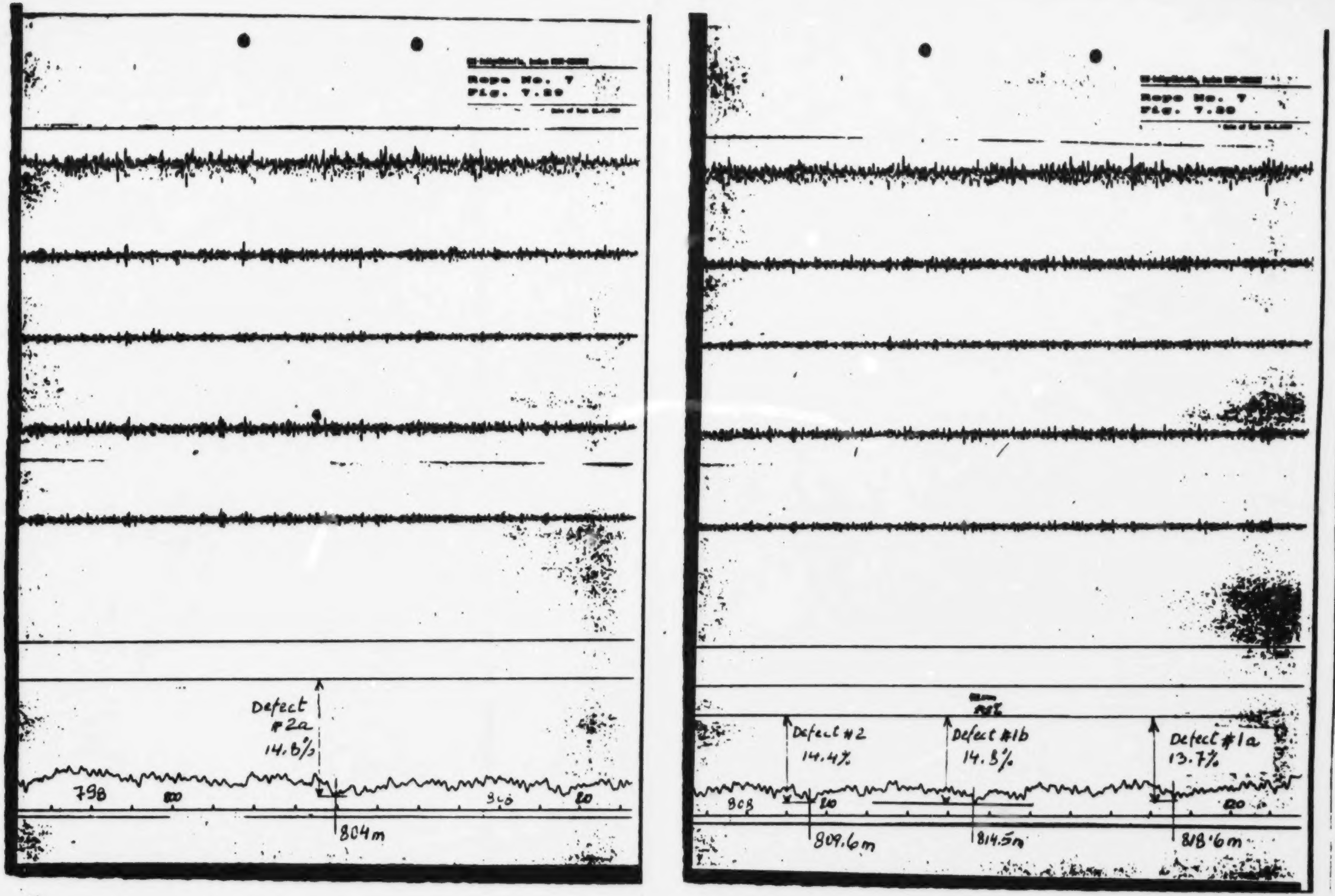

Fig. 5 (continued) — 10.4.89 shop-floor WBK test: as submitted by the operators and additionally marked by authors

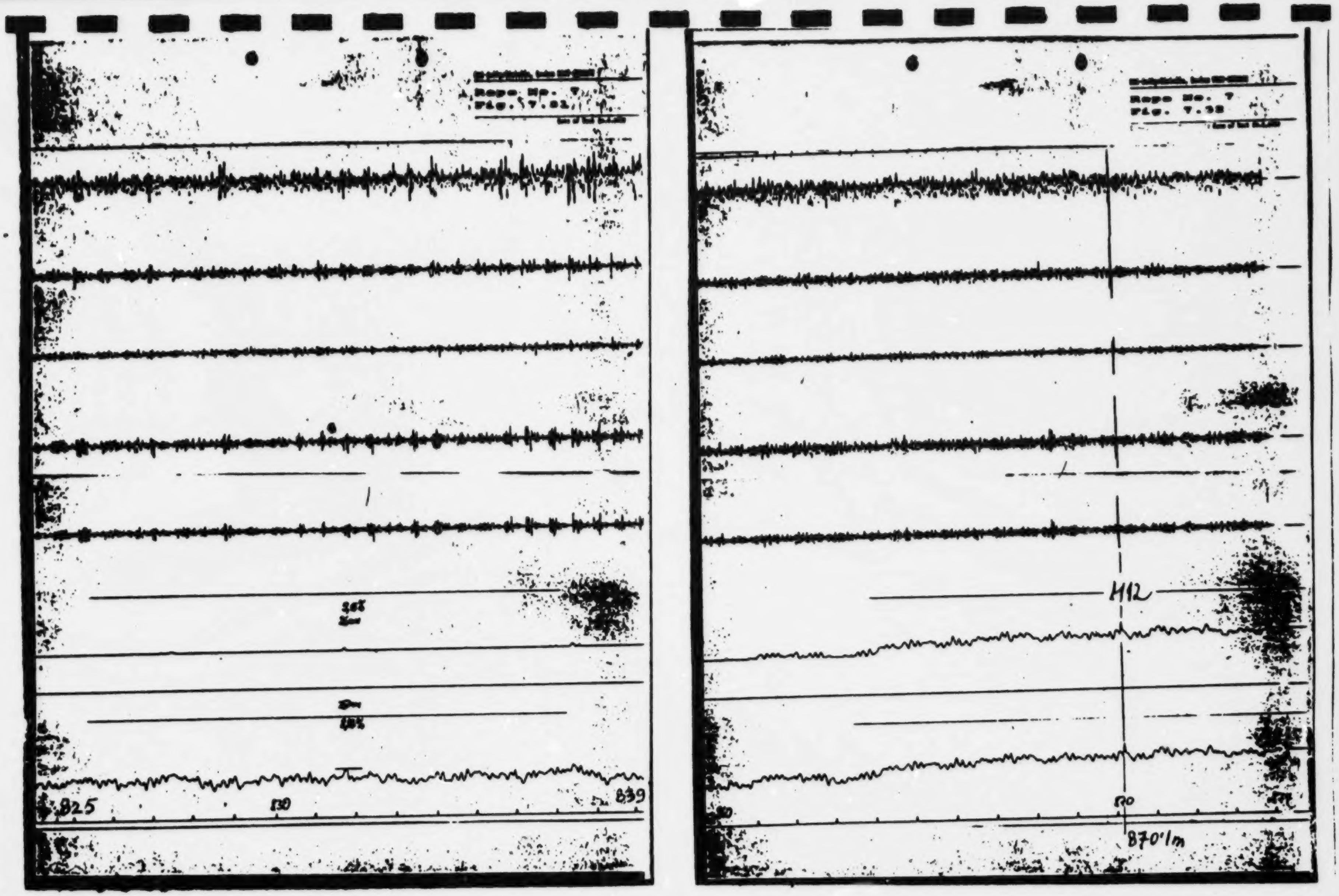

Fig. 5 (continued) — 10.4.89 shop-floor WBK test: as submitted by the operators and additionally marked by authors

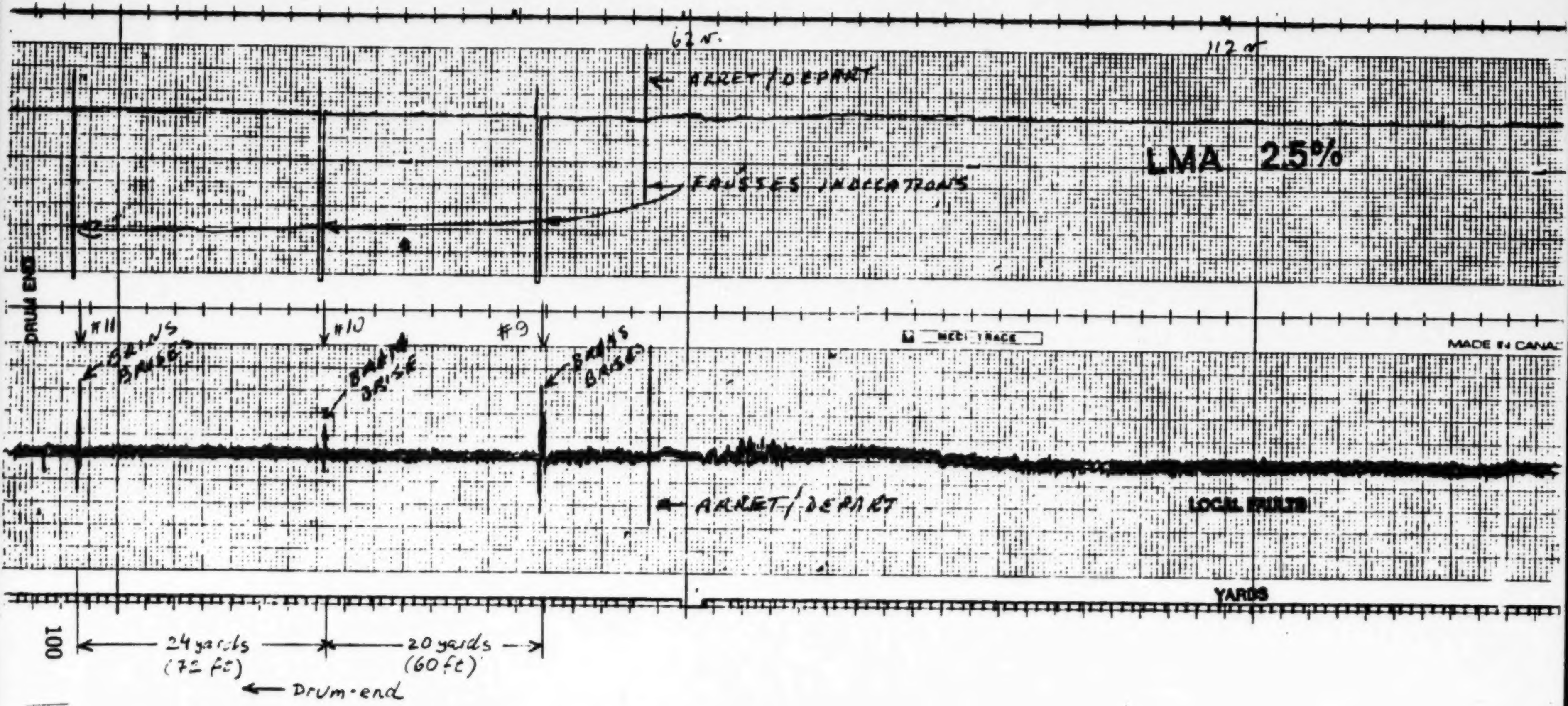

Fig. $6a_1$ — Rope-flaws #9 to #11 from Fig. 1e

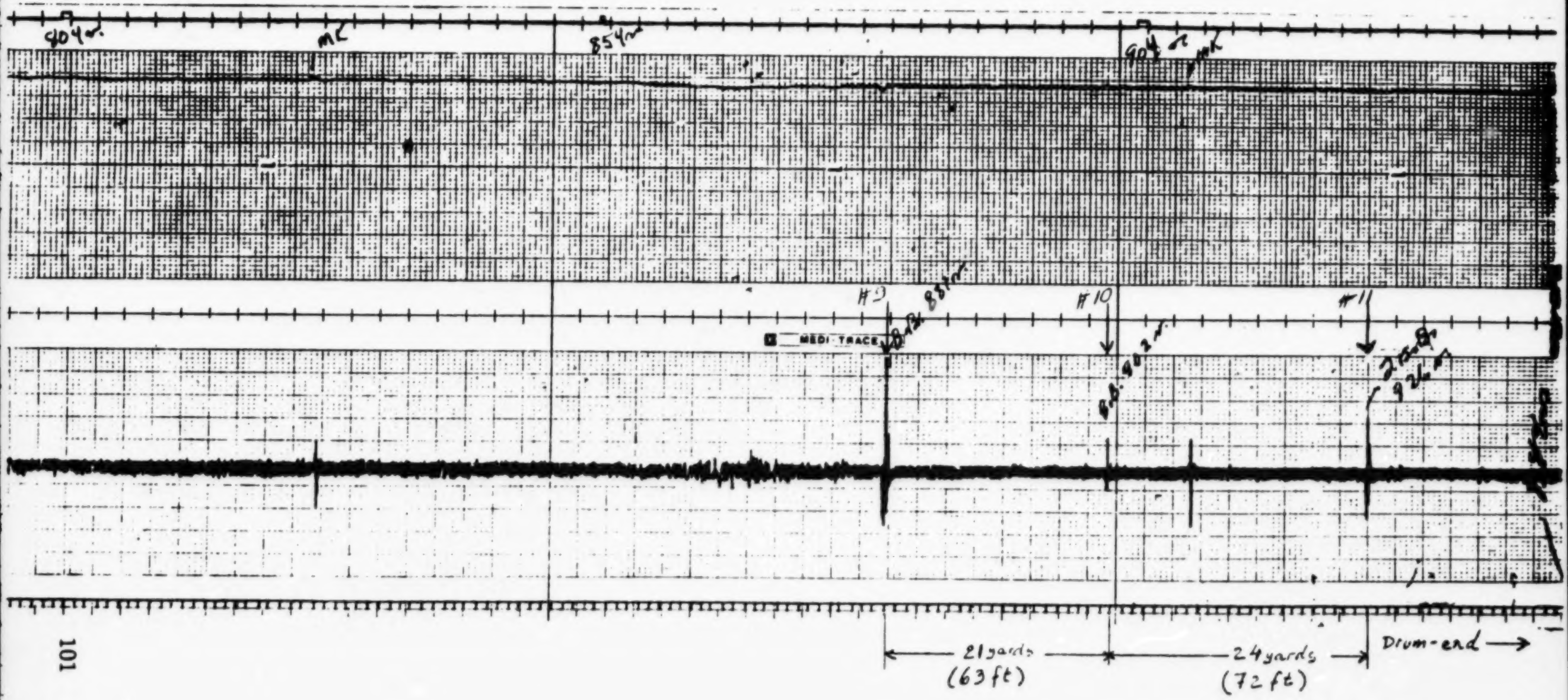

Fig. $6a_2$ — Rope-flaws #9 to #11 from Fig. 1f

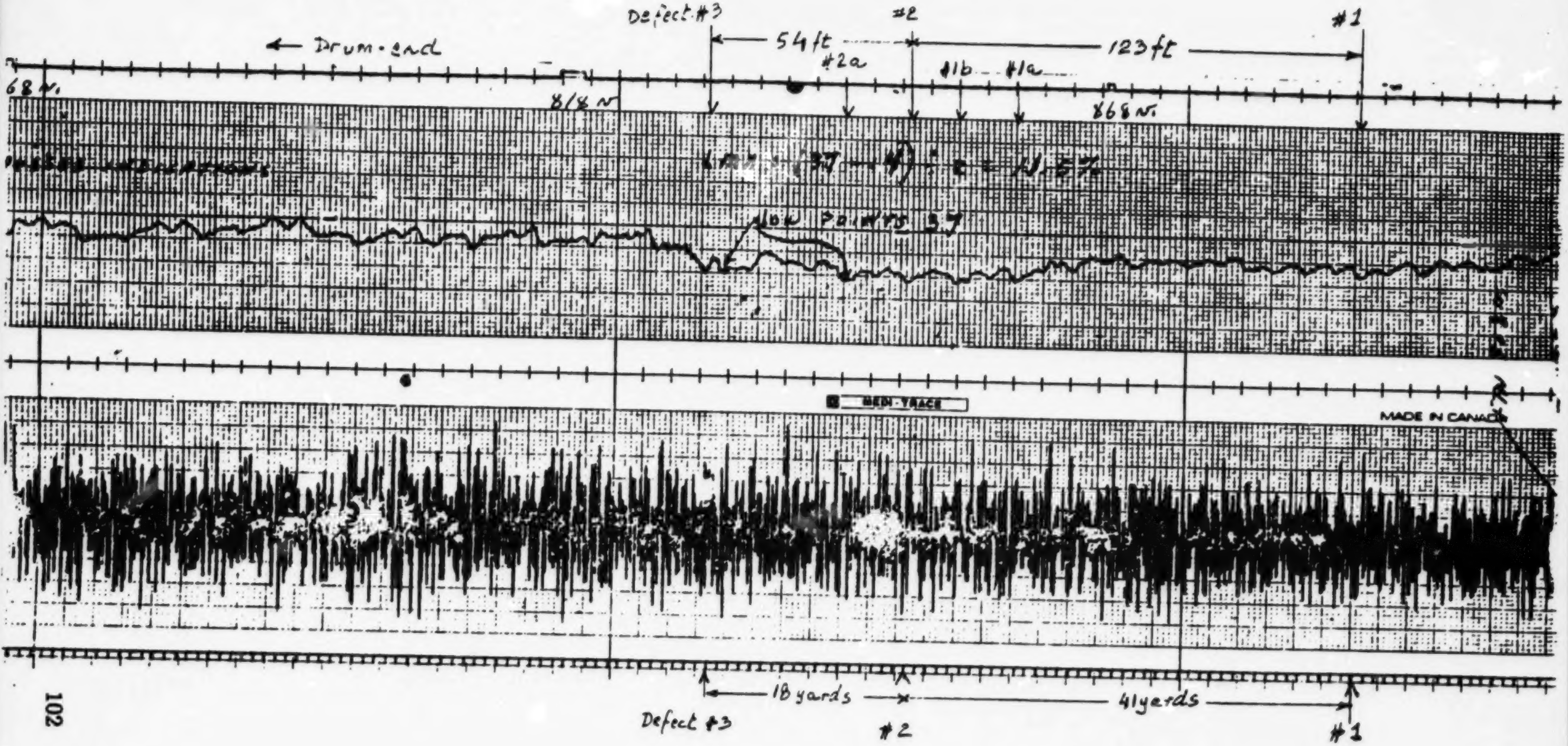

Fig. $6b_1$ — Rope-flaws #1 to #3 from Fig. 1e

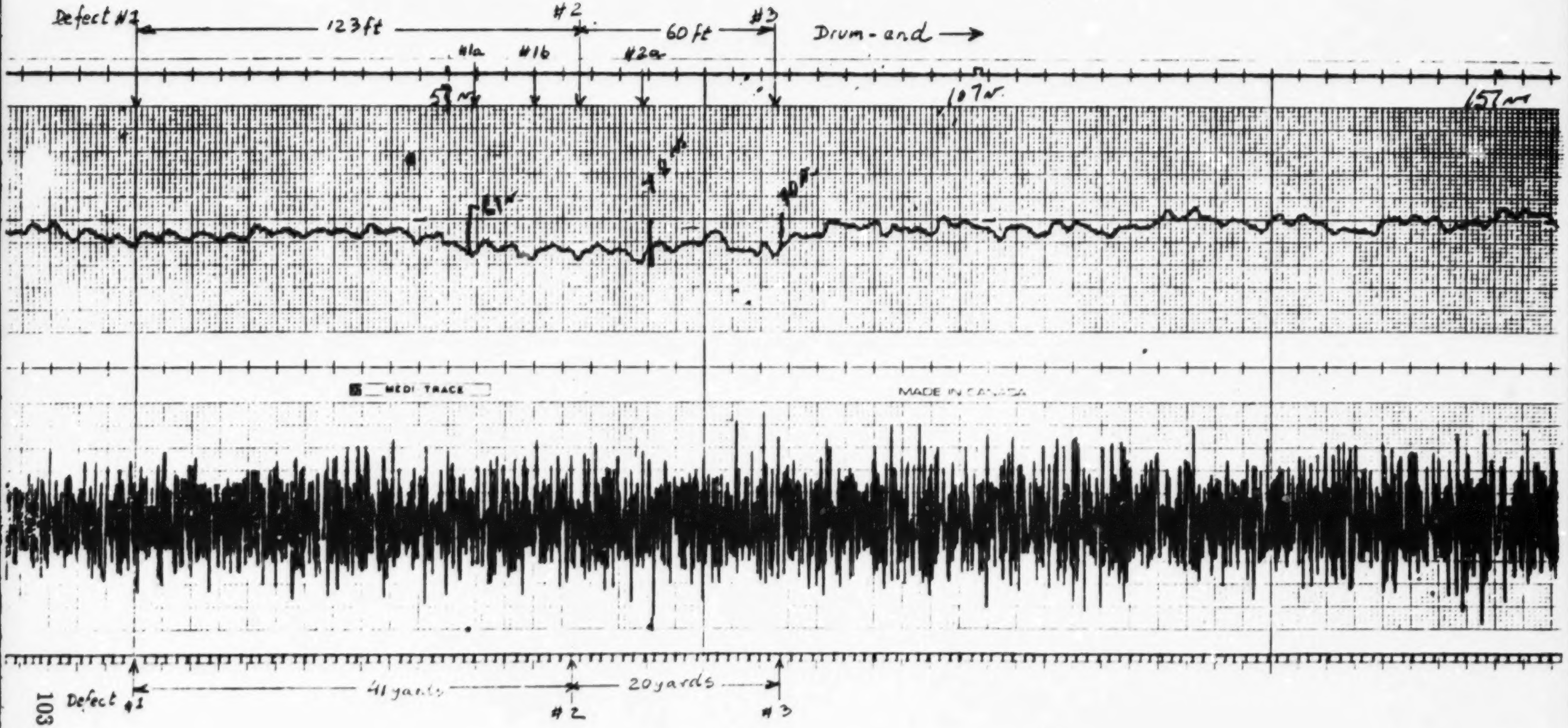

Fig. 6b$_2$ — Rope-flaws #1 to #3 from Fig. 1f

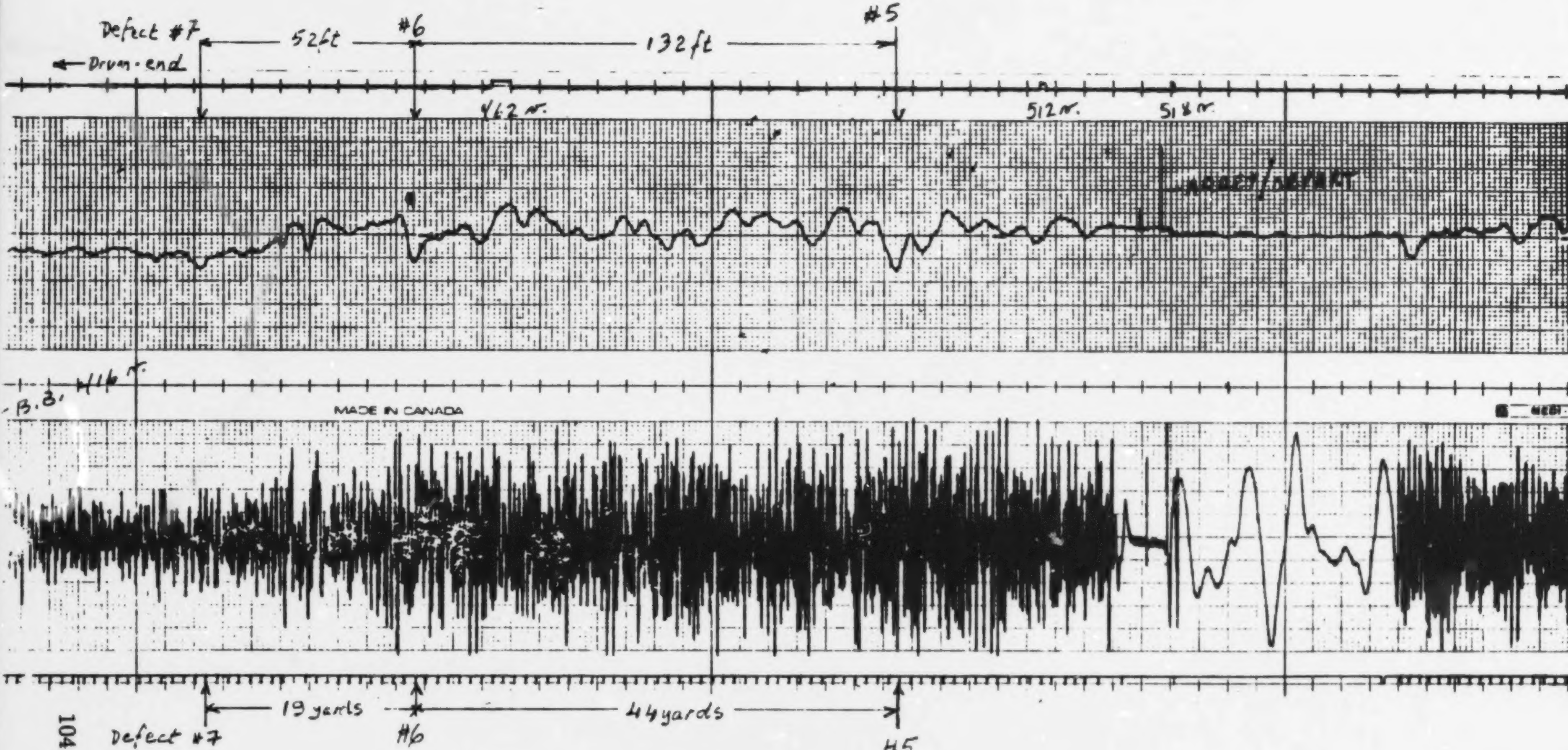

Fig. $6c_1$ — Rope-flaws #5 to #7 from Fig. 1e

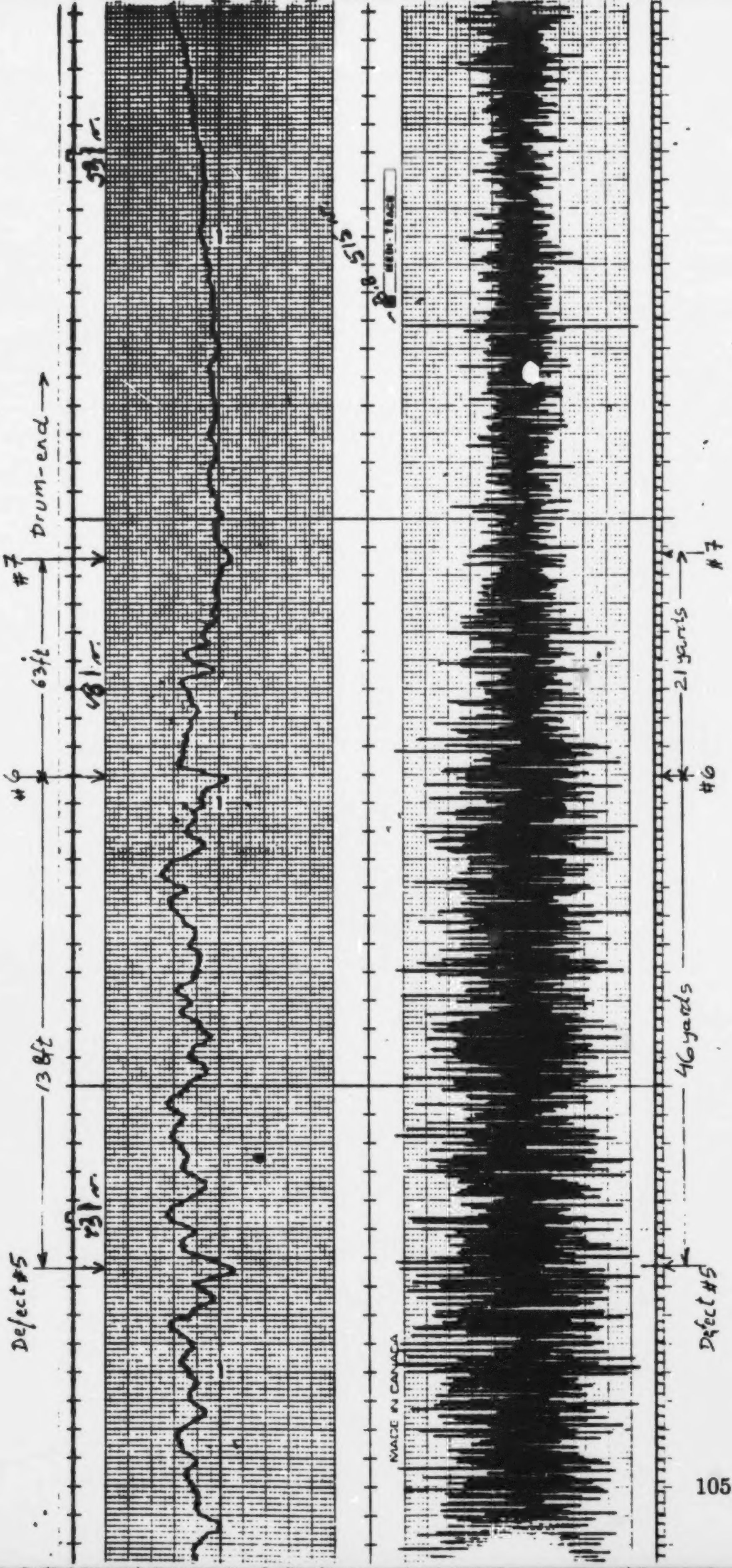

Fig. 6c₂ — Rope-flaws #5 to #7 from Fig. 1f

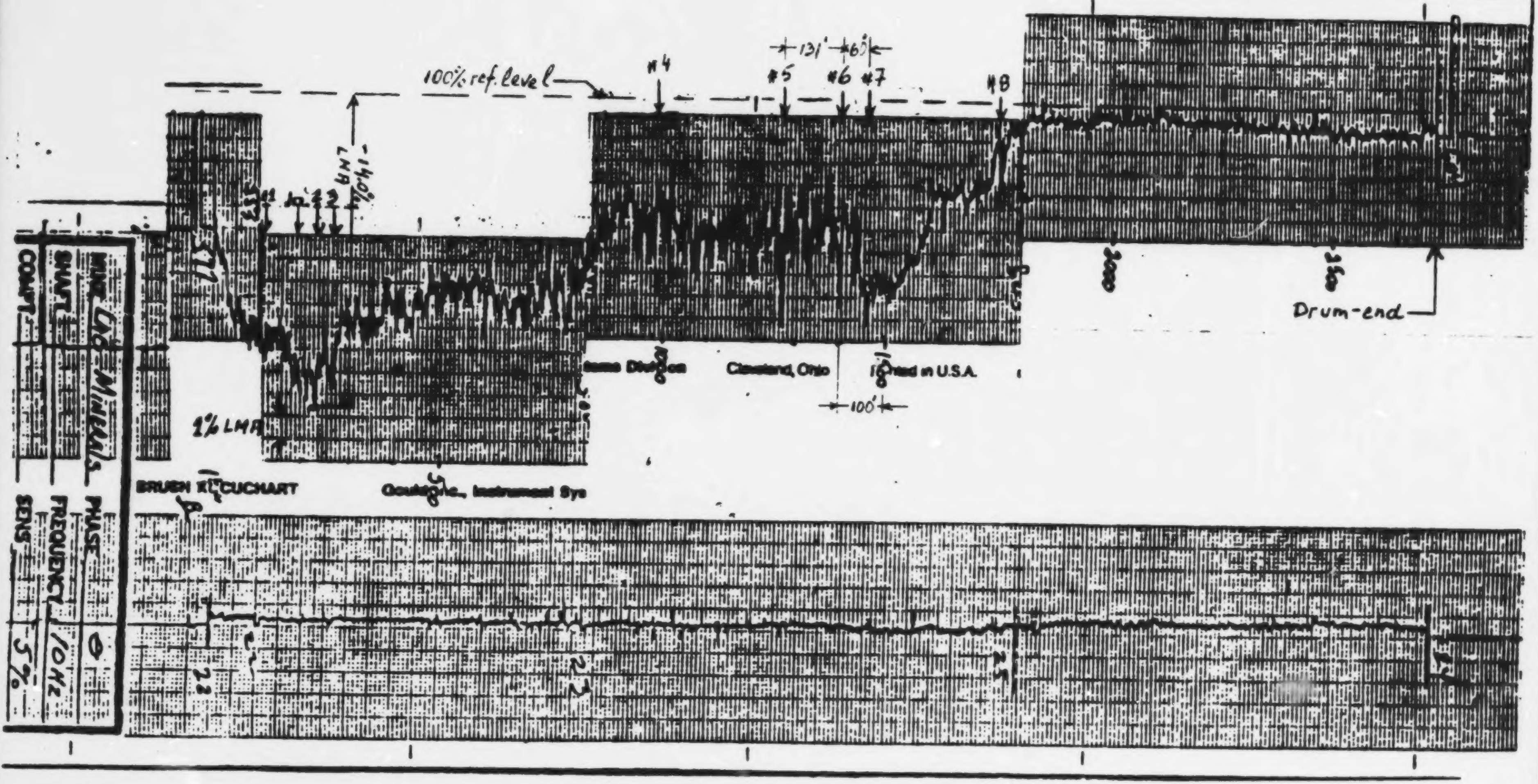

Fig. 7 — Rope-flaws #1 to #8 from Fig. 2c

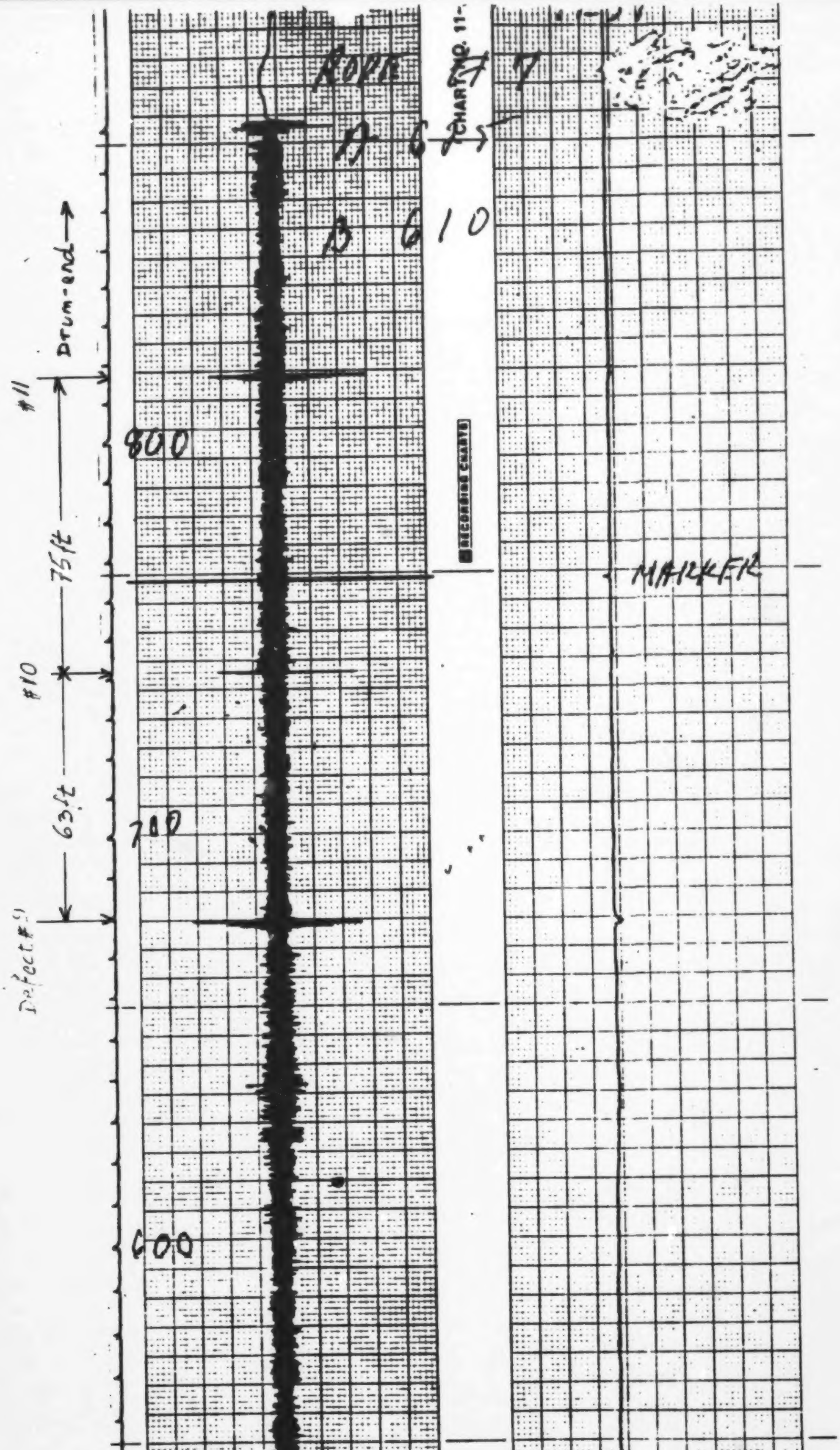

Fig. $8a_1$ — Rope-flaws #9 to #11 from Fig. 3b

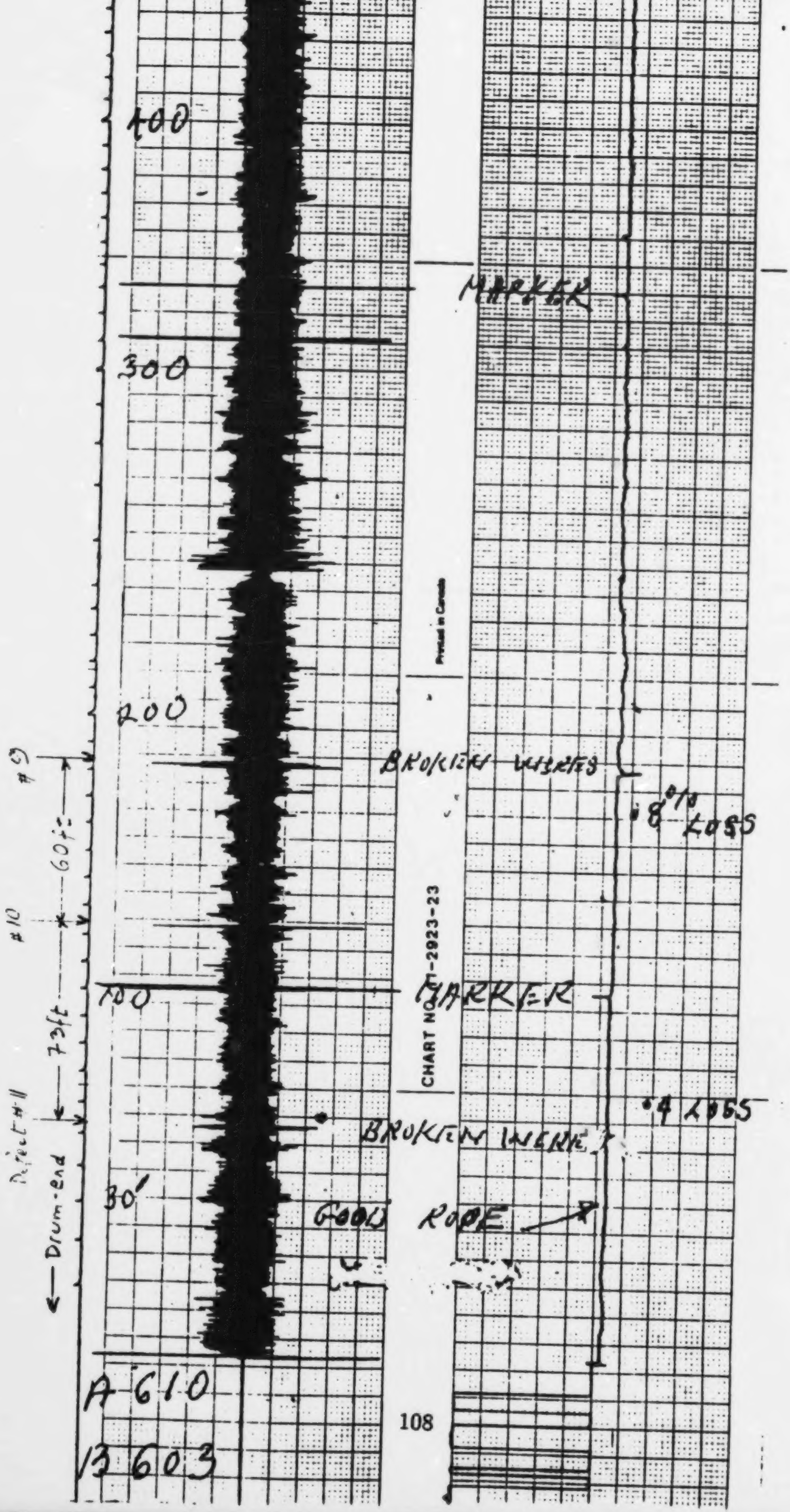

Fig. 8a$_2$ — Rope-flaws #9 to #11 from Fig. 3c

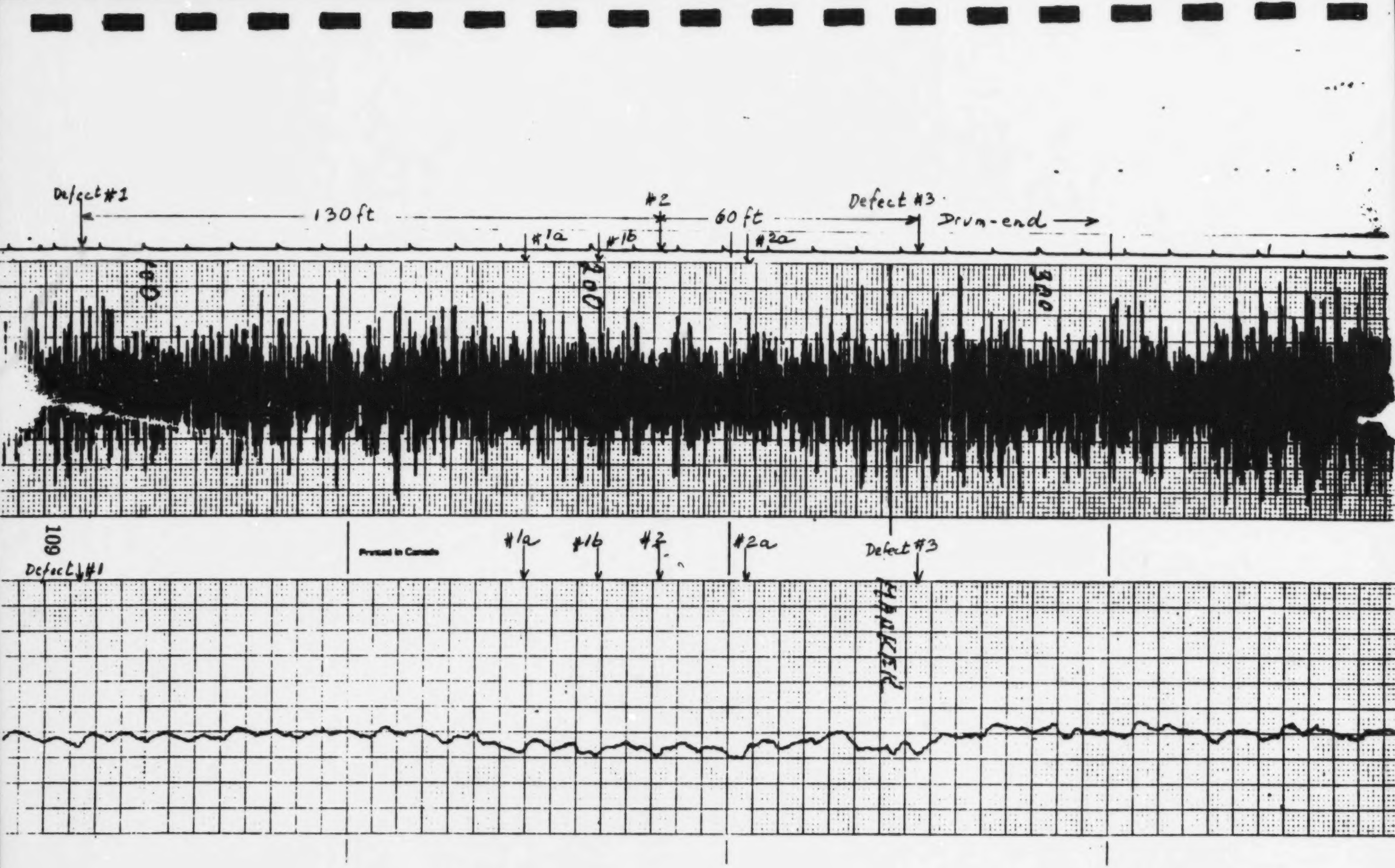

Fig. 8b$_1$ — Rope-flaws #1 to #3 from Fig. 3b

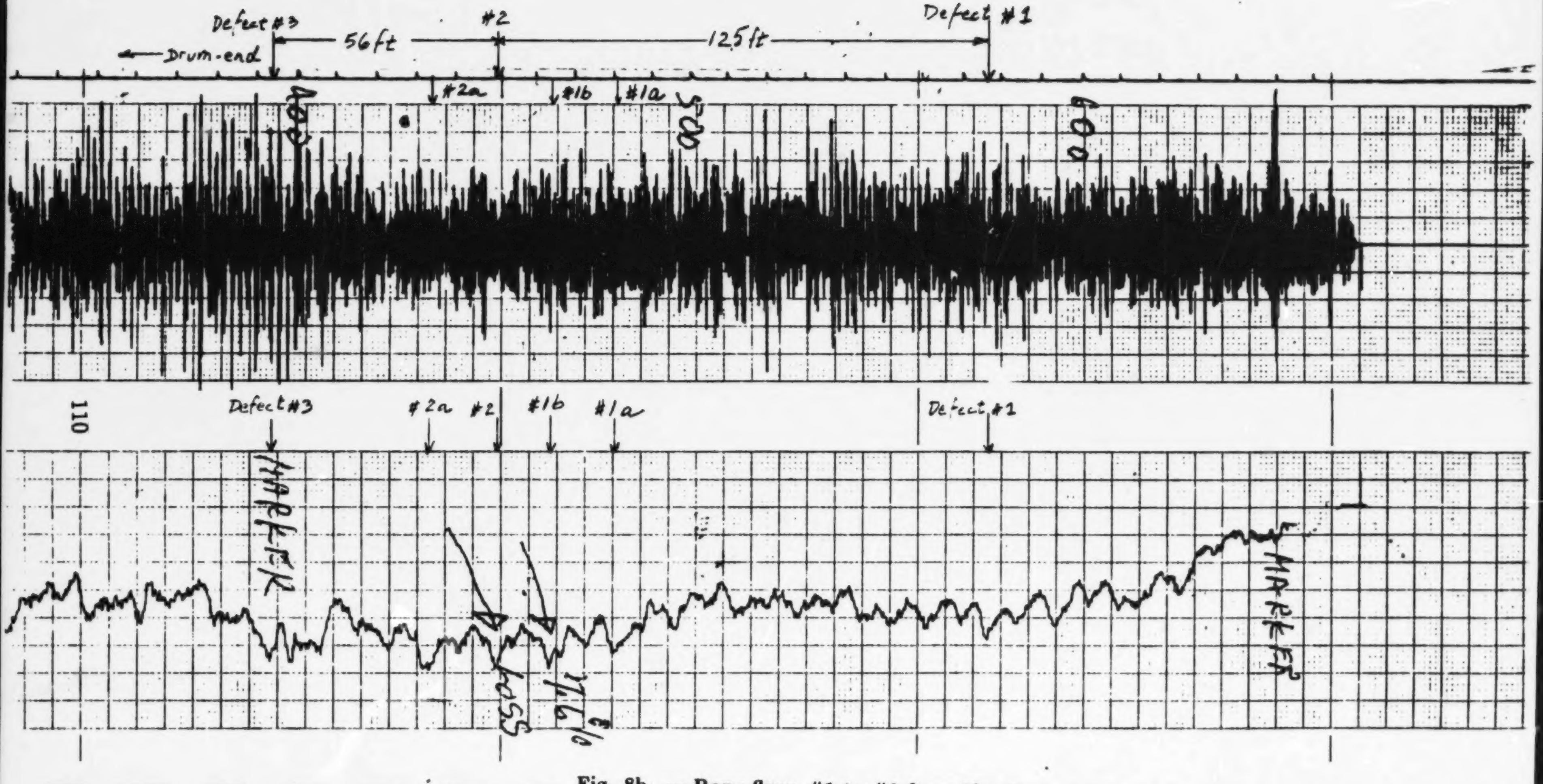

Fig. 8b$_2$ — Rope-flaws #1 to #3 from Fig. 3a

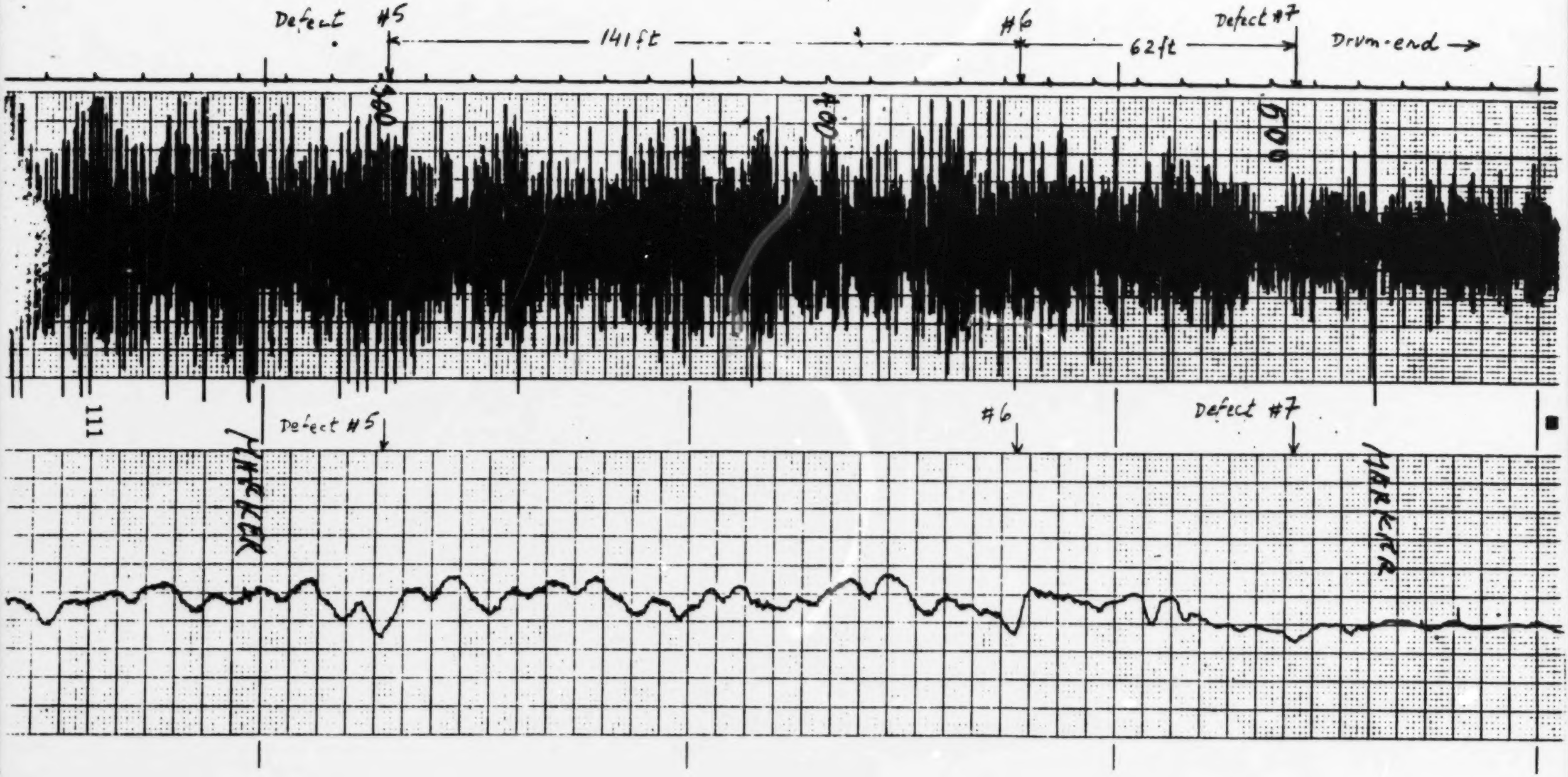

Fig. 8c$_1$ — Rope-flaws #5 to #7 from Fig. 3b

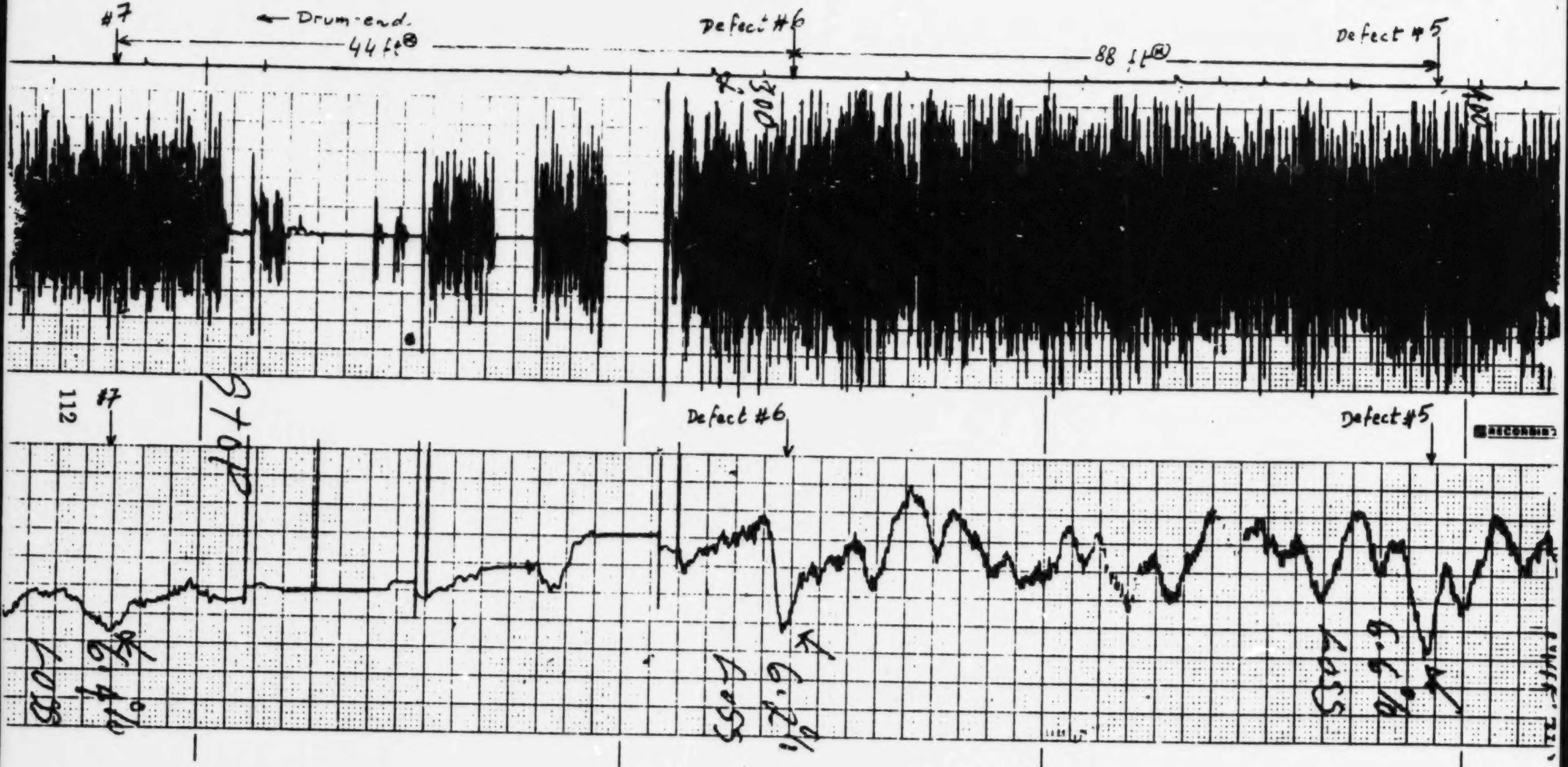

® these footages are in error

Fig. 8c$_2$ — Rope-flaws #5 to #7 from Fig. 3c

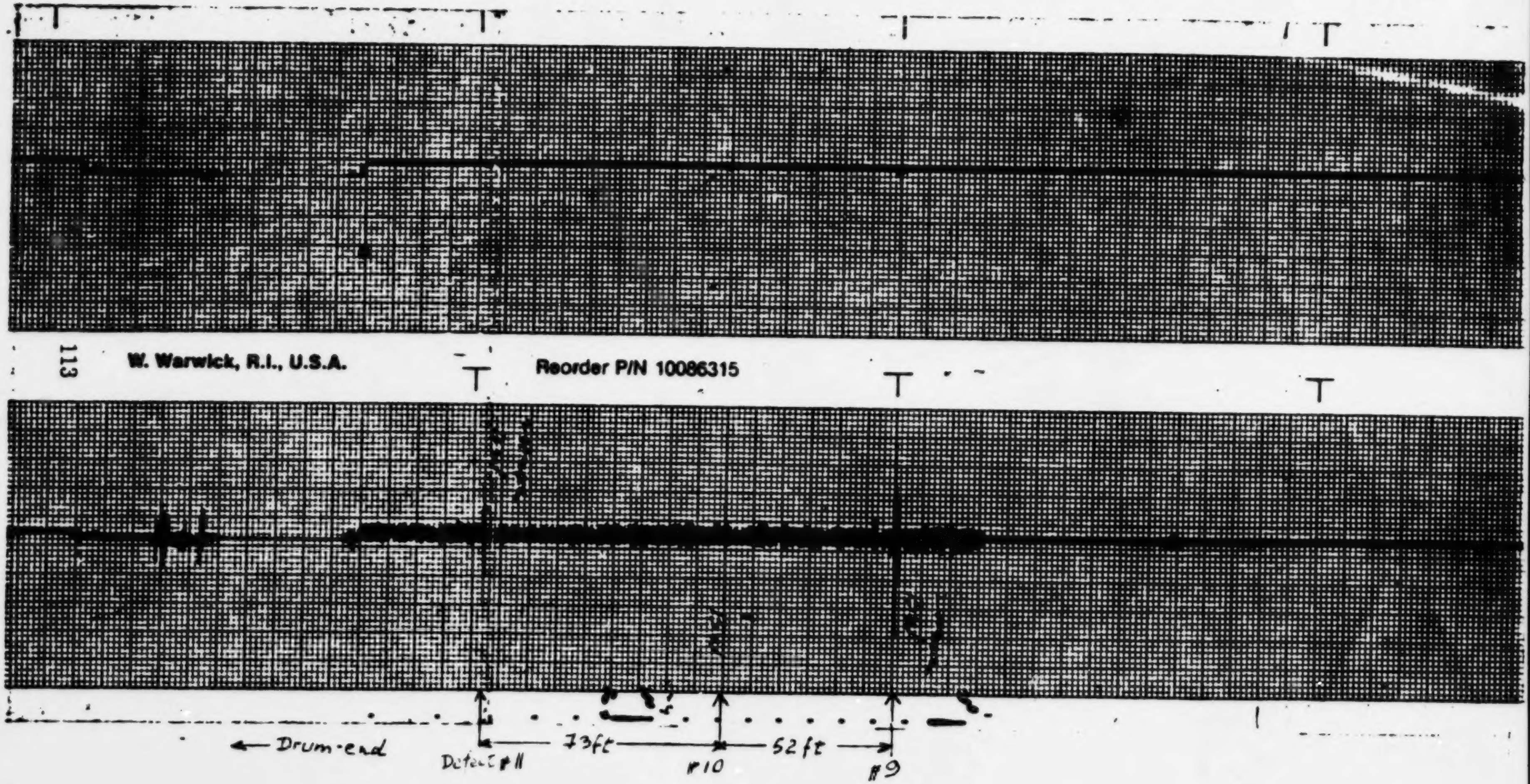

Fig. 9a$_1$ — Rope-flaws #9 to #11 from Fig. 4c

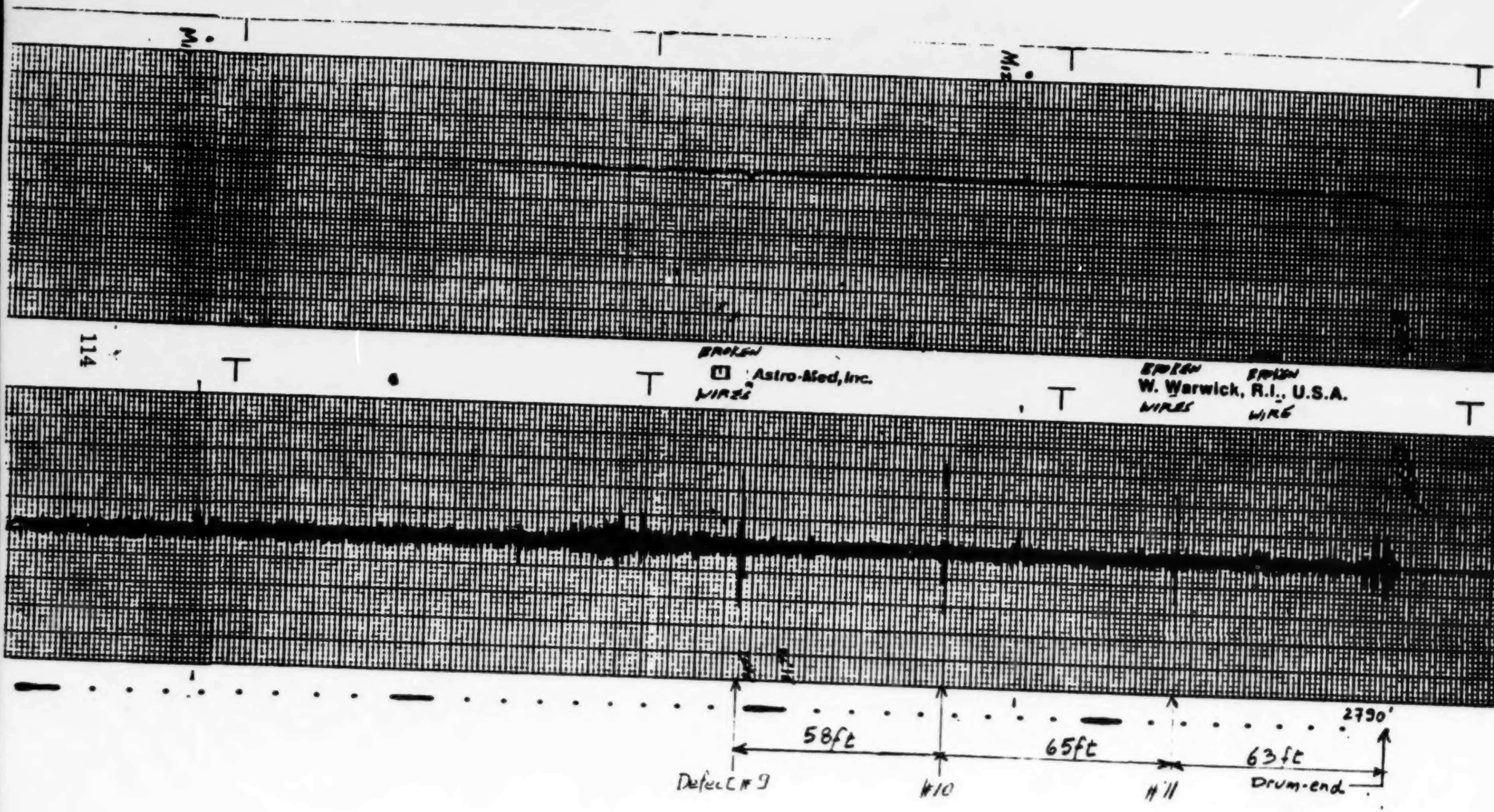

Fig. $9a_2$ — Rope-flaws #9 to #11 from Fig. 4d

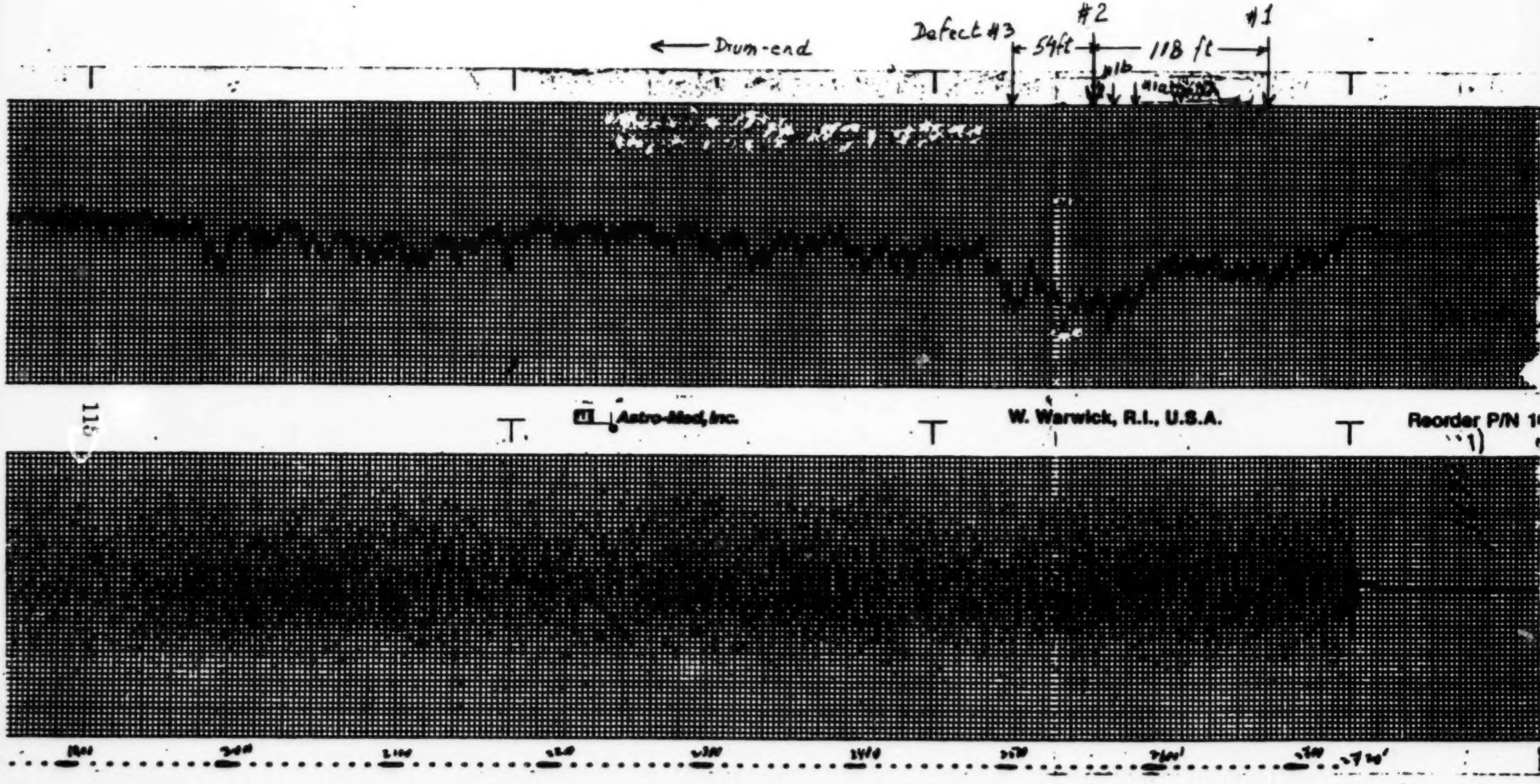

Fig. $9b_1$ — Rope-flaws #1 to #3 from Fig. 4c

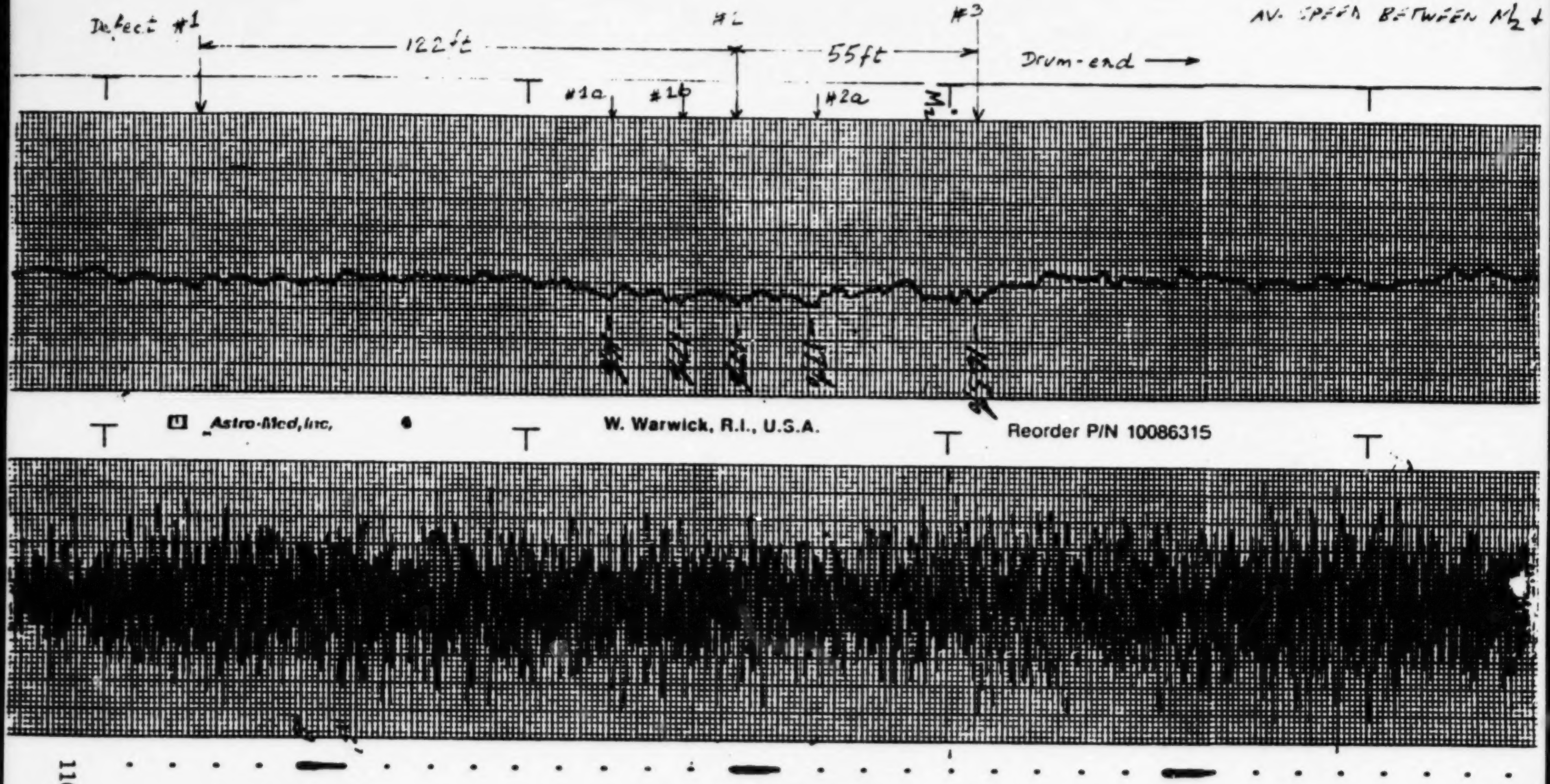

Fig. $9b_2$ — Rope-flaws #1 to #3 from Fig. 4d

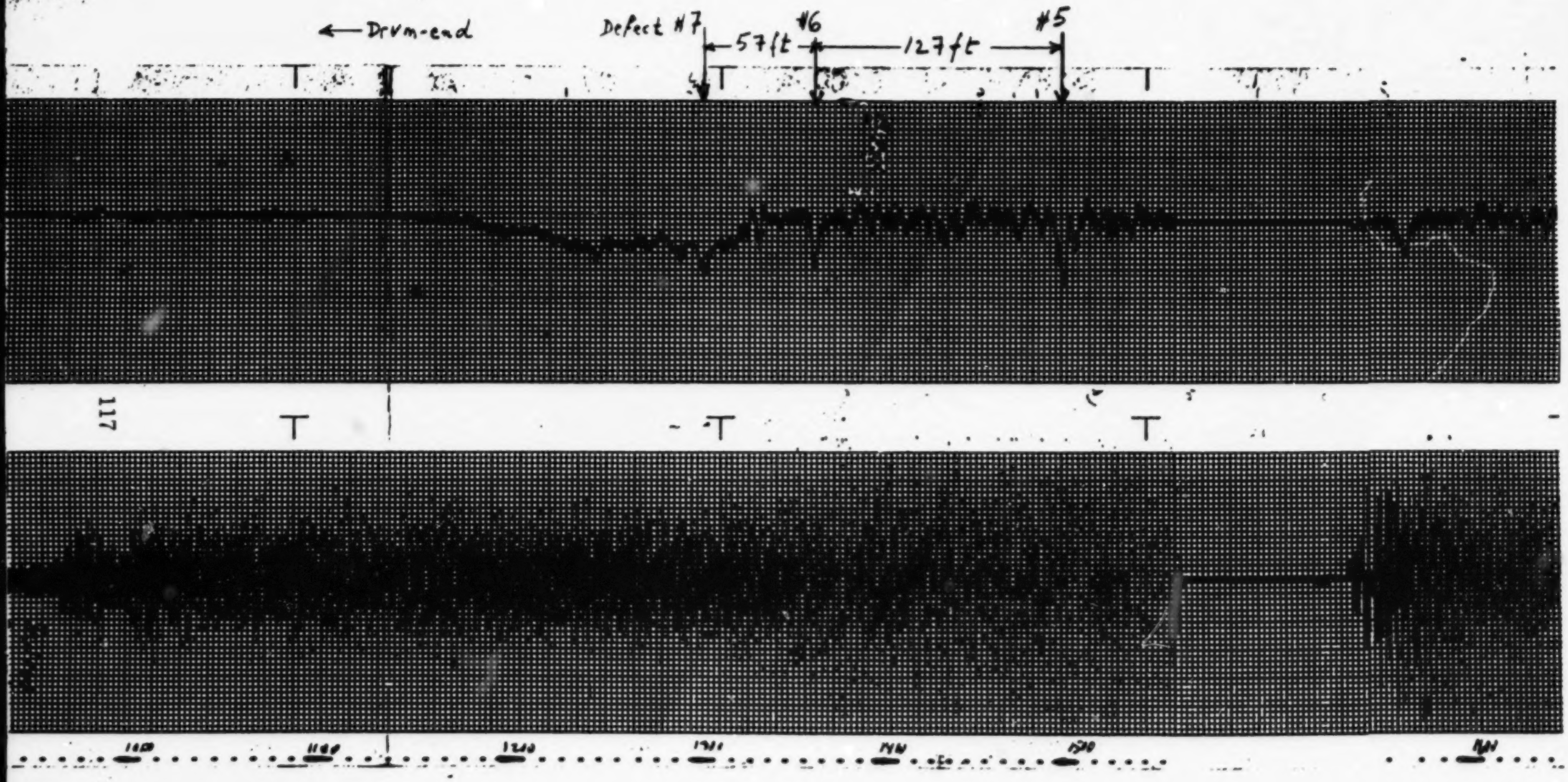

Fig. $9c_1$ — Rope-flaws #5 to #7 from Fig. 4c

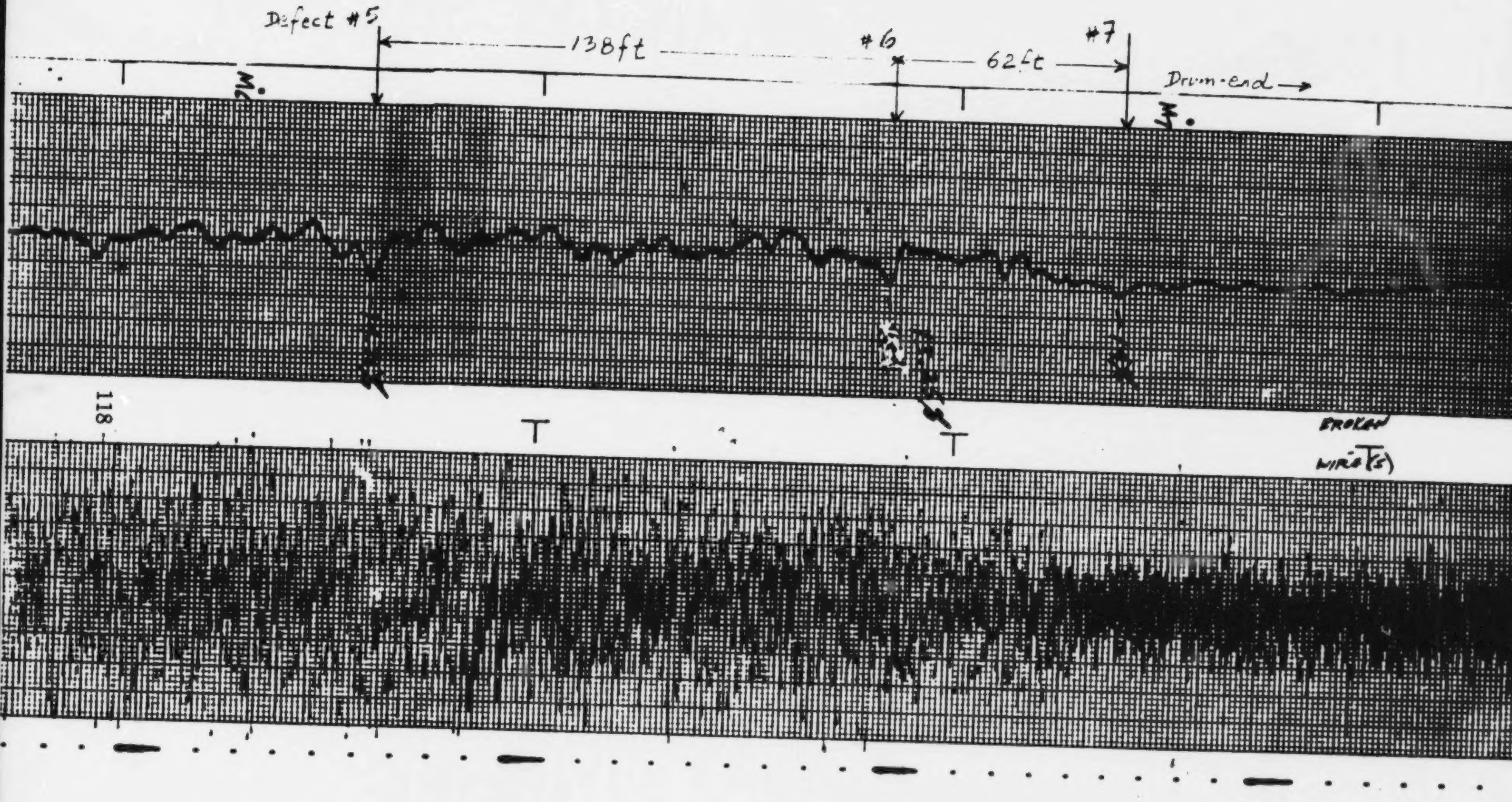

Fig. $9c_2$ — Rope-flaws #5 to #7 from Fig. 4d

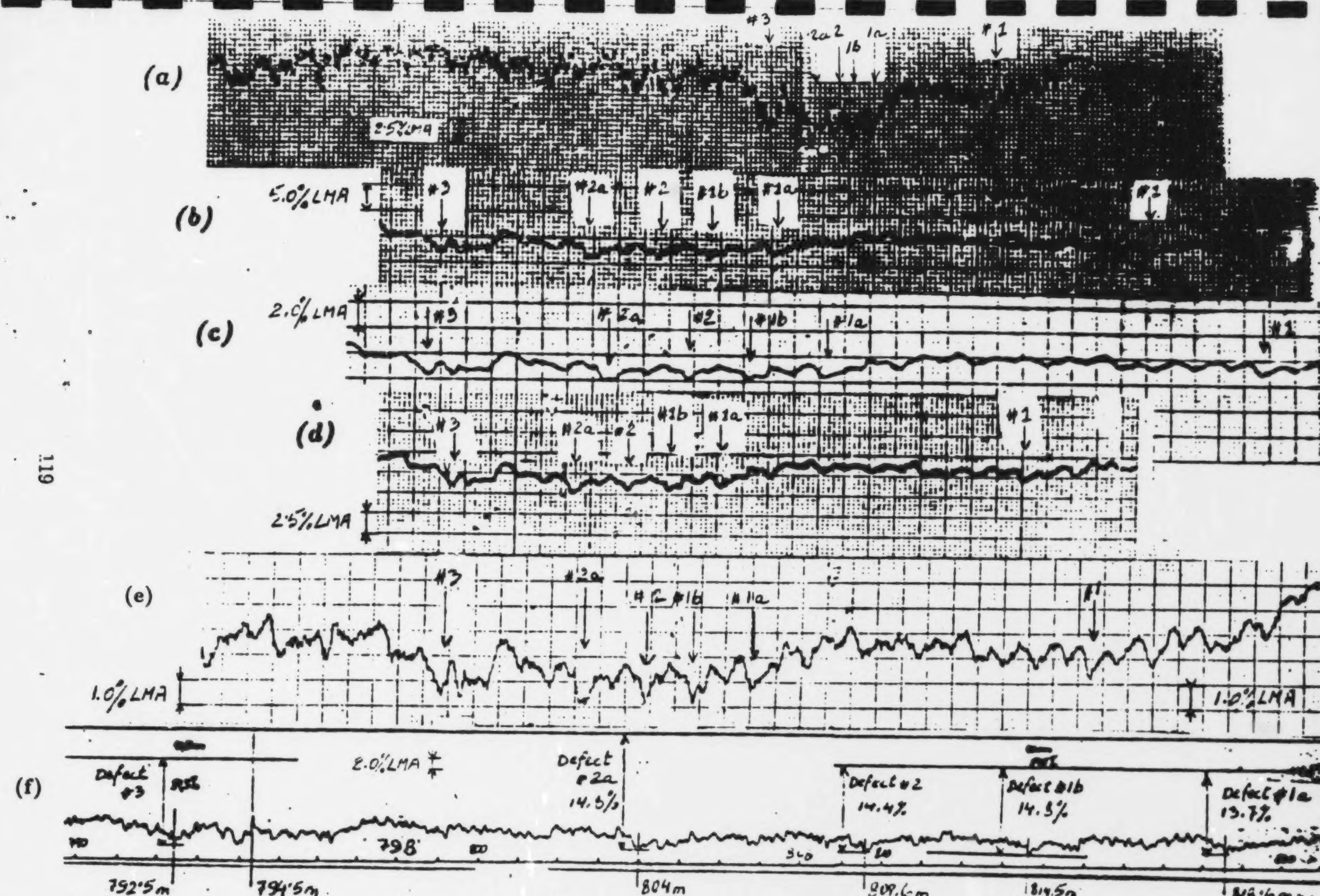

Fig. 10a — Juxtaposition of %LMA-trace 'fingerprints' of defects #1 to #3: (a) LMA-250, shop-floor, 18.1.89; (b) LMA-250, shop-floor, 4.4.89; (c) Rotescograph, shop-floor, 5.4.89; (d) Magnograph, shop-floor, 4.4.89; (e) Rotescograph, shop-floor, 10.4.89; (f) WBK, shop- floor, 10.4.89

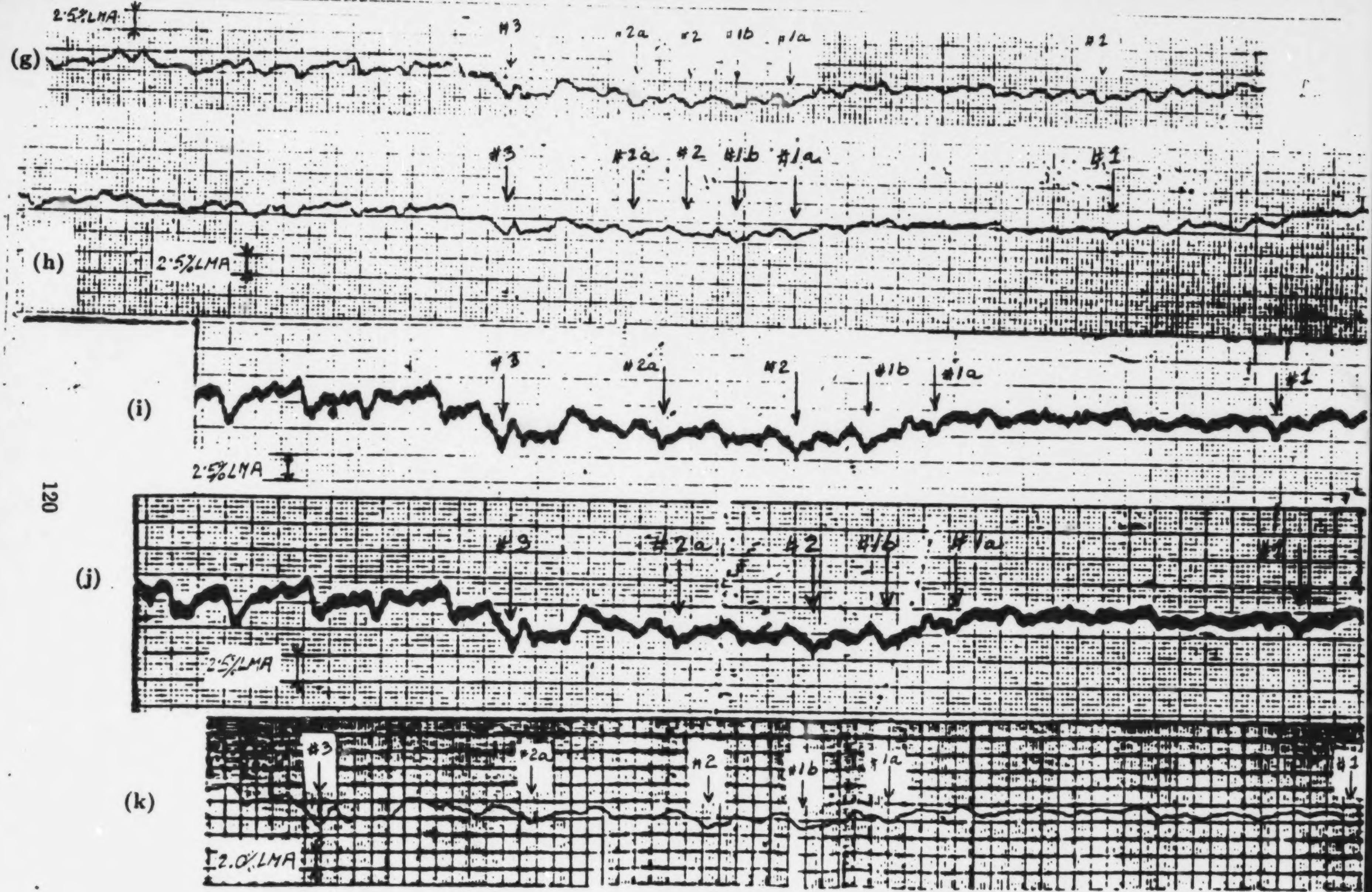

Fig. 10a (continued) — Juxtaposition of %LMA-trace 'fingerprints' of defects #1 to #3: (g) Magnograph, shop-floor, 18.1.89; (h) Magnograph, in situ, 23.8.88; (i) LMA-250, in situ, 9.9.88 (rope 'descending'); (j) LMA-250, in situ, 9.9.88 (rope 'rising'); (k) Rotescograph, in situ, 9.9.88

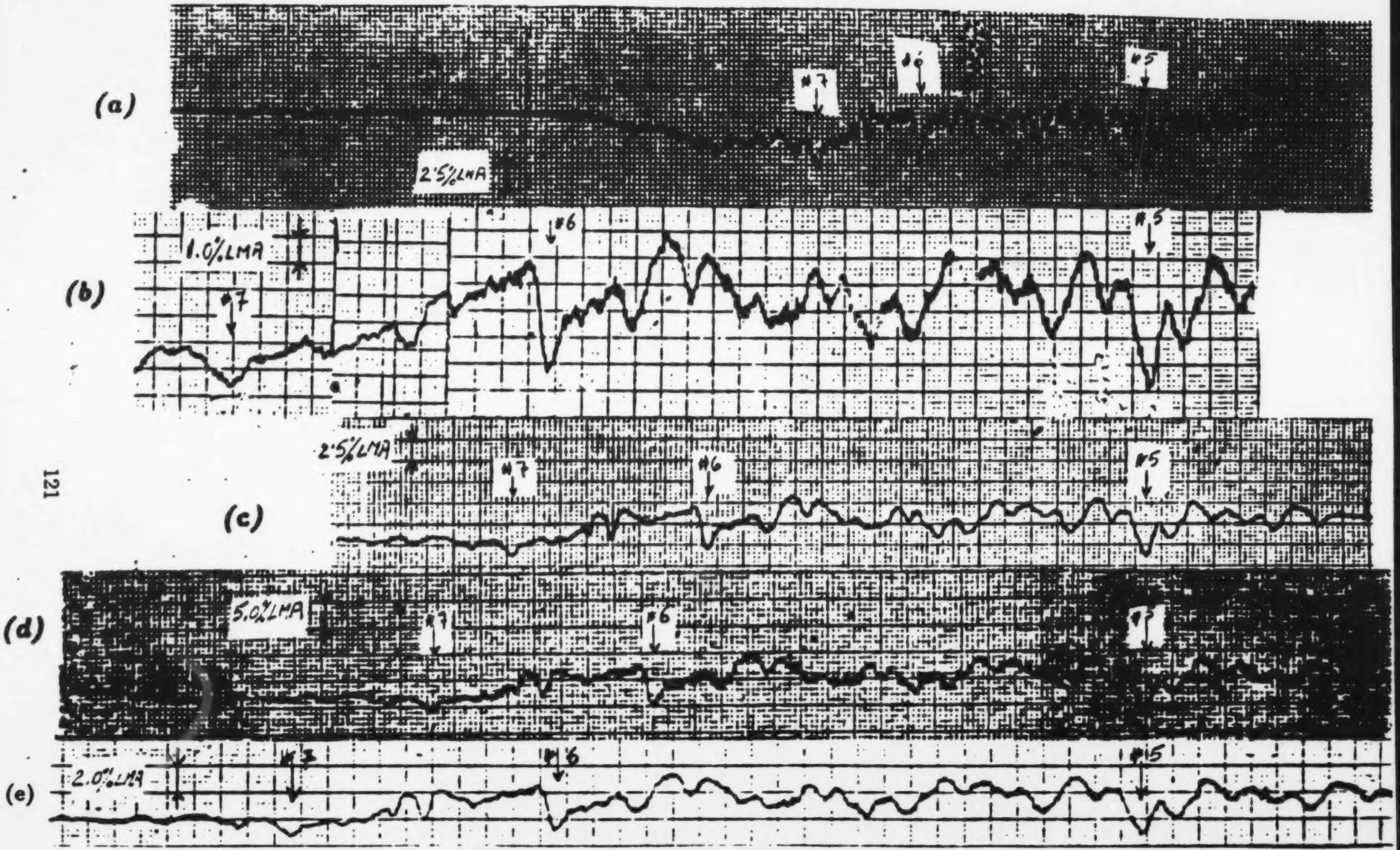

Fig. 10b — Juxtaposition of %LMA-trace ‘fingerprints’ of defects #5 to #7: (a) LMA- 250, shop-floor, 18.1.89; (b) Rotescograph, shop-floor, 10.4.89; (c) Magnograph, shop-floor, 18.1.89; (d) LMA-250, shop-floor, 4.4.89; (e) Rotescograph, shop-floor, 5.4.89

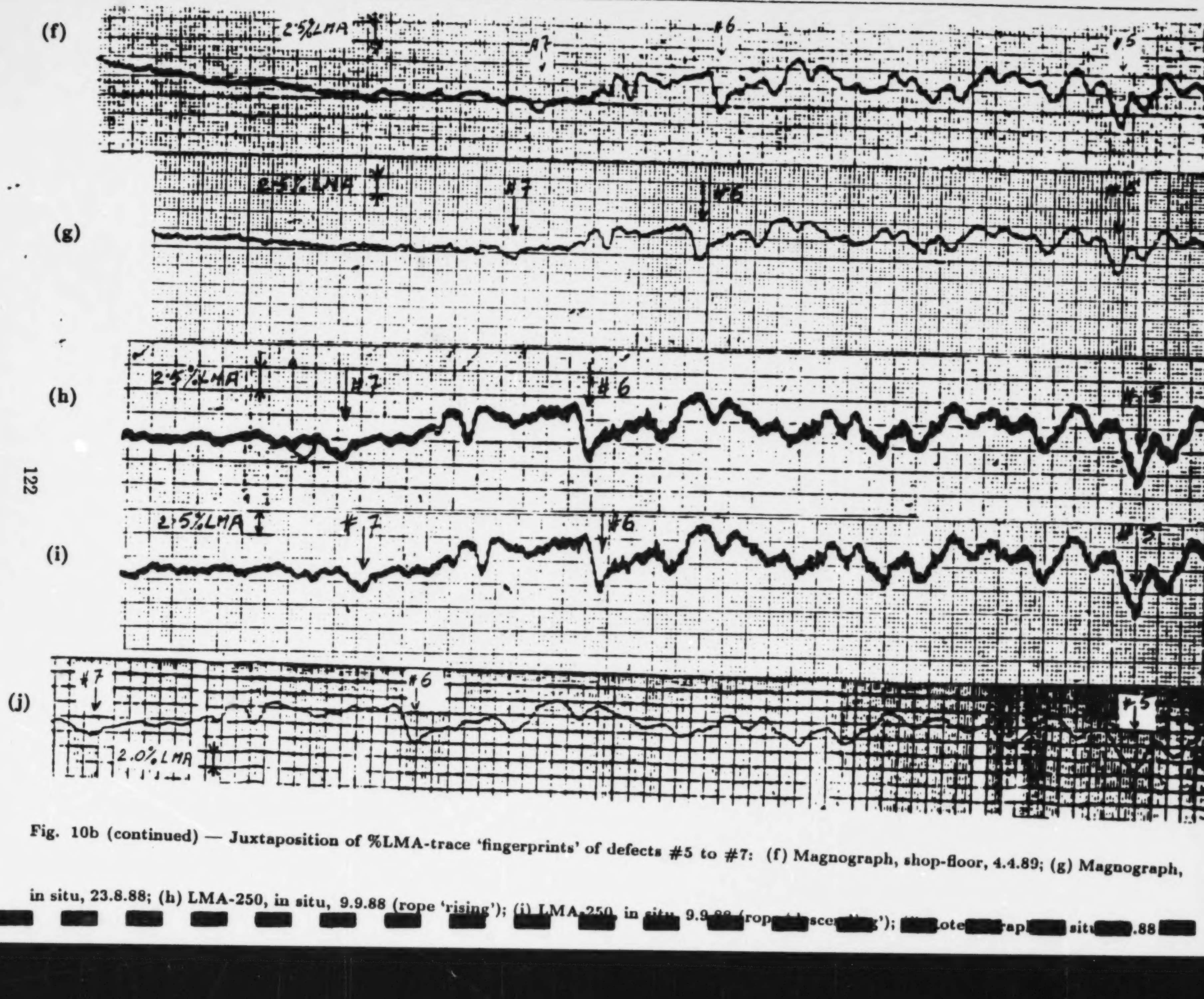

Fig. 10b (continued) — Juxtaposition of %LMA-trace 'fingerprints' of defects #5 to #7: (f) Magnograph, shop-floor, 4.4.89; (g) Magnograph, in situ, 23.8.88; (h) LMA-250, in situ, 9.9.88 (rope 'rising'); (i) LMA-250, in situ, 9.9.[illegible] (rop[illegible]scen[illegible]'); [illegible]ote[illegible]rap[illegible] situ[illegible].88

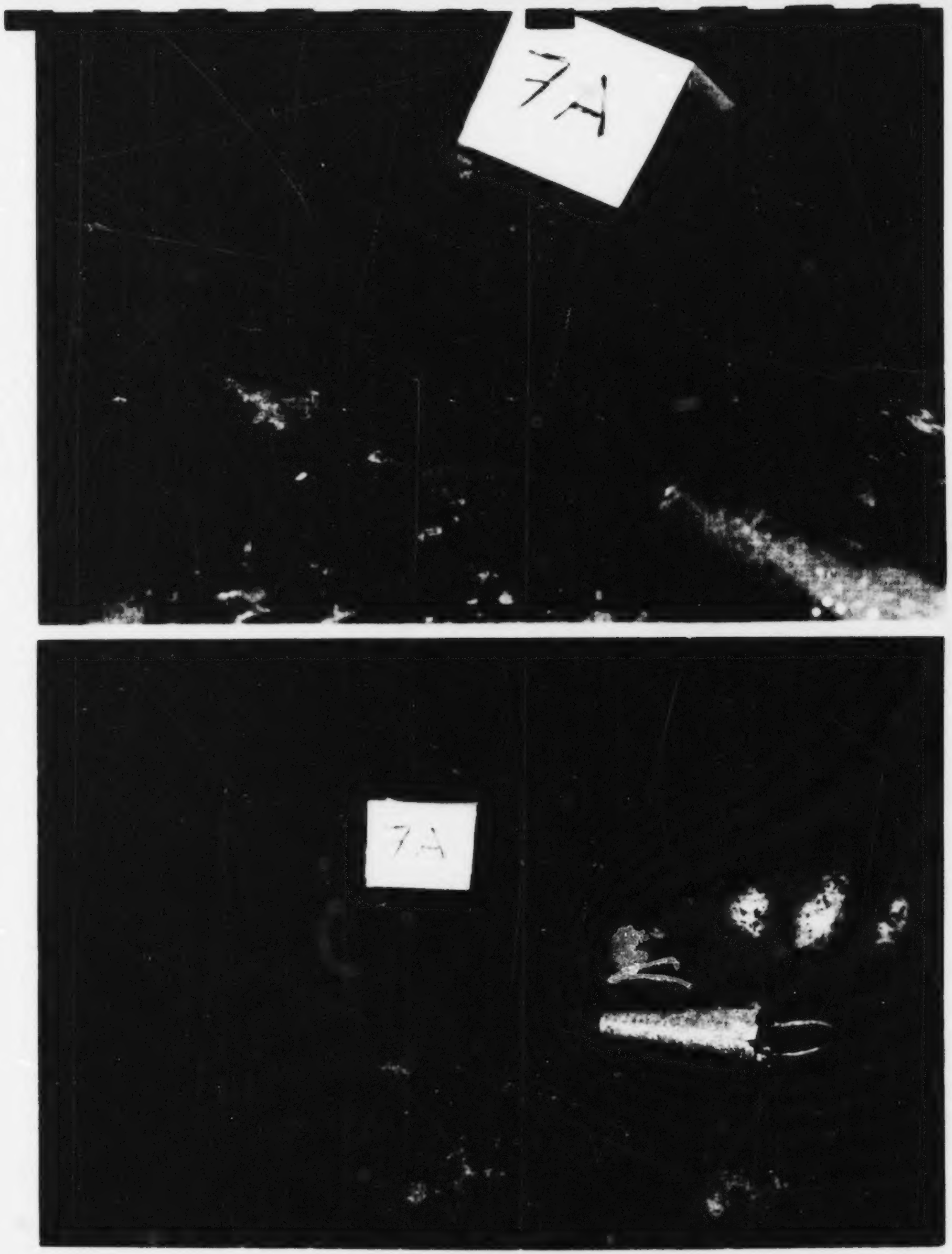

Fig. 11 — Two views of broken sample #7a

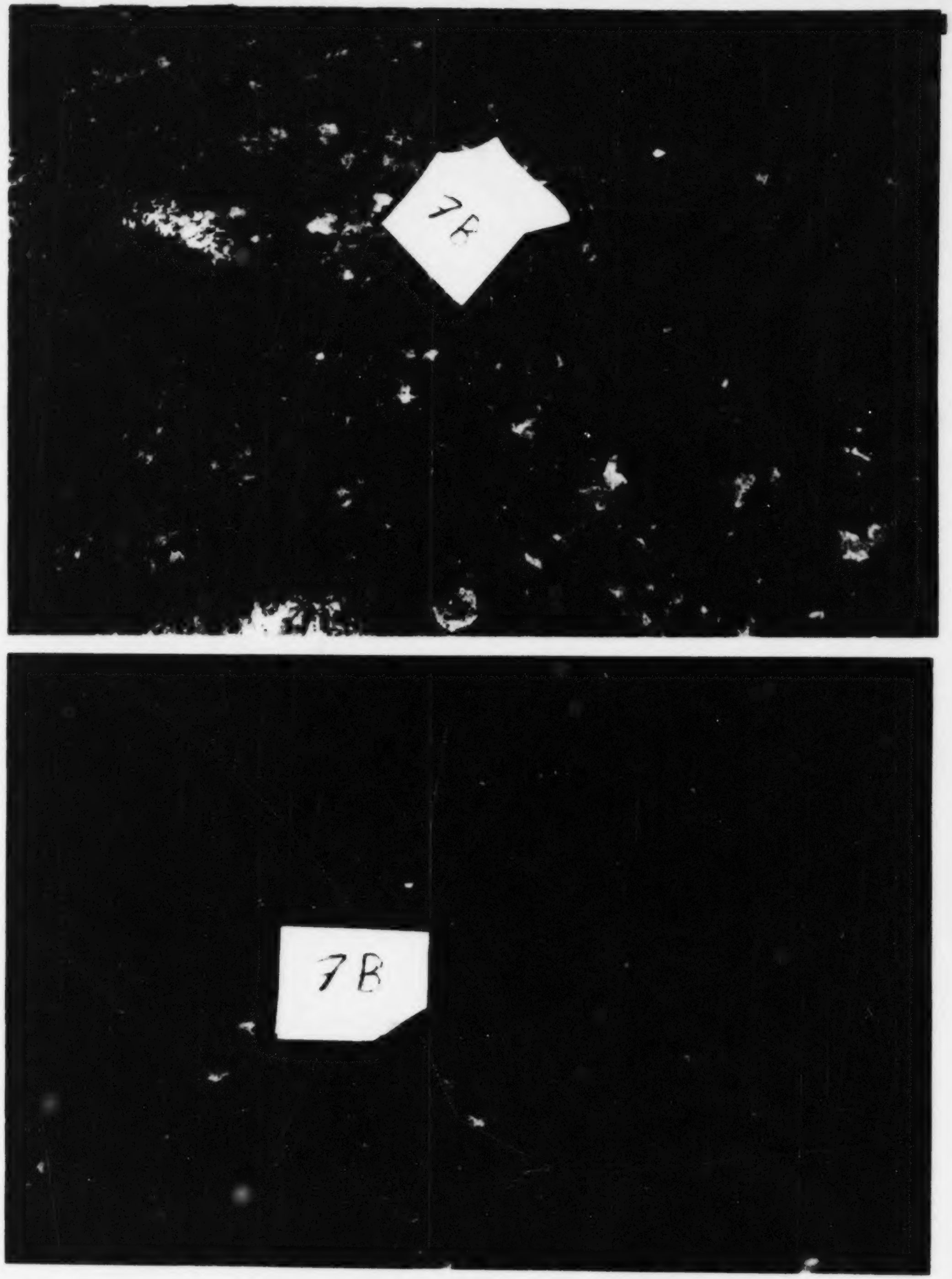

Fig. 12 — Two views of broken sample #7b

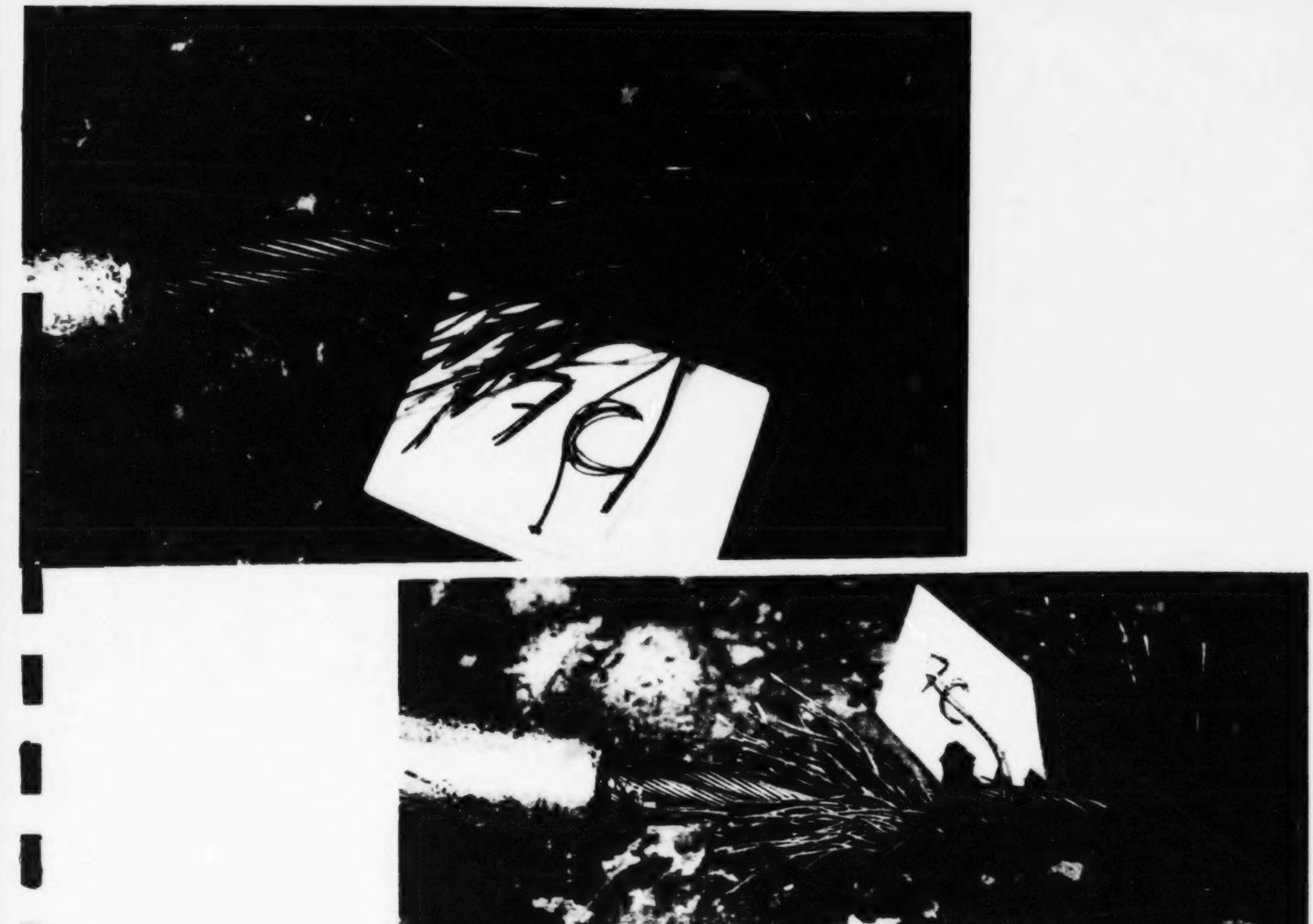

Fig. 13 — Three views of broken sample #7c

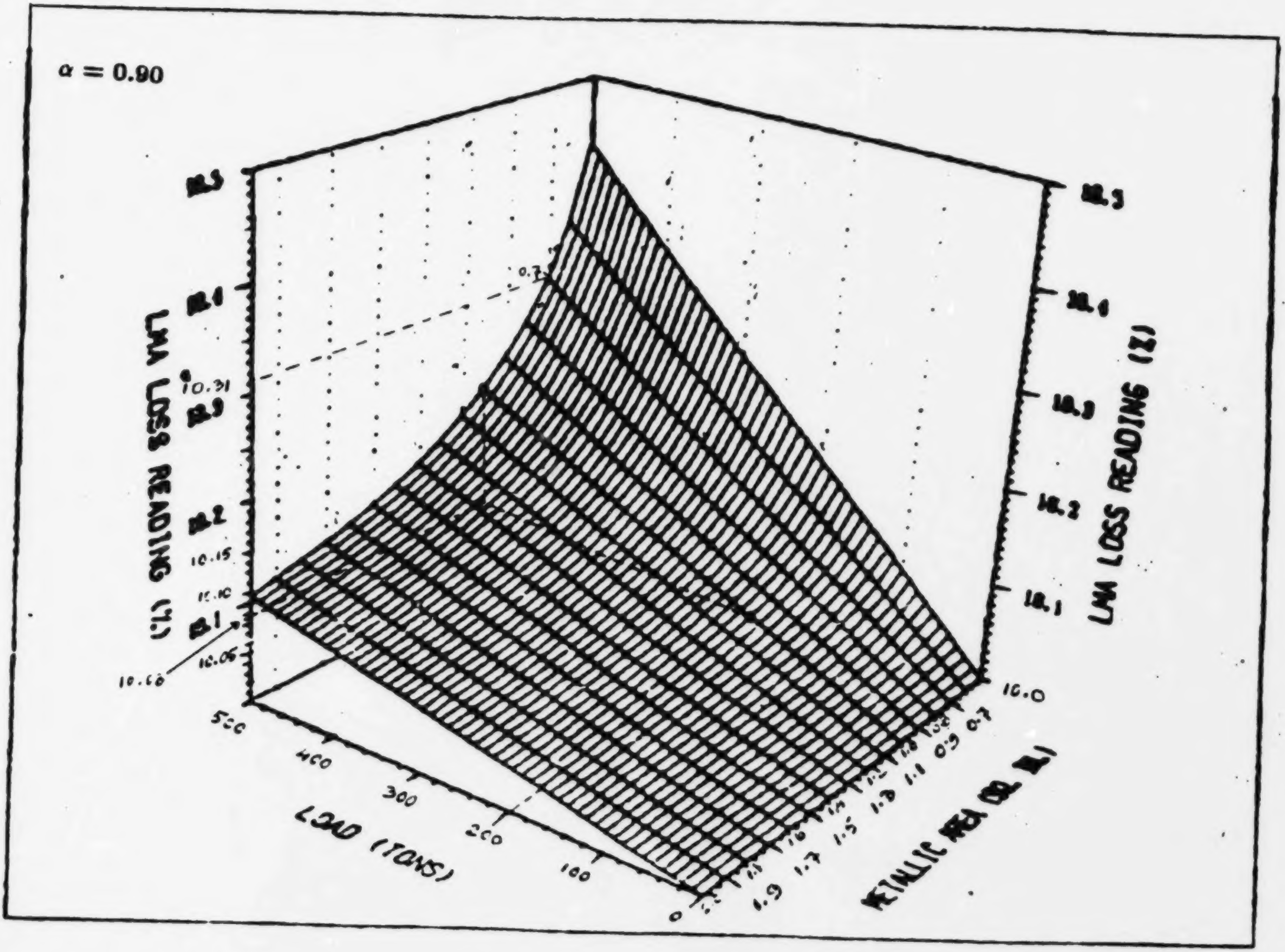

Fig. 14a — %Error, on comparing reel-to-reel with in situ %LMA chart readings: α = 0.90 (using program #1)

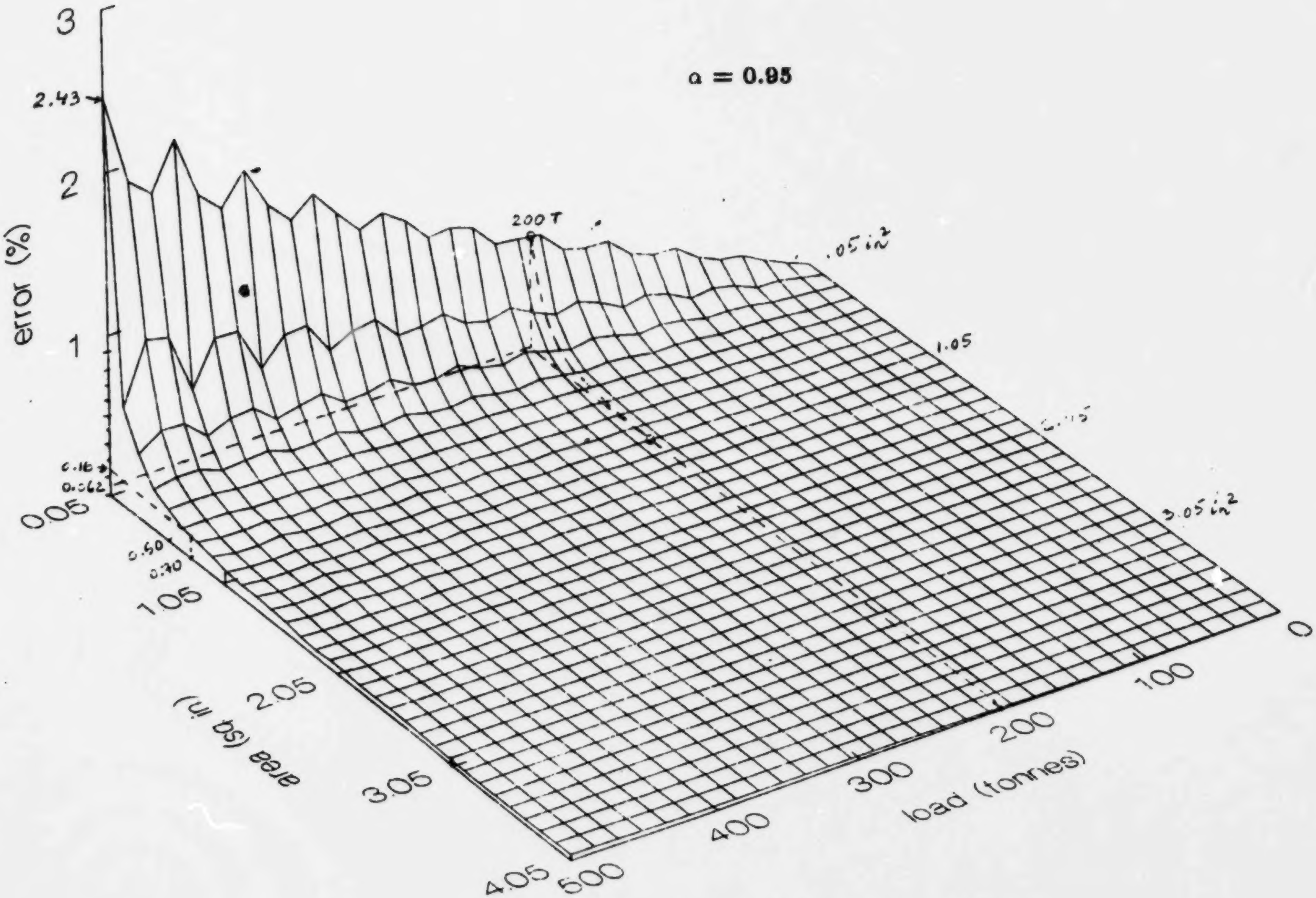

Fig. 14c — %Error, on comparing reel-to-reel with in situ %LMA chart readings: α = 0.95 (using program #2)